PRODUCTION FLUX OF SEA SPRAY AEROSOL

Gerrit de Leeuw,[1,2,3] Edgar L Andreas,[4] Magdalena D. Anguelova,[5] C. W. Fairall,[6] Ernie R. Lewis,[7] Colin O'Dowd,[8] Michael Schulz,[9,10] and Stephen E. Schwartz[7]

[1] Knowledge of the size- and composition-dependent production flux of primary sea spray aerosol (SSA) particles and its dependence on environmental variables is required for modeling cloud microphysical properties and aerosol radiative influences, interpreting measurements of particulate matter in coastal areas and its relation to air quality, and evaluating rates of uptake and reactions of gases in sea spray drops. This review examines recent research pertinent to SSA production flux, which deals mainly with production of particles with r_{80} (equilibrium radius at 80% relative humidity) less than 1 μm and as small as 0.01 μm. Production of sea spray particles and its dependence on controlling factors has been investigated in laboratory studies that have examined the dependences on water temperature, salinity, and the presence of organics and in field measurements with micrometeorological techniques that use newly developed fast optical particle sizers. Extensive measurements show that water-insoluble organic matter contributes substantially to the composition of SSA particles with $r_{80} <$ 0.25 μm and, in locations with high biological activity, can be the dominant constituent. Order-of-magnitude variation remains in estimates of the size-dependent production flux per white area, the quantity central to formulations of the production flux based on the whitecap method. This variation indicates that the production flux may depend on quantities such as the volume flux of air bubbles to the surface that are not accounted for in current models. Variation in estimates of the whitecap fraction as a function of wind speed contributes additional, comparable uncertainty to production flux estimates.

1. INTRODUCTION

[2] Sea spray aerosol (SSA) consists of a suspension, in air, of particles that are directly produced at the sea surface. These particles exist mainly in the liquid phase (i.e., as drops). The radii of these particles vary from around 10 nm to at least several millimeters, and the atmospheric residence times vary from seconds to minutes for larger particles, for which gravitational sedimentation is the principal removal mechanism, to days for smaller particles, for which removal is primarily by precipitation.

[3] SSA particles, because of their hygroscopicity and size, function readily as cloud condensation nuclei (CCN) [e.g., *Andreae and Rosenfeld*, 2008, and references therein], and can thus play a major role in determining the number concentration and size distribution of drops in marine clouds. In the absence of perturbations by anthropogenic aerosols, SSA exerts an even stronger influence on cloud properties; thus understanding SSA is necessary to evaluate the influences of anthropogenic aerosols on cloud reflectivity and persistence (so-called indirect radiative forcing) and on precipitation. A major contributor to uncertainty in evaluating the indirect forcing by anthropogenic aerosols is a lack of knowledge on the background natural aerosol and the associated cloud properties.

[4] SSA provides a major contribution to scattering of electromagnetic radiation over much of the world's oceans. The annual global average magnitude of upward scattering of radiation in the solar spectrum at wavelengths 0.3–4 μm by SSA particles, which results in a cooling influence on Earth's climate by decreasing the amount of radiation absorbed by the oceans, has been estimated in various investigations as 0.08–6 W m^{-2} [*Lewis and Schwartz*, 2004,

[1]Climate Change Unit, Finnish Meteorological Institute, Helsinki, Finland.
[2]Department of Physics, University of Helsinki, Helsinki, Finland.
[3]Department of Air Quality and Climate, TNO Built Environment and Geosciences, Utrecht, Netherlands.
[4]Seattle Division, NorthWest Research Associates, Inc., Lebanon, New Hampshire, USA.
[5]Naval Research Laboratory, Washington, D. C., USA.
[6]NOAA Earth System Research Laboratory, Boulder, Colorado, USA.
[7]Brookhaven National Laboratory, Upton, New York, USA.
[8]School of Physics and Centre for Climate and Air Pollution Studies, Environmental Change Institute, National University of Ireland, Galway, Galway, Ireland.
[9]Laboratoire des Sciences du Climat et de l'Environnement, Gif-sur-Yvette, France.
[10]Now at Meteorologisk Institutt, Oslo, Norway.

hereinafter LS04, p. 183]. Quantifying light scattering by SSA is thus important for understanding the perturbation by anthropogenic aerosols to Earth's shortwave radiation budget during the industrial period (so-called aerosol direct forcing) [*Charlson et al.*, 1992; *Intergovernmental Panel on Climate Change*, 2007]. This cooling influence is partly offset by absorption of longwave (thermal infrared) radiation [*Reddy et al.*, 2005a; *Satheesh and Moorthy*, 2005]. Production and properties of SSA as CCN are of interest also in proposals to modify climate to offset global warming ("geoengineering") by alteration of the properties of marine clouds [e.g., *Latham*, 1990; *Bower et al.*, 2006].

[5] SSA often dominates the mass concentration of marine aerosol, especially at locations remote from anthropogenic or other continental sources, and SSA is one of the dominant aerosols globally (along with mineral dust) in terms of mass emitted into the atmosphere. Estimates of global annual mass emission of sea salt (calculated as the integral over the size-distributed number production flux times the volume per particle times the mass of sea salt per unit volume of seawater) with current chemical transport models (CTMs) and global climate models (GCMs), using various parameterizations of the sea spray source function (SSSF), range over nearly 2 orders of magnitude, from 0.02 to 1×10^{14} kg yr^{-1} (Figure 1 and Table 1) [*Textor et al.*, 2006]. Much of this variation is due to the different dependences on wind speed and to the upper size limit of the particles included. This wide range emphasizes the necessity of specifying the particle size range and the height or residence time in reporting sea spray emission fluxes. Critical analysis of SSA production leads to the conclusions that there are large uncertainties in SSA fluxes and that SSSF parameterizations must be viewed as little more than order-of-magnitude estimates [*Hoppel et al.*, 2002; LS04, section 5.11].

[6] In the past several years, the contribution of organic species to SSA has been quantitatively examined in laboratory studies and field measurements, and measurements of SSA concentrations and production have been extended to sizes smaller than were previously thought to be important. In this paper we provide an overview of recent measurements and experimental investigations pertinent to SSA and its production, with the purpose of examining this work and placing it in the context of previous understanding. The starting point is the review of SSA production by LS04. Since that time, marine aerosol production has been reviewed by *Massel* [2007] and by *O'Dowd and de Leeuw* [2007]. *Massel* [2007] focused mainly on wave breaking and provided an overview of sea spray aerosol production based primarily on work prior to 2000, complemented with more recent studies by Polish investigators. *O'Dowd and de Leeuw* [2007] reviewed both primary and secondary particle formation in the marine atmosphere. With regard to primary SSA production, these investigators reviewed SSSF formulations presented in the period 2000–2006, results from laboratory studies concerning the sizes of the sea spray drops produced, and the first findings by *O'Dowd et al.* [2004] and *Cavalli et al.* [2004] regarding organic matter in sea spray aerosol. The current review differs from those in

that work published since LS04, including laboratory and field experimental results on sea spray production, on the enrichment in organic matter, and on the measurement and parameterization of whitecap coverage, is critically examined and compared with results summarized by LS04 to identify progress.

[7] Throughout this paper, we follow the common convention of specifying the size of an SSA particle by its equilibrium radius at a relative humidity (RH) of 80%, r_{80}. For sea salt particles originating from seawater with typical salinity (34–36), r_{80} is about one-half the radius at formation. For such particles, to good accuracy $r_{80} = 2r_{dry}$, where r_{dry} is the volume-equivalent dry radius. A simple approximation for the RH dependence of the equilibrium radius ratio of an SSA particle in the liquid phase r/r_{80} is

$$\frac{r}{r_{80}} = 0.54\left(1.0 + \frac{1}{1-h}\right)^{1/3}, \qquad (1)$$

where h is the fractional relative humidity ($h \equiv RH/100$) [LS04, p. 54]. This equation applies in situations for which the effect of surface tension can be neglected (i.e., particles sufficiently large and RH sufficiently low); for other situations a more detailed treatment is required [*Lewis*, 2008].

[8] SSA particles are considered in three distinct size ranges based on their behavior in the atmosphere and considerations of the processes that affect this behavior [e.g., LS04, p. 11]: $r_{80} \lesssim 1$ μm for small SSA particles, 1 μm $\lesssim r_{80} \lesssim 25$ μm for medium SSA particles, and 25 μm $\lesssim r_{80}$ for large SSA particles. This review is restricted to particles with $r_{80} \lesssim 25$ μm. Special attention is paid to new information on composition, concentration, and production of SSA particles with $r_{80} < 0.1$ μm.

[9] Many measurements indicate that the relative concentrations of the major solutes in sea spray particles are similar to their relative concentrations in bulk seawater, although this may not be the situation for some substances as a consequence of the formation process or of exchange with the atmosphere subsequent to formation. SSA particles are said to be enriched in such substances, and the enrichment factor, defined as the ratio of the concentration of a substance to the concentration of one of the major constituents of bulk seawater (typically sodium) in the particle to the same ratio for bulk seawater, may be less than or greater than unity.

[10] In biologically productive seawater, accumulation of organic substances at the sea surface can result in formation of sea spray particles that are considerably enriched in these substances, especially for particles with $r_{80} < 1$ μm [*Blanchard*, 1964; *Middlebrook et al.*, 1998; *O'Dowd et al.*, 2004]. As far back as 1948, *Woodcock* [1948] showed that drops produced by bubbles bursting in areas with high concentrations of plankton (dinoflagellates) in red tide could carry irritants across the air-sea interface into the atmosphere. *Blanchard* [1963] documented enrichment of organic matter in sea spray and discussed the sea-to-air transport of surface-active material [*Blanchard*, 1964]. *Blanchard and Syzdek* [1970] further confirmed that bacteria are concen-
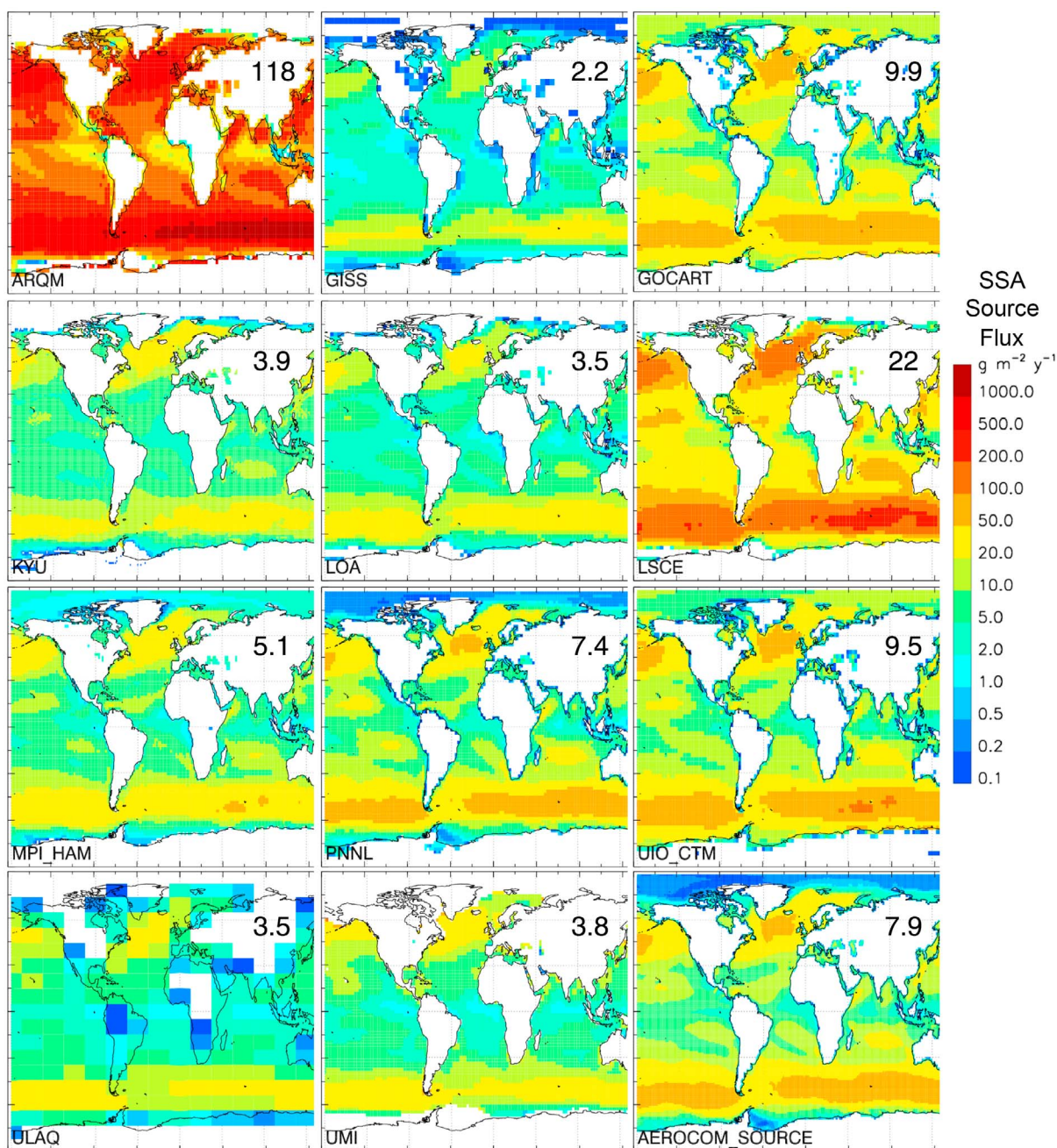
Figure 1. Annual average dry SSA mass production flux as computed by several chemical transport and general circulation models participating in the AeroCom aerosol model intercomparison [*Textor et al.*, 2006]. A global mean production flux of 10 g m^{-2} yr^{-1} over the world ocean corresponds to a total global production rate of approximately 3.5×10^{12} kg yr^{-1}. For identification of the models, production methods employed, and references see Table 1. Number given in top right denotes global annual SSA production in 10^{12} kg yr^{-1}.

trated at the sea surface, leading to enrichment of bacteria in SSA particles. Later, factors influencing the organic content of marine aerosols were investigated in laboratory studies by *Hoffman and Duce* [1976]. More recently, the use of instruments such as aerosol mass spectrometers has demonstrated and quantified the presence of organic species in individual particles. For instance, *Middlebrook et al.* [1998] reported that more than half of all marine particles with dry diameters greater than 0.16 μm at Cape Grim, Tasmania,

contained organics during clean marine conditions and that the organics were nearly always found internally mixed with sea salt. *Novakov et al.* [1997], based on measurements in a region minimally affected by continental emissions, reported that the contribution of organic substances to the aerosol mass from particles with dry aerodynamic diameter less than 0.6 μm was greater than that of sulfate, nitrate, or chloride (which would be indicative of sea salt) and suggested a marine source for these particles. *Putaud et al.* [2000]

TABLE 1. Sea Salt Production Methods for Model Calculations in Figure 1[a]

Model	Sea Salt Module	Winds	SSA Production Method	Reference for SSA Production Method	Global Dry SSA Mass Production (10^{12} kg yr^{-1})	Maximum r_{80} of Emitted Particles (μm)
ARQM	*Gong et al.* [2003]	model derived	interactive	*Gong et al.* [2003]	118	41
GISS	*Koch et al.* [2006]	model derived	interactive	*Monahan et al.* [1986]	2.2	8.6
GOCART	*Chin et al.* [2002]	GEOS DAS	interactive	*Monahan et al.* [1986]; *Gong et al.* [2003]	9.9	10
KYU (Sprintars)	*Takemura et al.* [2002]	model derived	interactive	*Erickson et al.* [1986]; *Takemura et al.* [2000]	3.9	10
LOA	*Reddy and Boucher* [2004]; *Reddy et al.* [2005a, 2005b]	model derived	interactive	*Monahan et al.* [1986]	3.5	20
LSCE	*Schulz et al.* [2004]	ECMWF	interactive	*Schulz et al.* [2004] fit to *Monahan et al.* [1986]; *Smith and Harrison* [1998]	21.9	15[b]
MPI_HAM	*Stier et al.* [2005]	model derived	interactive	*Schulz et al.* [2004] fit to *Monahan et al.* [1986]; *Smith and Harrison* [1998]	5.1	8[b]
PNNL	*Easter et al.* [2004]	model derived	interactive	*Gong et al.* [2002]	7.4	15[b]
UIO-CTM	*Myhre et al.* [2003]	ECMWF	interactive	*Grini et al.* [2002]	9.5	50
ULAQ	*Pitari et al.* [2002]	ECMWF	precalculated monthly	*Gong et al.* [1997]	3.5	20.5
UMI	*Liu and Penner* [2002]	ECMWF	precalculated monthly	*Gong et al.* [1997]	3.8	10
Aerocom source[c]	*Dentener et al.* [2006]	ECMWF	precalculated daily	*Gong et al.* [2003]	7.9	10

[a]Adapted from *Textor et al.* [2006]. GEOS DAS, Goddard Earth Observing System Model Data Assimilation System; ECMWF, European Centre for Medium-Range Weather Forecasts.
[b]Estimated radius below which 95% of sea salt mass is emitted, using respective geometric mean diameter and lognormal width.
[c]The "Aerocom source" refers to a source function employed in joint Aerocom B experiments that compared the consequences of differences in representation of processes comprising the life cycles of aerosol species in the atmosphere by removing diversity in the different models caused by differing emissions [*Dentener et al.*, 2006].

reported that organics contributed roughly 20% to the mass of aerosol particles with r_{80} less than ~1.3 μm in the marine boundary layer, less than non-sea salt sulfate but about the same as sea salt.

[11] The aerosol consisting of sea spray particles in the atmosphere has traditionally been termed "sea salt aerosol," but in this review it is denoted "sea spray aerosol" in recognition of the fact that the composition of the particles may differ from that of bulk seawater. One consequence of this difference is that the hygroscopic and cloud droplet activation properties of sea spray particles may differ from those calculated under the assumption that the particles are composed only of sea salt.

2. PRODUCTION OF SEA SPRAY AEROSOL AND FLUX FORMULATION

[12] SSA particles are formed at the sea surface mainly by breaking waves via bubble bursting and by tearing of wave crests. When a wave breaks, air is entrained into the water and dispersed into a cloud of bubbles [*Thorpe*, 1992], which rise to the surface and burst. The resulting white area of the sea surface is often denoted a "whitecap" on account of enhanced, wavelength-independent scattering of visible radiation by the interfaces between water and bubbles, and the fraction of the sea surface covered by white area is defined as the whitecap fraction, W. When an individual bubble bursts, the bubble cap (or film) may disintegrate into so-called film drops, which are ejected at a wide distribution of angles relative to the vertical. Up to a thousand such film drops may be produced per bubble, with the number and

size distribution (and whether or not film drops are produced) depending largely on bubble size [LS04]. These film drops have radii at formation ranging from smaller than 10 nm to several hundreds of micrometers, but most are less than 1 μm [e.g., *Blanchard*, 1963, 1983; *Day*, 1964]. Individual bubbles with radius less than ~1 mm typically do not form film drops [LS04, p. 208]. The majority of SSA particles in the atmosphere with $r_{80} < 1$ μm are probably film drops.

[13] After the bubble cap has burst, a vertical cylindrical jet forms in the middle of the cavity left by the bubble. This jet may break up into as many as 10 jet drops, with the number depending largely on bubble size, that are ejected vertically to heights of up to ~20 cm above the surface [e.g., *Blanchard*, 1963, 1983; *Spiel*, 1995]. The initial radii of these drops are roughly 10% of the radius of the parent bubble and thus range from slightly less than 1 μm to more than 100 μm. Individual bubbles of radius greater than 2 mm typically do not form jet drops [LS04]. The majority of SSA particles in the atmosphere with r_{80} between 1 and 25 μm are probably jet drops.

[14] SSA particles of the sizes considered in this review are formed mainly from bursting bubbles. Another production mechanism is the formation of spume drops by tearing of wave crests by the wind when the wind speed near the sea surface exceeds about 10 m s^{-1} [*Monahan et al.*, 1983]. These drops, which are transported nearly horizontally by the wind, are typically quite large, with radii from several tens of micrometers to several millimeters, and consequently fall back to the sea surface within seconds to minutes [*Andreas*, 1992]. Spume drops are not considered further here.

[15] The SSSF is a numerical representation of the size-dependent production flux of SSA particles. The following form of this function is employed in this review:

$$f(r_{80}) \equiv \frac{dF(r_{80})}{d\log_{10} r_{80}}, \qquad (2)$$

where the quantity $f(r_{80})$ denotes the number of particles in a given infinitesimal range of the common logarithm of r_{80}, $d\log_{10} r_{80}$, introduced into the atmosphere per unit area per unit time and $F(r_{80})$ is the total number flux of particles of size less than r_{80}. (The subscript 10 denoting the base of the logarithm is suppressed in the remainder of this paper.) Implicit in this definition is that this quantity is averaged over areas and times sufficiently large that rapid fluctuations caused by individual breaking waves are smoothed out.

[16] Because SSA particles may be emitted with an initial upward velocity, because the sea surface is vertically disturbed by waves, and because SSA production is enhanced near wave crests, the nature of the air-sea interface and of interfacial production is difficult to characterize. Additionally, some SSA particles fall back to the sea surface before spending any appreciable time in the atmosphere, the fraction of such particles increasing with increasing r_{80}. For all these reasons, the concept of a source of SSA particles that may be said to be introduced into the marine atmosphere must also, implicitly or explicitly, take into account an effective source height, which may be the mean interfacial height or some specified height above it [LS04]. Recognition of the need to specify an effective source height leads to a useful distinction between the interfacial flux (for which the height is zero) and the effective flux at that height. The interfacial flux is defined as the flux of those particles leaving the sea surface, whereas the effective flux is defined as the flux of those particles produced at the sea surface that attain a given height, typically taken as 10 m above mean sea level (the value used throughout this review), and thus remain in the atmosphere sufficiently long to participate in processes such as cloud formation and atmospheric chemistry.

[17] For many applications such as large-scale models that describe the atmosphere in terms of multiple vertical layers and consider introduction of particles only into the lowest level, it is only this effective flux that is important. For small SSA particles (i.e., those with $r_{80} \lesssim 1$ μm), the effective flux can, for all practical purposes, be considered to be the same as the interfacial flux. For medium SSA particles (those with 1 μm $\lesssim r_{80} \lesssim 25$ μm), the effective flux becomes increasingly less than the interfacial flux with increasing r_{80}. For large SSA particles, which have short atmospheric residence times and typically do not attain heights more than a few meters above the sea surface, the effective flux is essentially zero.

[18] An expression for the SSSF required as input to models would represent the size-dependent production flux expressed by equation (2) as a function of the controlling ambient variables a, b, …; i.e., $f(r_{80}; a, b,…)$. Identifying these variables and developing specific parameterizations for equation (2) rest on recognizing and understanding the controlling processes. Wind speed plays a dual role in influencing the effective production flux of SSA: first, by being the dominant factor controlling wave generation (and subsequent breaking) and second, through upward turbulent transport of newly formed particles. The near-surface wind speed, commonly measured and expressed at a reference height of 10 m, U_{10}, is thought to be the dominant factor affecting sea spray production. However, different formulations of the size-dependent SSSF in terms of only U_{10} vary widely for the same U_{10}. Considerable effort has been devoted to linking SSA production to more fundamentally relevant physical parameters such as wind stress on the surface, τ (or the friction velocity, u_*, defined by $u_* \equiv (\tau/\rho_{air})^{1/2}$, where ρ_{air} is the density of air), or whitecap fraction, W, with the expectation that such approaches might lead to a tighter relation between production flux and one of these other variables than is currently the situation with wind speed. For example, at a given U_{10}, τ can vary by a factor of 2 [Drennan et al., 2005] and W by a factor of 10 or more [LS04; Anguelova and Webster, 2006]; this variation is likely due to variability in the wavefield, surface properties, and the like. However, such efforts have not resulted in substantial narrowing of the spread in the SSSF as a function of controlling variables. Other factors that are expected to affect the SSA production flux are those affecting sea state such as fetch (the upwind distance over the water of nearly constant wind velocity) and atmospheric stability (often parameterized by the air-sea temperature difference), which also affects vertical transport; seawater temperature and salinity; and the presence, amount, and nature of surface-active substances.

[19] A simplifying assumption that is sometimes made in parameterizing the SSSF is that the dependences on drop size and controlling variables can be separated into a dimensionless function $\varphi(a, b, …)$ that contains all of the dependences of the SSA production flux on environmental forcing parameters a, b,.., including wind speed, and a universal shape function $g(r_{80})$

$$\frac{dF(r_{80}, a, b, \ldots)}{d\log r_{80}} = \varphi(a, b, \ldots)g(r_{80}). \qquad (3)$$

However, this assumption has relatively little observational support, and there are several reasons why it would not be expected to hold; for instance, under higher winds more larger particles could be transported upward and thus contribute to, and change the size distribution of, the effective production flux.

3. METHODS OF DETERMINING SSA PRODUCTION FLUXES

[20] Methods that can be used to infer the size-dependent production flux of SSA particles (Table 2) were discussed in detail by LS04. Methods relevant to this review are the steady state dry deposition method, the statistical wet deposition method, micrometeorological methods, and the whitecap method. These methods are briefly reviewed, and for each the following topics are discussed: the basic

TABLE 2. Methods Used to Determine SSA Production Flux

Method	Flux[a]	r_{80} Range[b] (μm)	Comments
Steady state dry deposition	Eff	3–25	Easy to apply
Concentration buildup	Eff	≲10	Has been applied only once; holds promise
Statistical wet deposition	Eff	≲1	Simple, provides constraint on production flux
Micrometeorological	Eff	≲10	Several such methods
Whitecap	Int	≲10	Several approaches; typically measures production flux from laboratory-generated whitecaps
Bubble	Int	≲100	Requires knowledge of several quantities
Along-wind flux	Int	≳50	Laboratory measurements; often incorrectly applied
Direct observation	Int	≳500	Has been applied only in laboratory
Vertical impaction	Int	≳250	Has been applied once in oceanic conditions

[a]Int and Eff refer to interfacial and effective SSA production fluxes, respectively.

[b]Approximate range of r_{80} (μm) to which the method can or has typically been applied.

assumptions inherent in its application, the quantities required and how they are determined, the size range to which the method can be applied and what precludes its application to other sizes, and concerns with its use. Some of the commonly used production flux formulations are also discussed here and presented in Appendix A. New formulations are discussed in section 5.

3.1. General Considerations

[21] The steady state dry deposition method, the statistical wet deposition method, and micrometeorological methods use field measurements of concentrations and/or fluxes, as do some applications of the whitecap method; thus, these methods infer the effective production flux. Most applications of the whitecap method use SSA size distribution measurements from laboratory-generated whitecaps, which allow inference of the interfacial production flux.

[22] Methods that rely on field measurements of SSA concentrations involve counting and sizing SSA particles in the atmosphere. However, even such measurements, although seemingly straightforward, encounter practical difficulties as a consequence of the low number concentrations of SSA particles, with values for SSA particles with $r_{80} > 1$ μm typically reported as less than several per cubic centimeter and for all SSA particles typically reported as at most a few tens per cubic centimeter [LS04, section 4]. Such low concentrations, the consequences of which become even more pronounced when size-segregated measurements are made, can result in poor counting statistics and require long sampling times to achieve adequate signal-to-noise ratios.

[23] Another difficulty arises from the presence in the marine atmosphere of particles other than SSA particles, because in some size ranges and locations SSA particles are not the most numerous. Typical concentrations of all aerosol particles in clean marine conditions are several hundred per cubic centimeter. Thus, techniques are required to distinguish SSA particles from particles composed of other substances. This concern becomes increasingly important with decreasing particle size, as SSA particles with radii less than several tenths of a micrometer may constitute only a small fraction of all aerosol particles in this size range [e.g., LS04, Figure 16]. This concern pertains especially to coastal regions or other areas where continental aerosols may be present in high abundances. Additionally, enrichment of SSA particles either during formation at the sea surface or due to atmospheric uptake and exchange may make it difficult to determine whether or not an aerosol particle is an SSA particle based on composition or on other properties such as hygroscopicity or thermal volatility.

[24] Field measurements of SSA particle concentrations or fluxes are often made at coastal regions because of cost, accessibility, ability to install permanent equipment, and other factors. Such measurements offer the possibility of long-term data sets that encompass a wider variety of conditions than may be feasible from an individual cruise. However, concerns with measurements from these locations are coastal influences such as surf-produced SSA and differences in flow properties and upward transport, in addition to the greater possibility of influences of continental aerosol. Typically data are screened so that they are used only when airflow is from ocean to land.

[25] Each of the methods that use field measurements requires certain conditions for its successful application. One such condition is often referred to as "steady state," but this phrase has been used to mean different things in different applications, and this ambiguity can and has led to confusion. In some instances this phrase refers to conditions in which there is no mean vertical flux of SSA particles, whereas in other instances it refers to conditions in which mean quantities affecting the SSA flux such as wind speed are unchanged over times of interest (e.g., the sampling time required to obtain a statistically representative sample) although there may still be a net upward flux of SSA particles. Whether the required conditions are satisfied is rarely discussed in presentations of SSA flux determinations, but spurious results can occur through failure to take into account other factors that affect measurements. Key among these are time-dependent meteorological conditions, which confound flux measurements, and entrainment of free tropospheric air into the marine boundary layer, which causes a growth in height of this layer and a decrease in particle number concentration through dilution.

3.2. Steady State Dry Deposition Method

[26] The steady state dry deposition method infers the size-dependent effective production flux of SSA particles by assuming that production of SSA particles with r_{80} in the

size range of interest at a given time and location is balanced by removal at the same time and location through dry deposition, such that the net upward flux of particles of any given r_{80} in that size range is zero. The effective production flux is thus equal to the dry deposition flux, which in turn is equal to the product of the size-dependent number concentration, $dN/d\log r_{80}$, and the dry deposition velocity, v_{dd}, also a function of r_{80}

$$\frac{dF_{eff}}{d\log r_{80}} = \frac{dN}{d\log r_{80}} \times v_{dd}(r_{80}). \qquad (4)$$

The size-dependent SSA number concentration, which is determined by measurements at a given reference height, typically near 10 m, is often parameterized only in terms of wind speed at 10 m, U_{10}. The size-dependent dry deposition velocity is modeled, also usually as a function only of U_{10}. Nearly all such parameterizations are based ultimately on *Slinn and Slinn* [1980], whose treatment accounts for gravitational sedimentation, turbulent transport, impaction to the sea surface, Brownian diffusion, and growth of particles near the sea surface due to the higher RH there, although for a given size range only some of these processes are important.

[27] The assumption of local balance requires steady state conditions with respect to dry deposition during the lifetimes of SSA particles in the atmosphere and thus that the meteorological conditions (i.e., wind speed and other pertinent parameters) under which the particles were produced are the same as those under which they are measured. It further requires that dry deposition be the dominant removal mechanism of SSA particles (i.e., that little or no rainfall has occurred during the lifetimes of these particles in the atmosphere), that there has been negligible decrease in concentration by entrainment and mixing of free tropospheric air, and that the mean size-dependent SSA concentration is independent of time. These assumptions restrict the mean atmospheric residence times of SSA particles for which this method can be accurately applied to a few days at most, corresponding to an approximate size range of 3 μm < r_{80} < 25 μm.

[28] There are several concerns with this method in addition to those listed in section 3.1. The large range of values of SSA concentrations reported for nominally the same wind speed, an order of magnitude or more [LS04], results in a correspondingly large range of values for the inferred production flux. Uncertainties in modeled dry deposition velocities can likewise lead to uncertainties in the inferred production flux, and systematic errors can occur if the required conditions for successful application of this method are not satisfied.

[29] This approach, which is appealing because it is seemingly easy to apply, has been used by several investigators (10 formulations based on this method are compared by LS04). One widely used formulation (Appendix A) is that of *Smith et al.* [1993], who measured size-dependent aerosol concentrations with optical particle counters (OPCs) for more than 700 h from a 10 m tower on an island off the west

coast of Scotland. They used measurements only from maritime air masses and assumed that the majority of particles measured were SSA particles. Their formulation consists of two lognormal size distributions with coefficients that exhibit different dependences on U_{10}; such a formulation is, of course, inconsistent with the separability assumption (equation (3)).

[30] The steady state dry deposition method together with numerous measurements of sea salt aerosol concentration taken from the literature was used by LS04 to determine a formulation (Appendix A) for the effective production flux over the r_{80} range 3–25 μm as a power law in r_{80} with exponent −2.5, with the amplitude varying directly as U_{10} to the 2.5 power. This formulation is characterized by an associated uncertainty of a multiplicative factor of 4 above and below the central value resulting from the variability in size-dependent number concentrations in a given range of wind speeds and from estimated uncertainties in the modeled dry deposition velocity.

3.3. Statistical Wet Deposition Method

[31] The statistical wet deposition method infers the effective SSA production flux necessary to account for measured number concentrations under the assumptions that SSA particles in the size range of interest are removed from the atmosphere only by wet deposition (coagulation being negligible for SSA particles primarily because of their low concentrations) and that precipitation, when it occurs, removes nearly all SSA particles in this size range. These assumptions restrict application of this method to SSA particles with $r_{80} \lesssim 1$ μm and imply that for this size range the size dependence of the number concentration of SSA particles is the same as that of their production.

[32] This method is essentially a budget argument that provides a consistency check, ensuring that unrealistically high production fluxes are not calculated. On average, the total number of SSA particles in a given size range produced since the last precipitation event, per unit area of sea surface, is equal to the column burden (i.e., integral over height) of the concentration of such particles. Because SSA particles in this size range are expected to be nearly uniformly mixed over the height of the marine boundary layer H_{mbl} and because concentrations of SSA particles are quite low above the marine boundary layer relative to concentrations within this layer, this column burden can be approximated by the product of the number concentration at an arbitrary measurement height (typically near 10 m) and H_{mbl}. Consequently, the production flux required to produce the measured concentration is equal to that column burden divided by the time between rainfall events, τ_{wet}

$$\frac{dF_{eff}}{d\log r_{80}} = \frac{dN}{d\log r_{80}} \times \frac{H_{mbl}}{\tau_{wet}}. \qquad (5)$$

This method was applied by LS04 (Appendix A) with the parameters τ_{wet} = 3 days, H_{mbl} = 0.5 km, and the value $dN/d\log r_{80}$ = 5 cm^{-3} (based on numerous measurements reported in the literature at typical wind speeds) to yield an

estimate of $dF/d\log r_{80} \approx 10^4$ m^{-2} s^{-1}, nearly independent of r_{80}, over the range 0.1 μm $\lesssim r_{80} \lesssim 1$ μm, with an associated uncertainty of a factor of 5 above and below the central value based on uncertainties in the above quantities.

3.4. Micrometeorological Methods

[33] Micrometeorological methods infer the effective SSA production flux from measurements of fluctuations or gradients of concentration in the lowest portion of the marine boundary layer (typically within several tens of meters from the sea surface). Techniques such as eddy correlation, eddy accumulation, relaxed eddy accumulation, and gradient methods are commonly used to determine net vertical turbulent fluxes of other quantities such as heat, momentum, or gases. Both eddy correlation and gradient methods have been used to determine fluxes of SSA particles. These methods assume that the production of SSA particles is not in steady state with respect to removal of these particles through dry deposition, although steady state conditions in the sense of time invariance of mean quantities over the duration of the measurement are assumed.

3.4.1. Eddy Correlation Method

[34] Eddy correlation [e.g., *Businger*, 1986; *Kaimal and Finnigan*, 1994] determines the net vertical flux, $F\chi$, of a quantity, χ, such as the number concentration of SSA particles in a given size range by decomposing the vertical wind speed, w, into a mean component, $\overline{w}$, and a fluctuating component, w', as $w = \overline{w} + w'$, and similarly for χ, where the overbar denotes an average over a time sufficiently long that meaningful statistics are obtained but sufficiently short that environmental conditions do not appreciably change. Because $\overline{w}$ is zero, the net vertical flux is $F_\chi = \overline{w'\chi'}$.

[35] In contrast to the situation for heat, momentum, and gases for which the measured fluxes are due to turbulent transport alone, for SSA particles, dry deposition and gravitational settling, which act as downward fluxes, must be taken into account in determining production fluxes [LS04, p. 81]

$$\frac{dF_{\text{eff}}}{d\log r_{80}} = \overline{w'\left(\frac{dN}{d\log r_{80}}\right)'} + \overline{\left(\frac{dN}{d\log r_{80}}\right)} \times \left[v_{\text{dd}}(r_{80}) - v_{\text{grav}}(r_{80})\right].$$
(6)

Hence the effective production flux of SSA particles exceeds the net flux measured by eddy correlation (the first term on the right-hand side of equation (6)) by the difference between the dry deposition flux, which is calculated from the mean SSA particle number concentration and the dry deposition velocity, and the gravitational flux. As gravitational settling does not contribute to the measured eddy correlation flux, the dry deposition velocity, which includes gravitational settling, must itself be diminished by the gravitational settling velocity. Either of the terms on the right-hand side of equation (6) can be confounded by the presence of other types of aerosol particles.

3.4.2. Gradient Method

[36] Another micrometeorological method is the gradient method, by which the effective production flux of particles

sufficiently small that the effect of gravity is negligible compared to upward turbulent diffusion (i.e., r_{80} smaller than a few micrometers) can be determined from measurements of the dependence of the concentration on height. This approach was proposed by *Petelski* [2003] as an extension of Monin-Obukhov similarity theory, which is commonly used to relate fluxes of quantities such as momentum and heat to the vertical gradients of wind speed and temperature, respectively. *Petelski and Piskozub* [2006, 2007] and *Andreas* [2007] have argued that in steady state conditions (which in this sense refers to mean quantities being independent of time) and neutral atmospheric stability the height dependence of the number concentration can be written as

$$\frac{dN}{d\log r_{80}}(z) = \left(\frac{-1}{\kappa u_*}\right)\left(\frac{dF}{d\log r_{80}}\right)\ln\left(\frac{z}{z_{\text{ref}}}\right) + \frac{dN}{d\log r_{80}}(z_{\text{ref}}),$$
(7)

where u_* is the friction velocity, κ is the von Karman constant (approximately 0.40), and z_{ref} is an arbitrary reference height. Thus, the production flux of SSA particles of a given size could, in principle, be determined from the difference in number concentrations at two heights or from the slope of the number concentration plotted against the logarithm of the height. Because of the small change in the number concentration over heights at which measurements are typically made, accurate determination of this difference, or slope, imposes high-accuracy and -precision requirements on the concentration measurements. For particles with $r_{80} < 1$ μm, concentration differences are extremely difficult to measure; for larger particles, the concentrations are so small that accurate measurements require very long sampling times. Determination of SSA production fluxes by this approach is discussed in section 4.2.2.

3.4.3. Discussion of Micrometeorological Methods

[37] Successful application of micrometeorological methods requires that the downward flux of SSA particles due to dry deposition, if not negligible, be taken into account. However, because there is typically no discrimination with regard to particle composition, dry deposition of other aerosol particles can lead to spurious results if not accurately taken into account. This effect also reduces the signal-to-noise ratio because uncertainties of modeled dry deposition fluxes of small particles may be greater than the measured upward fluxes themselves. Use of micrometeorological methods implicitly assumes that the ocean surface is a uniform source of particles, but fluctuations caused by the discrete nature of breaking waves would interfere with measurements or at least require long times for averaging. Implementation of these methods also involves several practical difficulties. Gradients and fluctuations in RH must be accurately taken into account, and measurements from a ship at sea, for example, must take into account perturbation of the turbulent characteristics of the flow by the ship or sampling devices and the motion of the ship.

[38] There are several concerns with micrometeorological methods. Because of the relatively low concentrations of

SSA particles in the atmosphere, accurate results require long sampling times, which may be beyond practical limits or extend through meteorological conditions that are changing. The consequences of these low concentrations are more pronounced for micrometeorological methods than for other methods because micrometeorological methods determine the SSA production flux from small differences of much larger quantities; uncertainties can thus result in much greater fractional uncertainty for the estimated flux.

[39] The SSA production flux determined by eddy correlation measurements is based on turbulent deviations of the concentrations from the mean values for a sampling rate on the order of a few tenths of a second. These concentration fluctuations inherently have large uncertainties which are enhanced when concentrations are small. In effect, this approach also determines the production flux as a difference of two much larger values, as the dominant contribution to this flux is provided by the sum of the positive values of $w'(dN/d\log r_{80})'$ minus the sum of the negative values of this quantity. The concern of long sampling times required for accurate results is sometimes addressed by determining total number fluxes at the cost of size resolution. These long sampling times, which become more pronounced with increasing particle size due to the associated decreasing concentrations, provide a practical limit on the size to which these methods can be applied to values of r_{80} less than several micrometers.

[40] Eddy correlation has been used to infer SSA fluxes in only a few studies. *Nilsson and Rannik* [2001] and *Nilsson et al.* [2001] made 175 h of measurements of all particles with dry mobility diameter (roughly equal to r_{80}) greater than 0.01 μm from a ship in the Arctic at wind speeds (at 35 m above sea level) from 4 to 13 m s^{-1}. Measured number concentrations of particles of these sizes were reported as 100–200 cm^{-3}. Using modeled dry deposition fluxes, the investigators converted the measured net total (as opposed to size-dependent) flux to a total effective production flux, which they fitted to an exponential dependence on wind speed (Appendix A). There are concerns as to the confidence that can be placed in their formulation because of the large magnitude of the modeled dry deposition flux (which sometimes exceeded the net upward flux), the lack of any significant correlation between wind speed and sea salt mass for dry mobility particle diameter $d_p < 0.16$ μm, discrepancies in the relations between wind speed and concentrations of total aerosol number and those of sea salt mass for larger and for smaller particles, and ambiguity about what types of particles contributed to the upward fluxes. Recognizing these concerns, *Nilsson et al.* [2001] stated that "a more careful examination of all data is needed before we can make any conclusion about the source and characteristics of the upward aerosol number flux." An additional concern with the expression presented by *Nilsson et al.* [2001] is that it yields an unrealistically high production flux; for $U_{10} = 10$ m s^{-1}, this expression would result in a rate of increase in the number concentration of aerosol particles (assumed to be uniformly distributed over a marine boundary layer height of 0.5 km) of approximately

320 cm^{-3} d^{-1}. Such a rate would be inconsistent with measured concentrations and a typical residence time against precipitation of ~3 days [LS04, p. 72].

3.5. Whitecap Method

[41] The whitecap method infers the SSA production flux from measurements of size-dependent SSA production from laboratory simulations or from the surf zone, as a proxy for oceanic whitecaps, by scaling the production flux per white area, $dF_{wc}/d\log r_{80}$, to the ocean using the oceanic whitecap fraction, W. The oceanic production flux is thus given by

$$\frac{dF}{d\log r_{80}} = W \times \frac{dF_{wc}}{d\log r_{80}}. \tag{8}$$

The fundamental assumption of this method is that the number of SSA particles of any given size produced per unit time and area is the same for any white area, either in the laboratory, the surf zone, or over the ocean, independent of the means by which this white area was produced, provided the whiteness exceeds some threshold.

3.5.1. Determination of the Oceanic Whitecap Fraction

[42] The oceanic whitecap fraction has been determined from photographs or video recordings of the sea surface from ships, towers, or aircraft, with aircraft measurements typically yielding values of W that are up to an order of magnitude greater than those from shipboard photographs [LS04]. In the past, video determinations of W have typically resulted in values roughly an order of magnitude less than those determined by photographs, although technological improvements in video and use of digital video may have changed this situation (an intercomparison of whitecap determination from film, video, and digital images would provide much needed information on this subject). However, for both photos and videos, regardless of the medium (i.e., film, analog magnetic tape, or digital), the decision on what is "white" must be made arbitrarily, introducing unavoidable subjectivity in determining W and thus in the production flux. Moreover, nothing in the choice of this threshold ensures that the resulting values of W are the pertinent ones for determining SSA production and, in fact, what is "suitable" cannot be determined from image analysis.

[43] Observations from space-based sensors offer the prospect of routinely determining W on regional and global scales and of determining parameterizations by use of local (in situ) or remote-sensing measurements of controlling variables such as wind speed and air and sea temperatures. Such observations would permit characterizing the whitecap fraction, its temporal and spatial variability, and its dependence on controlling variables, with the expectation of leading eventually to improved models of W and with this of SSSF via equation (8).

[44] The whitecap fraction can be detected with satellite-based instruments because of the distinct remote-sensing signature of whitecaps in several regions of the electromagnetic spectrum [*Koepke*, 1986]. In the visible region, the whitecap fraction can be quantified photographically on the basis of enhanced reflectivity of solar radiation by whitecaps

[*Whitlock et al.*, 1982; *Frouin et al.*, 1996; *Kokhanovsky*, 2004]. In the infrared (IR), both reflectivity and emissivity contribute to the signal from the whitecaps [*Jessup et al.*, 1997; *Marmorino and Smith*, 2005]. In the microwave region, for which measurements yield the surface brightness temperature T_B, whitecaps are highly emissive compared to adjacent nonwhite areas [*Nordberg et al.*, 1971; *Rose et al.*, 2002; *Aziz et al.*, 2005; *Padmanabhan et al.*, 2006].

[45] Different regions of the electromagnetic spectrum exhibit different advantages and challenges for remote sensing of the whitecap fraction. Measurements in the visible region have the advantage of the direct relation of the signal to the white area commonly characterized in laboratory experiments, but correction for extinction and for scattering of light out of and into the optical path through the atmosphere (atmospheric correction) is especially demanding in the visible and IR regions. The advantages of using microwave frequencies, specifically the ability to determine whitecap fraction at night, penetration of microwave radiation through clouds, and minimal difficulty in atmospheric correction, make this approach very attractive. However, difficulties arise in modeling the sea surface emissivity, especially in distinguishing signals emanating from foamy regions (i.e., whitecaps) from those emanating from areas where the sea surface has been roughened by the wind. As noted above, there is no demonstration that the whitecap fraction determined by remote sensing in any region of the electromagnetic spectrum is the most pertinent to SSA production.

[46] The oceanic whitecap fraction, W, has typically been parameterized as a function of only U_{10}. Numerous expressions for $W(U_{10})$ have been proposed, many of which are power laws with an exponent near 3. The expression of *Monahan and Ó Muircheartaigh* [1980, hereinafter MO'M80]

$$W(U_{10}) = 3.84 \times 10^{-6} U_{10}^{3.41}, \tag{9}$$

where U_{10} is in m s^{-1}, is frequently used, despite nearly 30 years of subsequent measurements. These later measurements have demonstrated many uncertainties regarding the dependence of W on U_{10}; as noted in section 2, W can vary by over an order of magnitude for the same U_{10} [LS04; *Anguelova and Webster*, 2006]. W must thus depend also on other atmospheric and/or oceanic properties in addition to U_{10}; attempts to include additional variables in the parameterization of W are examined in section 4.1.1.

3.5.2. Determination of the SSA Particle Flux per White Area

[47] Determinations of the SSA production flux per white area have employed several types of laboratory "whitecaps," both continuous (such as those formed by a falling stream of water or by forcing air through a frit below the water surface) and discrete (such as those formed by simulating a wave-breaking event by colliding two parcels of water). For experiments using the former approach, bubbles and resulting SSA are generated by one of two basic mechanisms: the first being air forced through diffusers, sintered glass filters, or other porous material and the second being plunging water

jets or weirs. Each mechanism produces a continuous whitecap from which the resultant SSA is entrained into an air stream in which the number concentration is measured. Measurements of size-dependent number concentrations, $dN/d\log r_{80}$, can be used to determine the size-dependent SSA production flux per white area, $dF_{wc}/d\log r_{80}$, using the flow rate, Q, of air entraining the resultant SSA and the area of the surface covered by bubbles, A, according to

$$\frac{dF_{wc}}{d\log r_{80}} = \frac{Q}{A} \frac{dN}{d\log r_{80}}. \tag{10}$$

Such an approach requires determination of the "white" area, the criterion for which, as in field measurements, is necessarily somewhat arbitrary.

[48] Estimation of the SSA production flux from measurements involving discrete whitecaps additionally requires knowledge of lifetimes of oceanic whitecaps; these have been determined from photographs or videos of laboratory whitecaps. The SSA production flux per white area has also been estimated from measurements in the surf zone. Specifically, the integral over height of the number concentration of the aerosol resulting from the surf zone is used together with the wind speed and the fraction of the white area in the surf zone to estimate the production flux per white area. For both the surf zone and laboratory approaches, the contribution from background aerosols must be subtracted out, although in many situations this is negligible compared to the much larger signal resulting from active production by the surrogate whitecap.

[49] Interpretation of the type of flux determined by the whitecap method requires some care. The production flux per white area determined from laboratory whitecaps is an interfacial flux, whereas that determined from measurements of aerosol production in the surf zone more closely approximates an effective flux. Additionally, because laboratory experiments are currently incapable of simulating upward entrainment of SSA particles, they are restricted to determining the interfacial production flux. However, such laboratory experiments determine the flux of only bubble-produced drops and not spume drops and thus yield only a fraction of the interfacial production flux. Because nearly all applications of the whitecap method have been restricted to particles with $r_{80} \lesssim 10$ μm, over which range the interfacial and effective production fluxes are nearly the same, no further distinction is made regarding the type of flux determined by investigations involving the whitecap method, and it is assumed that such fluxes can be compared with those inferred by other methods discussed here.

[50] Laboratory investigations allow for controlled experiments on the effects of parameters such as salinity, water temperature, and surface-active substances on the magnitude and size distribution of the production flux. However, interpretation of laboratory experiments requires assumptions regarding the applicability of laboratory conditions to conditions representative of breaking waves in the open ocean. Laboratory breaking waves and whitecaps have different characteristics from those over the ocean and vastly

different sizes. Few laboratory experiments have employed more than a single method for producing whitecaps or determined whether scaling holds over a range of sizes of these whitecaps; such work might enhance confidence in extrapolating results from laboratory whitecaps to SSA production by oceanic whitecaps.

[51] A concern with investigations involving bubbles produced by frits is the accuracy with which the size-dependent SSA production flux (including its salinity and temperature dependences) characteristic of breaking waves in the open ocean is modeled by the laboratory study because the bubble formation process at the frit is an entirely different physical process than that by which bubbles are produced in the ocean. Additionally, because bubbles produced by frits are typically smaller than those thought capable of producing film drops and the particles produced are smaller than those reported for jet drops, the question arises as to the extent to which production fluxes determined from these measurements might be artifacts of the experimental approach.

[52] Similarly, a concern with the surf zone approach is the representativeness of surf zone white area as a model for breaking waves and SSA production in the open ocean. In contrast to the open ocean, wave breaking in the surf zone is strongly influenced by drag against the shallow seafloor, whose depth is comparable to that to which air bubbles are entrained by breaking waves. Interaction with the seafloor almost certainly modifies the wave-breaking process and bubble production. The width of the surf zone, the turbulent dispersion velocity, and the height of the plume of the aerosol produced by the surf zone are influenced by wind speed, and these quantities are also affected by local conditions and topography. These influences further call into question the assumption of constant flux per white area needed to extrapolate results from the surf zone to SSA production in the open ocean.

3.5.3. SSA Production Flux Formulations

[53] The whitecap method of estimating the SSA production flux has seen and continues to see widespread use; 10 formulations based on this method are compared by LS04. One widely used formulation (Appendix A) is that of *Monahan et al.* [1986], who combined results from measurements of SSA production from a discrete laboratory whitecap of initial area 0.35 m^2, the lifetime of other laboratory whitecaps calculated assuming exponential decay, and equation (9) for W; the stated range of validity was $r_{80} = 0.8–8$ μm. Other formulations from the same group differed from this one by as much as an order of magnitude over this size range. A modification of this formulation (Appendix A), which extended the r_{80} range of applicability to 0.07–20 μm, was proposed by *Gong* [2003], who tuned the formulation so that size-dependent SSA number concentrations calculated with a 1-D column model matched those reported by *O'Dowd et al.* [1997] from measurements on a single cruise in the North Atlantic. The limits attributed to this formulation might also be questioned; Gong stated (incorrectly) that the *Monahan et al.* [1986] formulation applied for r_{80} up to 20 μm (instead of 8 μm) and that their new formulation

yields "reasonable" size distributions for r_{80} as low as 0.07 μm, despite the fact that the measurements of *O'Dowd et al.* [1997] were limited to $r_{80} > 0.1$ μm.

[54] Another formulation of the SSA production flux based on the whitecap method was presented by *Mårtensson et al.* [2003], who measured the flux of particles produced from a white area of 3×10^{-4} m^2 formed by forcing air through a frit with pore size (presumably diameter) 20–40 μm that was located 4 cm below the water surface. Based on such measurements at four different temperatures and three different salinities (but only a single frit size and flow rate), Mårtensson et al. presented a formulation for the size- and temperature-dependent production flux per white area at salinity 33 (near that of seawater) for dry mobility particle diameter d_p (approximately equal to r_{80}) between 0.02 and 2.8 μm. They combined this result with the MO'M80 formula given above for W (equation (9)) to arrive at a formulation for the oceanic SSA production flux (Appendix A). The temperature dependence of this formulation accounts only for the temperature dependence of SSA production per white area determined in the laboratory and does not account for any possible temperature dependence of the whitecap fraction, although there are indications that such a dependence exists [LS04]. For $U_{10} = 10$ m s^{-1}, this formulation yields a rate of increase in the SSA number concentration (assumed to be uniformly distributed over a marine boundary layer height of 0.5 km) of near 170 cm^{-3} d^{-1} at 25°C and near 270 cm^{-3} d^{-1} at 5°C, resulting in atmospheric number concentrations much greater than those typically measured.

[55] The surf zone approach was used by *de Leeuw et al.* [2000], who reported concentration measurements at piers at two locations on the coast of California and presented a formulation for the SSA production flux per white area (Appendix A) over the r_{80} range ~0.4–~5 μm on the assumption that the entire surf zone acted like a whitecap (i.e., the whitecap fraction in the surf zone was unity); note that as originally presented, this formulation was missing a factor of 10^6 [LS04, p. 222]. The integral of the number concentration over the height of the plume was based on concentration measurements at two heights (7 and 15 m in La Jolla and 5 and 12 m in Moss Landing) under the assumption of an exponential decrease with height. According to this formulation, the production flux per white area depends exponentially on wind speed, with nearly an order of magnitude difference between the flux at the lowest wind speeds ($U_{10} = 0$–2 m s^{-1}) and the highest (9 m s^{-1}). This dependence likely reflects transport phenomena and possibly higher swell, resulting in more vigorous wave breaking with increasing wind speed, but such a dependence calls into question the extent to which this approach simulates production in the open ocean and additionally violates the assumption of constant production flux per white area.

3.6. Summary

[56] Intrinsic to any formulation for the SSA production flux, either effective or interfacial, is an associated uncertainty. In view of the large spread of determinations of

production flux for a given set of environmental conditions, LS04 characterized this uncertainty as a multiplicative quantity, denoted by $\overset{\times}{\div}$, equivalent to an additive uncertainty of $\pm$ associated with the logarithm of the production flux, and thus in a plot of the logarithm of the production flux versus r_{80} such a measure of uncertainty corresponds to equal distances above and below the best estimate production flux. They intended this quantity to provide an estimate of the range about the central value within which the actual production flux might be expected to lie such that it would be difficult to restrict the range to much less than this factor. Presenting the uncertainty associated with a given formulation provides a criterion for whether or not two different formulations can be said to "agree" and allows a means for determining the precision to which a formulation should be presented. Additionally, such an uncertainty provides context for deciding whether features in the size distribution might be considered to be characteristic of actual production fluxes rather than statistical fluctuations. This uncertainty is essential also as input to subsequent use of a formulation, for example, in assessing the relative enhancement of CCN number concentration pertinent to the enhancement of cloud albedo by anthropogenic aerosols.

[57] Some 40 SSA production flux formulations were presented and compared by LS04. Based on their analysis of these formulations and numerous other data sets, LS04 proposed a formulation (Appendix A) for the effective SSA production flux for particles with $0.1\ \mu m < r_{80} < 25\ \mu m$ as a lognormal size distribution of the form $dF/d\log r_{80}$ with a single mode and a 2.5 power wind speed dependence for $5\ m\ s^{-1} < U_{10} < 20\ m\ s^{-1}$. Associated with this formulation is a multiplicative uncertainty of a factor of 5 about the central value. Because of the large number of data sets upon which this formulation was based, LS04 expressed the view that a substantial reduction of this uncertainty would require more than close agreement of a few new formulations.

[58] Although it had been conclusively demonstrated that sea spray particles with $r_{80} < 0.1\ \mu m$ are formed by the bursting of individual bubbles [e.g., *Blanchard*, 1963; *Day*, 1964; *Resch and Afeti*, 1992] and from bubble bursting associated with swarms of bubbles [*Cipriano and Blanchard*, 1981; *Cipriano et al.*, 1983, 1987; *Mårtensson et al.*, 2003], extensive measurements from a large number of investigators led LS04 to conclude that sea salt particles with $r_{80} < 0.1\ \mu m$ constitute only a small fraction of the number of aerosol particles present in that size range in the marine atmosphere and only a small fraction of the number of sea spray particles produced. However, recent observations (section 4) suggest that SSA particles with $r_{80} < 0.1\ \mu m$ may occur in appreciable concentrations in the marine atmosphere. If these observations are correct, then one possibility is that the particles detected are *sea spray* particles, that is, particles formed at the sea surface by bursting bubbles consisting mostly of organics or other substances but containing little *sea salt*. A possible explanation for the previous results is that differences in composition would result in differences in hygroscopic and other properties, causing the particles not to have been recognized as SSA particles. This issue remains qualitatively and quantitatively unresolved, and the production and fate of SSA particles in this size range are currently major topics in this field.

4. RECENT EXPERIMENTAL AND OBSERVATIONAL FINDINGS

[59] Experimental and data processing techniques have been further developed in the last several years, and results from laboratory and field experiments have provided new insights pertinent to the SSA production flux. These results relate, in particular, to the whitecap method, micrometeorological methods, and the chemical composition of SSA. Sections 4.1–4.3 discuss each of these aspects.

4.1. Whitecap Method
4.1.1. Photographic Measurements of Whitecap Fraction

[60] Five new data sets of whitecap fraction have been reported, four in coastal regions under fetch-limited conditions [*Lafon et al.*, 2004, 2007; *Sugihara et al.*, 2007; *Callaghan et al.*, 2008a] and one in open ocean (unlimited fetch) conditions [*Callaghan et al.*, 2008b]. Details of these data sets (Table 3) show the ranges of various meteorological and oceanographic variables (in addition to wind speed) that were recorded to investigate possible dependencies on these other quantities and the means by which the images were collected and processed.

[61] Recent developments in image processing of sea state photographs have aimed at decreasing the uncertainty in measured whitecap fraction in two ways, both of which have been facilitated by developments in digital technology. One is removing the subjectivity in determining the intensity threshold that distinguishes whitecaps from the surrounding water. The other is averaging a large number of "instantaneous" W values measured during an observation period to obtain a single W data point.

[62] To determine more objectively the intensity thresholds separating whitecaps from the surrounding water, the change in instantaneous W values when the threshold was varied was examined by *Sugihara et al.* [2007, Figure 5]. An optimum threshold was identified for which a change in threshold of $\pm 6\%$ resulted in a relative change in W of 10–20%; this same threshold was selected and applied to all processed images. An automated whitecap extraction technique was devised by *Callaghan and White* [2009] that involved two major elements: an "image structure," defined as the fraction of pixels with intensities greater than a given threshold, which decreased as the threshold was increased from a predetermined minimum intensity to the maximum intensity of the image, and analysis of the first, second, and third derivatives of this image structure with respect to the threshold intensity. The image structure was used to identify whether an image contains a whitecap, and the derivative analysis was used to determine the intensity threshold for an image containing a whitecap. This procedure yielded a unique threshold applicable to an individual image [*Callaghan et al.*, 2008a].

TABLE 3. Location and Time of Observations and Accompanying Meteorological and Oceanographic Factors (U_{10}, X, T_w, ΔT) for New Measurements of Whitecap Fraction Shown in Figure 2[a]

Reference	Platform	Location	Time Period	U_{10} Range (m s^{-1})	X (km)	T_w (°C)	ΔT (°C)	Additional Parameters[b]	Data Points	Images per Data Point	Averaging Period (min)	Medium	Image Rate (s^{-1})	Geometric Mean of Ratio to MO'M80[c]
Lafon et al. [2004]	ship	Gulf of Lyon, Mediterranean	Mar–Apr 1998	6–17	8–90	13	−2.65 to +6.25	u_*, f_p, H_s	45	10–25	5 to 12.5	film	0.033	0.64
Lafon et al. [2007]	tower	Toulon-Hyères Bay, Mediterranean	Oct–Nov 2001	10–18	<30	14	NA	u_*, f_p, H_s	29	24	12	film	0.033	0.52
Sugihara et al. [2007]	tower	Tanabe Bay, Wakayama, Japan	Nov–Dec 2003; Feb–Mar 2004	4.4–16.4	coastal	NA	−11 to 0	u_*, T_p, c_p, H_s	91	600	10	digital video	1	0.35
Callaghan et al. [2008a]	tower	Martha's Vineyard, Massachusetts, USA	Nov 2002	3–12	3–20	NA	NA	φ_w, f_p, c_p/u_*, $\bar{u}_c$	73	400–1200	20	digital photo	1	0.24
Callaghan et al. [2008b]	ship	Northeast Atlantic	Jun–Jul 2006	4.5–23	200, 500, >500	13–14	−3.86 to −0.13	T_a, T_w for 44 data points	107	100–782	30	digital video	0.5	0.46

[a]Meteorological and oceanographic factors are as follows: U_{10}, wind speed at 10 m above the sea surface; X, fetch (the length of water over which wind has blown); T_w, water temperature; $\Delta T = T_a − T_w$, difference between air temperature T_a and water temperature.

[b]Additional parameters (directly measured or calculated) are as follows: u_*, wind friction velocity; H_s, significant wave height; f_p, frequency peak of wave spectrum; T_p peak wave period; c_p, phase speed of dominant waves; c_p/u_*, wave age; φ_w, wind direction; $\bar{u}_c$, ocean current velocity (magnitude and direction).

[c]Geometric mean of the ratios of measured values of W to those calculated using the formulation of *Monahan and Ó Muircheartaigh* [1980], equation (9) in the text.

[63] The changes in the value of W that resulted from increasing the number of individual determinations of W obtained in series of measurements during 30 min periods to yield an average was also investigated by *Callaghan and White* [2009]. The relative difference of each such value of W from the data set mean was as great as ±25% when 10–30 values were averaged, gradually decreasing to about ±10% when 100 values were averaged and to less than ±3% when about 500 values were averaged. Such decrease in the relative difference would be consistent with expectation for averages of independent measurements. Although use of a greater number of images reduced the difference from the mean calculated from 700 images, there did not appear to be any bias associated with using fewer images (as would also be consistent with expectation for averages of independent measurements). Similar findings were reported by *Callaghan et al.* [2008a]. Additionally, it was found that the value of W for many of the images would not be substantially different if sampled only 1 or 2 s apart. *Callaghan et al.* [2008a] noted that the optimal sampling frequency (beyond which little improvement is seen) was once every 3–4 s, approximately the lifetime of an individual whitecap. Several of these data sets would appear to contain valuable information concerning statistics on the lifetimes and sizes of individual whitecaps and on the temporal autocorrelation of W which have not yet been fully exploited.

[64] The new whitecap fraction data are plotted in Figure 2 as a function of wind speed, U_{10}, together with previous measurements that are summarized in Table 20 of LS04 and in Table 2 of *Anguelova and Webster* [2006]. The $W(U_{10})$ relationship from MO'M80 (equation (9)) is also shown. As determinations of W by analog video are thought to not be as accurate as those by film photography [LS04], the "previous" measurements in Figure 2 include only photographic determinations of W [LS04, Table 20]. Three of these new data sets were obtained using digital photography or digital video (Table 3); digital video has better resolution and lower noise than analog video, although it is not yet as good as film photography in spatial resolution and dynamic range [*Brady and Legge*, 2009; *Kroeker*, 2009].

[65] The newly measured values of W appear to exhibit less scatter than, but are consistently less than, the bulk of those of the previous data sets. Geometric means of the ratios of the new values of W to those calculated according to the MO'M80 relationship ranged from 0.24 to 0.64 for the new data sets (Table 3). Furthermore, the wind speed dependence of W for these new data sets seems to differ from that of the older data sets: At low wind speeds ($U_{10} < 7$ m s^{-1}), the new measurements indicate that $W(U_{10})$ increases faster than MO'M80, resulting in a strong increase of W (from $\sim10^{-5}$ to $\sim5 \times 10^{-4}$) over a narrow range of wind speeds (5–7 m s^{-1}). In contrast, and in agreement with the previous results, $W(U_{10})$ increases slowly for $U_{10} > 16$ m s^{-1}, and the few data for $U_{10} > 20$ m s^{-1} seem to plateau at a constant value; albeit the new data are consistently lower than the MO'M80 curve throughout the entire range of wind speeds. As the new data sets were based on both film photography (two sets) and digital imagery (three sets) and were
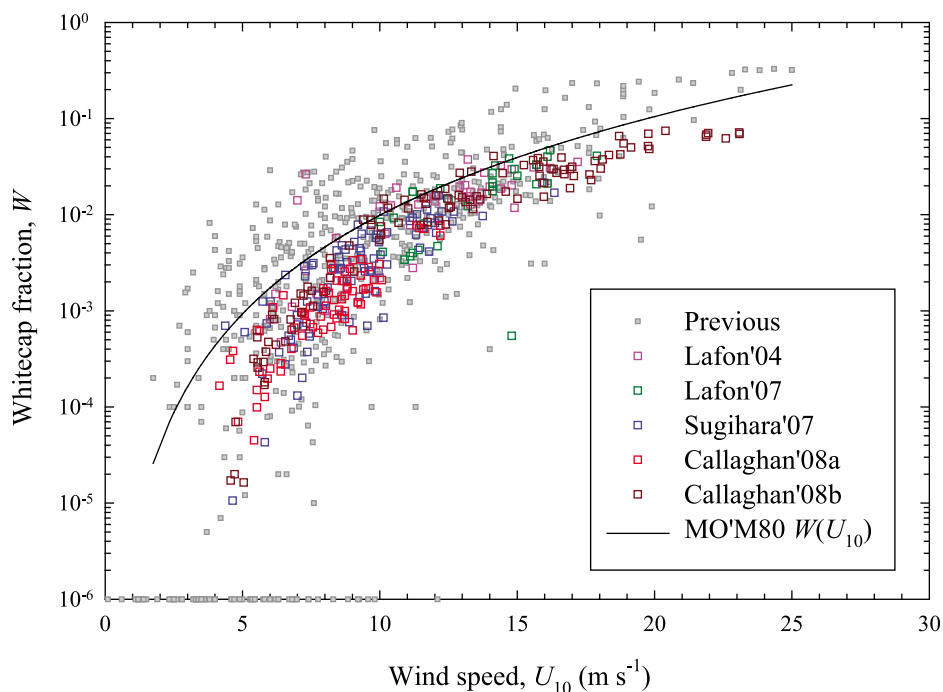
Figure 2. Whitecap fraction W as a function of wind speed at 10 m above the sea surface U_{10} from five new data sets (colors) and from previous studies that used film photography (gray) as summarized in Table 20 of *Lewis and Schwartz* [2004] and in Table 2 (data sets 1–5, 7–17, 21, 26) of *Anguelova and Webster* [2006]. Points on abscissa denote values less than or equal to 1×10^{-6}. The formulation of *Monahan and Ó Muircheartaigh* [1980], equation (9), is also shown.

characterized by both limited fetch (four sets) and open ocean (one set), there seems to be no obvious reason for the consistently lower values.

[66] Most of the new whitecap data [*Lafon et al.*, 2004, 2007; *Sugihara et al.*, 2007; *Callaghan et al.*, 2008a] have also been examined for their dependence on friction velocity u_*, but there seems to be little or no decrease of the scatter in plots of W versus u_* compared to that in plots of W versus U_{10}, a similar conclusion to that reached from the analysis of previous data by LS04. It has been suggested that u_* could be more accurately determined if the expression of roughness length explicitly included wavefield characteristics (or combinations of them) such as wave age (a measure of and proxy variable for fetch), significant wave height, wave steepness, or energy dissipation in the breaking waves [e.g., *Drennan et al.*, 2005]. By the same token, models of W that directly involve wavefield characteristics might better account for variability in whitecap fraction [cf. *Massel*, 2007, chapter 7]. For example, using the so-called breaking wave parameter or windsea Reynolds number, $R_b = u_*^2/(\nu_a f_p)$ [*Zhao and Toba*, 2001], where ν_a is the kinematic viscosity of air and f_p the frequency peak of the wave spectrum, to represent the sea state-dependent whitecap fraction has yielded improved prediction of the transfer velocity of CO_2 [*Woolf*, 2005; *Soloviev et al.*, 2007]. Consequently, it has been suggested that parameterizations of W in terms of wave age [*Lafon et al.*, 2004, 2007; *Guan et al.*, 2007; *Sugihara et al.*, 2007; *Callaghan et al.*, 2008a] might lead to similar improvement in predicting the SSA particle flux in equation (8) through improved estimates of W.

[67] The analysis of whitecap observations by *Callaghan et al.* [2008b] supports this premise. Callaghan et al. sorted data into periods with decreasing and increasing wind as surrogates for developed (old) seas (defined as a sea state produced by winds blowing steadily for fetch of hundreds of kilometers and duration of several days) and undeveloped (young) seas, respectively, and reported that for U_{10} below 9 m s^{-1}, there seemed to be no difference in the relation between W and U_{10} between the two data sets, whereas for U_{10} greater than 9 m s^{-1}, W values from periods of decreasing wind were 30–70% higher than those from periods of increasing wind. Although such measurements demonstrate the contribution of sea state to the variability of W at a given U_{10}, the reported dependence accounts for only a small fraction of this order-of-magnitude variability.

4.1.2. Satellite-Based Measurements of Whitecap Fraction

[68] Measurements made with satellite-borne microwave sensors infer W from surface brightness temperature, T_B, determined from the emitted radiance, which increases with increasing whitecap fraction, as opposed to detecting individual whitecaps. Although the dependence of W on T_B might be calculated from a simple empirical relationship [*Wang et al.*, 1995], a physically sound approach for obtaining W requires an algorithm containing multiple steps. The feasibility of acquiring whitecap fraction globally from space using T_B and variables necessary for the atmospheric correction (columnar water vapor and cloud liquid water path) from the Special Sensor Microwave/Imager (SSM/I) was demonstrated by *Anguelova and Webster* [2006].
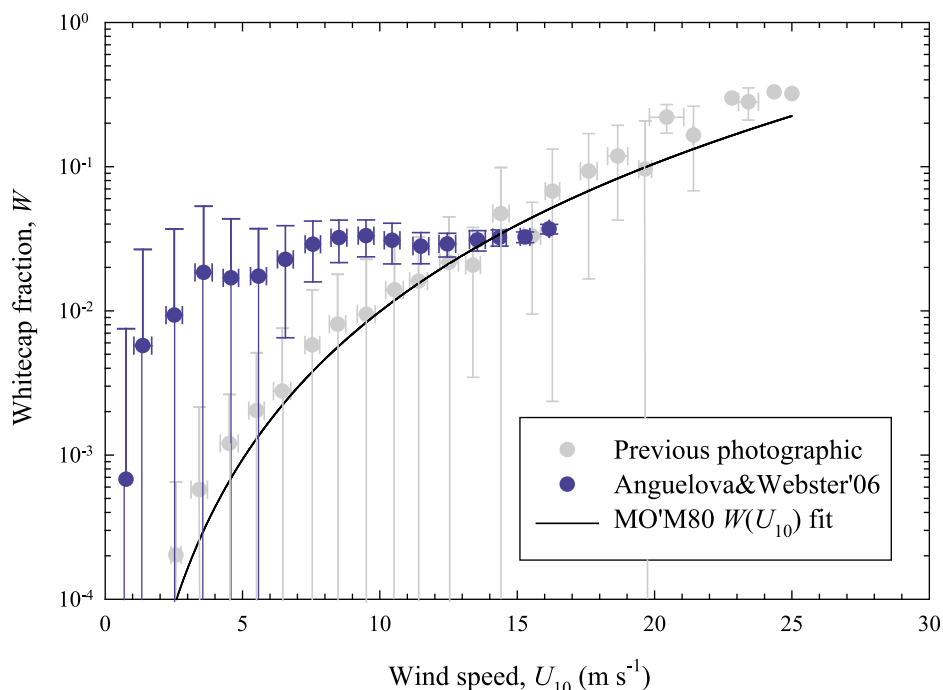
Figure 3. Whitecap fraction W as a function of wind speed at 10 m above the sea surface U_{10}, arithmetically averaged in intervals of 1 m s^{-1}, obtained with the algorithm of *Anguelova and Webster* [2006] (blue) using annually averaged (1998) observations of brightness temperature T_B from SSM/I in clear sky (no clouds) locations all over the globe. The corresponding U_{10} values are also from SSM/I. Error bars on W values represent 1 standard deviation of the data points falling in each U_{10} bin; the apparent asymmetry of the error bars is a consequence of plotting on the logarithmic ordinate scale. Also shown (gray) are bin-average values of W from previous photographic determinations shown in Figure 2 and the formulation of *Monahan and Ó Muircheartaigh* [1980], equation (9).

Because the algorithm uses satellite observations with a wide cross-track swath, W is determined twice a day (once in the daytime and once at night) at almost every oceanic location on Earth. Each satellite-based determination of W is a value spatially averaged over the sensor footprint (approximately 50 km × 50 km) at a specific local time for a given location.

[69] There are two main contributions to the uncertainty of satellite-based estimates of W. One is the error associated with the accuracy of models used in the algorithm that represent the various relationships needed for determining W, e.g., the emissivities of the rough sea surface and of whitecaps at microwave frequencies. This error might be characterized by comparing satellite- and surface- or aircraft-based observations collocated in time and space. The second source of uncertainty is the measurement error, which results from random and systematic errors in the data used in the determination of W. Random error is quantified as the variance, σ_W^2, of the calculated W. This method does not identify or quantify systematic errors. In their feasibility study, *Anguelova and Webster* [2006, section 3.4] evaluated the measurement error and assigned a standard deviation σ_W to each W estimate; lack of concurrent in situ measurements prevented evaluation of the modeling error. Analysis of whitecap fraction determined by the satellite-based method for all days in 1998 showed that the relative standard deviation, σ_W/W, was less than 30% for about half of the determinations, whereas less than one-third of the individual photographic measurements available at the time had this accuracy [*Anguelova and Webster*, 2006].

[70] The satellite-based results for W from the algorithm of *Anguelova and Webster* [2006], binned (as arithmetic means) by wind speed in intervals of 1 m s^{-1}, are compared in Figure 3 to bin (arithmetic) averages of W determined from photographic measurements and to the $W(U_{10})$ parameterization of MO'M80. These determinations of W yield a nearly constant value of approximately 0.03, independent of wind speed over the range 8 m s$^{-1} < U_{10} < 17$ m s^{-1}, with somewhat lower W as wind speed decreases for $U_{10} < 8$ m s^{-1}, in contrast to the much stronger wind speed dependence exhibited by the photographic data and MO'M80 parameterization.

[71] The differences between the satellite results and in situ photographic measurements are likely due to three factors. First, the signal from a whitecap may be different in different regions of the spectrum because of difference in the observed physical process, e.g., skin depth of the foam in the microwave region versus penetration depth of scattered visible radiation. Second, the satellite retrieval algorithm may be incomplete; for instance, simplified emissivity models were employed for foamy and rough surfaces by *Anguelova and Webster* [2006, section 5]. Finally, the influence of various geophysical factors captured by the satellite estimates of W, which are not currently extracted nor reliably

TABLE 4. Experimental Investigations of Sea Spray Production by Laboratory Bubble Plumes

Study	Medium	Organic Added	Bubble Production Method(s)	Bubble Rise Distance (cm)	White Area (cm^2)	Temperature (°C)	Salinity
Mårtensson et al. [2003]	artificial seawater	none	diffuser[a]	4	3	−2, 5, 15, 25	0, 9.2, 33
Sellegri et al. [2006]	artificial seawater	sodium dodecyl sulfate	weir, diffusers[b]	2	not stated	4, 23	not stated, presumably near 35
Tyree et al. [2007]	seawater, artificial seawater, mixtures	oleic acid	diffusers[c]	32–40	180	20–25	1, 10, 20, 33, 70
Keene et al. [2007]	seawater	none	diffuser[b]	~115	~150–300	~27	not stated, presumably near 35
Facchini et al. [2008]	seawater	none	water jet	not stated	400	not stated, presumably ~13	not stated, presumably near 35
Fuentes et al. [2010]	artificial seawater, seawater	*Thalassiosira rotula* exudate	water jets, diffusers[d]	4–10	200	18–20	35

[a]Pore size (presumably diameter) is 20–40 μm.
[b]Pore size(s) not specified.
[c]Pore sizes (presumably diameters) of 80 and 140 μm.
[d]One, a sintered glass filter with mean pore size (presumably diameter) of 30 μm; the other, an aquarium diffuser with unspecified pore size.

quantified, may be important. Improvement of the satellite-based estimates of W requires understanding and characterizing all these factors.

[72] In view of concerns over the accuracy of the space-based microwave determination of W, *Anguelova and Webster* [2006] suggested several possible modifications of their initial algorithm, including different models for foamy and rough surfaces and independent data sets for atmospheric correction. Microwave observations from the new satellite radiometric sensor WindSat [*Gaiser et al.*, 2004; *Bettenhausen et al.*, 2006; *Freilich and Vanhoff*, 2006] in addition to those of SSM/I provide a possibility to use independent data sets. To better represent the emissivity of whitecaps in different lifetime stages, Anguelova and Webster suggested using a depth profile of the void fraction within the thickness of the whitecaps instead of a constant value and assuming a distribution of whitecap thicknesses over the ocean. Details of these suggestions are given by *Anguelova* [2008] and *Reul and Chapron* [2003], respectively.

4.1.3. Laboratory Experiments on SSA Production

[73] Recent experimental studies of SSA production from laboratory-generated bubble plumes by *Sellegri et al.* [2006], *Tyree et al.* [2007], *Keene et al.* [2007], *Facchini et al.* [2008], and *Fuentes et al.* [2010] have provided new data on the effects of salinity, water temperature, means of bubble production, and surfactants on resulting SSA particle size distributions and the resultant size-dependent organic enrichment and hygroscopic properties of these particles. Key features of these experiments, and of prior similar experiments by *Mårtensson et al.* [2003], are summarized in Table 4.

[74] The range of conditions in these experiments could, in principle, provide a test of the key premise of the whitecap method (section 3.5), specifically the assumption that the size-dependent production flux per white area is independent of the means by which that white area is formed. However,

several of the investigations reported only normalized concentrations and/or did not report the white area characterizing their experiment. Nonetheless, under the assumption of negligible particle loss such normalized concentrations would exhibit the same size dependence as production fluxes, permitting comparison of the results of the several studies. Those experiments which provided sufficient data to allow determination of both a magnitude and size distribution of a production flux are discussed further in section 5.1.

[75] There are several concerns with laboratory experiments simulating SSA production. One is the extent to which laboratory whitecaps can accurately simulate breaking waves over the ocean as discussed in section 3.5. All of the laboratory whitecaps discussed in this section, whether formed by diffusers or water jets, were continuous, as opposed to open ocean whitecaps, which are discrete. Large bubbles (those thought to be responsible for the production of most of the small drops, i.e., those with r_{80} less than several tenths of a micrometer, which are thought to be film drops) rise quickly to the surface, and after several seconds the only bubbles that remain in the ocean are smaller ones, which are thought to be too small to produce film drops. Thus the vast majority of the film drops would be produced during only a small fraction of the lifetime of a whitecap in the ocean, in contrast to the laboratory whitecaps. Another concern with laboratory experiments is the possible influences of the sides of the container on the resultant whitecap. In some experiments [e.g., *Keene et al.*, 2007; *Tyree et al.*, 2007] the white area was constrained by the size of the tank such that the white area was nearly the same for a range of bubble volume fluxes (i.e., the rate of air volume in bubbles reaching the surface divided by the white area, which Tyree et al. called the superficial bubbling velocity). Other experiments used only one bubble volume flux or varied this quantity only slightly. However, whether the values chosen are in the range of those

in oceanic whitecaps, and the possible consequences of those values not being in the oceanic range, are not known.

[76] Another concern with laboratory experiments as models for oceanic behavior of bubbles is the short bubble rise times and distances compared to those for bubbles produced by breaking ocean waves, which reach depths of up to several meters, depending on wave height, as shown by acoustic observations of bubble plumes near the ocean surface [e.g., *Thorpe*, 1992]. Rise distances in laboratory studies are often much shorter. For example, *Sellegri et al.* [2006] and *Fuentes et al.* [2010] used bubble rise distances of only a few centimeters. *Tyree et al.* [2007] used rise distances of ~0.35 m, which they claimed approximated the circulation depth of oceanic bubbles. *Keene et al.* [2007] used bubble rise distances greater than 1 m, over which distance they assumed that the equilibrium size distribution would be attained before bubbles reached the surface and burst.

[77] A possible basis for a dependence of drop production on bubble rise times or distance is the time required for organic substances to equilibrate on the air-water interface of the bubbles. This equilibration time was examined by *Fuentes et al.* [2010], who provided a theoretical analysis demonstrating that equilibrium with respect to adsorption of organics would be reached within 0.05 ms, much shorter than rise times of bubbles even for the short distances of some of the laboratory studies. On the basis of this analysis, Fuentes et al. concluded that the depth of bubble generation would play little role in the effect of organics on production and properties of SSA. However, this result would seem to be in contradiction with findings reported in a series of laboratory studies by Blanchard and colleagues, which indicated that the equilibrium attachment of organics to the air-water interface of bubbles is attained much more slowly. *Blanchard and Syzdek* [1972, 1975] reported that ejection heights of jet drops exhibited a dependence on bubble rise distance over the range 6–23 cm and on bubble age for up to 10–20 s. *Detwiler and Blanchard* [1978] reported that both bubble rise speeds and top jet drop ejection heights decreased with increasing bubble age (time spent in the water), with rise speeds decreasing by nearly a factor of 2 over the first 10 s or so, effects that they attributed to attachment of organic material to the bubble interface. In several studies, Blanchard and colleagues examined the dependence of enrichment of bacterial concentration in drops relative to the bulk concentration on bubble age or rise distance. *Blanchard and Syzdek* [1970] reported that bacterial enrichment in the top jet drop increased by approximately a factor of 5 when the bubble rise distance increased from 1 to 30 cm. *Blanchard and Syzdek* [1972] and *Blanchard et al.* [1981] reported that bacterial enrichment in jet drops increased with increasing bubble age for ages of 20 s or more. All of these results, which were attributed to organic attachment to the bubbles, would appear to indicate that this process does not rapidly attain equilibrium.

[78] Several of the size-dependent production flux measurements obtained in the newly reported studies, normalized to the maximum values in the representation

$dF/d\log r_{80}$, are shown in Figure 4. A common feature is a rather broad maximum of the production flux in this representation at r_{80} near 0.05–0.1 μm, which is rather independent of the means of production and of the bubble size distribution, although the spectral shapes differ markedly among the different examples. The large differences in the size distributions of the normalized concentration (and thus of the production flux), which may be as great as 2 orders of magnitude at $r_{80} = 0.01$ μm, rather strongly refute the assumption that the production flux per white area is independent of the means by which the white area is produced. The results presented in Figure 4 were obtained for different conditions such as artificial versus natural seawater, water temperature, salinity, effects of surfactants, and bubble generation method, the effects of which were assessed in different studies. The results of these studies are presented here and possible causes for differences are examined.

[79] The effect of salinity on the production flux size distribution was examined by *Mårtensson et al.* [2003] (salinities 0, 9.2, and 33) and by *Tyree et al.* [2007] (salinities 1, 10, 20, 33, and 70). Both studies reported an increase in particle number production with increasing salinity. Mårtensson et al. (their Figure 5) reported that size distributions for r_{80} between ~0.05 and 0.1 μm were nearly the same for salinities 9.2 and 33 and that for larger SSA particles the number fluxes for salinity 33 were increasingly greater than for salinity 9.2 as r_{80} increased, up to nearly an order of magnitude for r_{80} larger than approximately 1 μm. Mårtensson et al. argued that the size distributions near $r_{80} = 0.05$ μm shifted to slightly lower sizes at lower salinity, consistent with the hypothesis that formation radii were independent of salinity, although this shift did not occur for larger particles. In contrast to these results, Tyree et al. observed little change in the shape of their size distributions, with only a small increase (~15%) in the value of r_{80} of particles with increasing salinity from 10 to 70 (their Figure 4). Tyree et al. did, however, report an increase in total particle number production by a factor of 2.5 with salinity increasing from 10 to 70. As discussed by LS04, there is a transition in the coalescence behavior of bubbles that occurs near salinity 10, which results in very different bubble size distributions and thus perhaps SSA particle size distributions between lower and higher salinities to which it may be possible to attribute some of these results.

[80] The effect of water temperature on the resultant size distribution was investigated by *Mårtensson et al.* [2003] (−2, 5, 15, and 25°C) and by *Sellegri et al.* [2006] (4 and 23°C). Mårtensson et al. found nearly identical size distributions for −2 and 5°C and little change between these and the size distribution at 15°C, although at both 15 and 25°C there was a decrease in the magnitude of the production flux by a factor of 2–3 for $r_{80} < 0.1$ μm and an increase by a factor of 5–10 for $r_{80} > 1$ μm. Sellegri et al. reported an increase in the production flux of particles with $r_{80} < 0.7$ μm at 4°C relative to that at 23°C and a decrease at greater r_{80}, although much of this difference could alternatively be attributed to a decrease in the values of r_{80} by ~30% at the lower temperature.
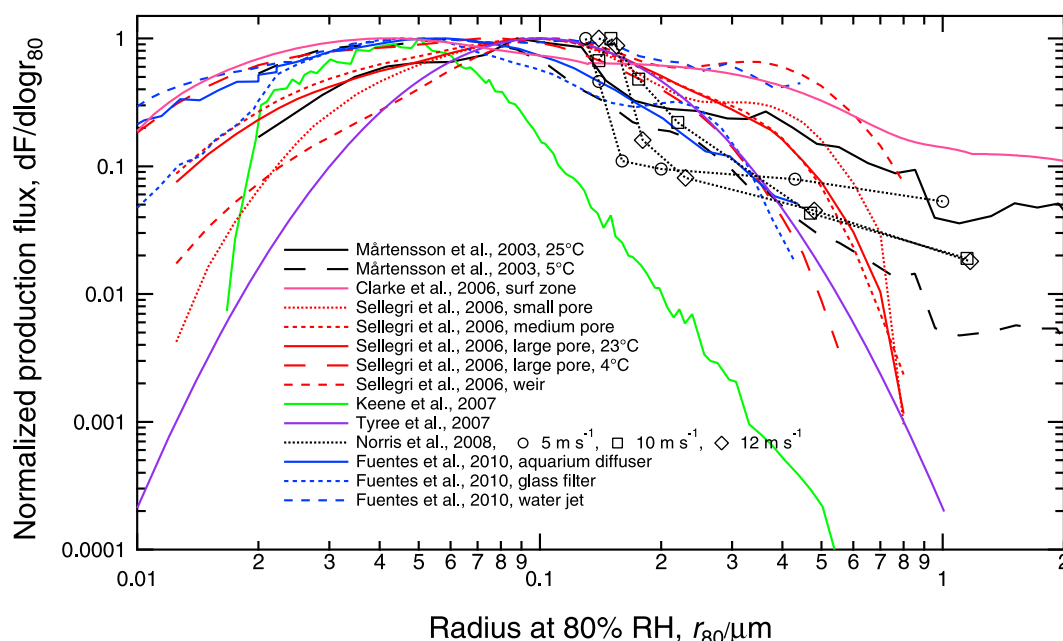
Figure 4. Size distributions of SSA production flux normalized to maximum value in representation $dF/d\log r_{80}$ as a function of r_{80} from laboratory experiments (*Mårtensson et al.*'s [2003] Figure 4c; *Sellegri et al.*'s [2006] Figures 2 and 4; *Keene et al.*'s [2007] Figure 3 for 5 L min^{-1}; *Tyree et al.*'s [2007] Table 1, artificial seawater, and salinity 33; and *Fuentes et al.*'s [2010] Figure 6) and field measurements (the *Clarke et al.* [2006] formulation which is presented in text and *Norris et al.*'s [2008] Figure 6 at U_{10} 5, 10, and 12 m s^{-1}). Uncertainties in the original data are not shown.

[81] The effects of different bubble generation methods on the resultant aerosol size distribution and properties were examined by *Sellegri et al.* [2006], *Tyree et al.* [2007], and *Fuentes et al.* [2010]. Sellegri et al. noted different size distributions (their Figure 2) for different methods, a weir and diffusers with three pore sizes, with $dN/d\log r_{80}$ exhibiting a maximum near $r_{80} = 0.1$ µm for each method but with the size distribution produced by the weir having a narrower distribution near this maximum and an additional contribution from particles with r_{80} near 0.35 µm. Tyree et al. reported that the production flux per white area obtained using a diffuser with a pore size (presumably diameter) 140 µm was up to a factor of 4 greater than when using one with pore size 80 µm at the same bubbling rate. Fuentes et al. reported large differences in the magnitude and shape of the number size distribution (their Figure 6) and hence of inferred SSA production flux, produced by plunging water jets and by diffusers with different pore sizes, with the size distribution (in the form $dN/d\log r_{80}$) produced by the water jets being bimodal with maxima at r_{80} near 0.05 and 0.15 µm, with that from an aquarium diffuser having a single broad maximum near $r_{80} = 0.06$ µm, and with that from a sintered glass filter (pore size, presumably diameter, 30 µm) having a narrow maximum near $r_{80} = 0.06$ µm with a much smaller secondary maximum near $r_{80} = 0.25$ µm. These size distributions are also shown in Figure 4.

[82] The dependence of production flux on bubble volume flux was investigated by *Tyree et al.* [2007] and *Keene et al.* [2007]. Tyree et al. reported that a higher bubble volume flux could yield more than an order of magnitude increase in

the total number production flux per white area. Keene et al. also reported an increase in the magnitude of this quantity with increased bubble volume flux, although shapes of size distributions were similar. These dependences together with results of *Mårtensson et al.* [2003] are shown in Figure 5. In
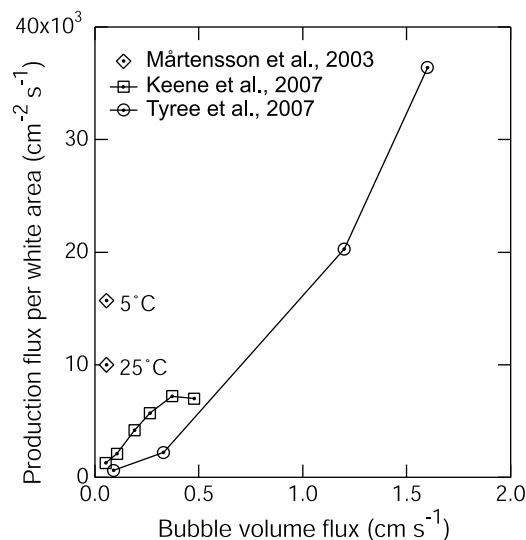

Figure 5. Dependence of total SSA number production flux per white area in laboratory experiments of *Mårtensson et al.* [2003] using artificial seawater (salinity 33) at two different temperatures, *Keene et al.* [2007] using natural (low productivity) seawater, and *Tyree et al.* [2007] using artificial seawater (salinity 33) on bubble volume flux (volume of air in bubbles rising to the water surface per unit area and time).

view of the strong dependences shown in Figure 5, bubble volume flux would seem to be an important property of whitecaps influencing the SSA production flux per white area. Certainly it would seem that a whitecap property such as this would be much more useful than an arbitrary threshold of "white" in relating SSA production flux to white area and ultimately in developing more accurate parameterizations for SSA production flux.

[83] The effects of surfactants on SSA production were investigated by *Sellegri et al.* [2006], who added sodium dodecyl sulfate (SDS) to artificial seawater; *Tyree et al.* [2007], who investigated natural seawater containing different organic compositions and artificial seawater to which 0.1 and 10 mg L^{-1} oleic acid was added; and *Fuentes et al.* [2010], who added exudate of the diatom *Thalassiosira rotula* to natural filtered seawater at a concentration 512 μM (representative of dissolved organic carbon (DOC) concentration in seawater in areas of high biological activity).

[84] Particle size distributions produced using artificial seawater were reported by *Sellegri et al.* [2006] as being similar to those using natural seawater, although they were shifted toward smaller values of r_{80} for SDS concentrations greater than 3 mg L^{-1}. The investigators stated that these results should be considered exploratory because their comparison to long-term, seasonally varying data of particle size distributions obtained at the Mace Head atmospheric research station (located on the west coast of Ireland) showed that SDS does not accurately simulate the effects of the surfactants present in the natural environment.

[85] The natural seawater samples of *Tyree et al.* [2007] exhibited differing organic composition because they had been collected in winter (DOC concentration = 2.3 mg C L^{-1}, chlorophyll concentration = 0.1 mg m^{-3}) and summer (DOC concentration = 3.1 mg C L^{-1}, chlorophyll concentration = 1.8 mg m^{-3}). The size distributions of the SSA particles produced in their experiments were nearly the same, regardless of the type of water (artificial, filtered, or unfiltered seawater), with little dependence on the amount of surfactant added. The winter samples of natural seawater produced 20–40% more SSA particles than the summer samples. Comparison of the size distributions of the SSA particles produced with the summer and winter samples showed that the natural organic matter exerted little effect on the numbers or radii of the produced SSA particles. Bubbling artificial seawater artificially enriched with oleic acid produced approximately twice as many drops as natural seawater. The investigators concluded that the nature of organic matter affects foam droplet production and that oleic acid is a poor surrogate for natural organic matter for studies of foam production. These findings, as well as those of *Sellegri et al.* [2006], would seem to raise questions over the accuracy of laboratory experiments as models for oceanic SSA production.

[86] Hygroscopic growth and CCN activity for artificial seawater were examined by *Fuentes et al.* [2010], who reported that these properties were not affected by the bubble generation technique; however, for the organically enriched natural seawater, hygroscopic growth was suppressed, with the degree of suppression depending on the aerosol generation technique. The main differences in hygroscopic growth resulting from different generation techniques were observed for RH > 75%, with the plunging water jet presenting the greatest suppression of growth. The influence of organics on the CCN activity exhibited little size dependence, with only a slight increase in the critical supersaturation compared to seawater samples to which no organics were added.

[87] Chamber studies aimed at determining the size-dependent mass fraction of organic material in SSA particles produced from natural seawater were conducted by *Keene et al.* [2007] and *Facchini et al.* [2008]. Keene et al. used highly oligotrophic seawater (concentrations of organic substances such as formate, acetate, oxalate, and methylsulfonate were below detection limits) pumped from the ocean into a laboratory near the coast of Bermuda and produced SSA by bubbling the water through diffusers. Facchini et al. used highly productive seawater (average chlorophyll-a concentration of 1.4 mg m^{-3}) pumped into a sealed tank on a ship in the North Atlantic west of Ireland during an algae bloom and produced SSA using a water jet.

[88] Enrichment of calcium with respect to surface water concentrations (median enrichment factor of 1.2), which may have been caused by fragments of biogenic $CaCO_3$ or from complexes with organic matter, was reported by *Keene et al.* [2007]. These investigators also reported that all size-resolved and bulk aerosol samples were highly enriched in organics, with the enrichment decreasing from greater than 10^5 for r_{80} near 0.06 μm (the lowest size range) to slightly greater than 10^2 for r_{80} near 4 μm and again increasing slightly to near 10^3 for r_{80} near 14 μm; the median enrichment factor for all samples was near 400. The organic mass fraction exhibited similar behavior, decreasing from near 80% for r_{80} near 0.06 μm to 40–50% for r_{80} between 0.06 and 0.6 μm and to less than a few percent for r_{80} between 0.6 and 4 μm then increasing again to near 40% for r_{80} near 14 μm. In all size ranges except the smallest, the dominant contribution to aerosol mass was provided by sea salt.

[89] A strong dependence of the organic (water-soluble and water-insoluble organic matter) mass fraction on particle size (Figure 6), with the enrichment factor (relative to the bulk seawater) increasing with decreasing particle size, was also reported by *Facchini et al.* [2008]. SSA particles with ambient radii greater than 0.5 μm contained more than 90% of the inorganic sea salt mass; particles with ambient radii less than 0.25 μm consisted mainly of organic matter, most of which was water insoluble. This water-insoluble organic matter (WIOM) exhibited substantial enrichment (relative to the bulk solution) with mass fraction increasing from 3 to 77% as radius (at 50–70% RH) decreased from 4 to 0.06 μm, with only a very minor fraction (~3%) of water-soluble organic matter (WSOM); the remaining mass was sea salt. The WIOM was attributed to colloids and aggregates exuded by phytoplankton on the basis of functional nuclear magnetic resonance spectroscopy. Such an increasing fraction of organic matter with decreasing drop radius is consistent with the volume fraction of adsorbed surfactant organic matter as
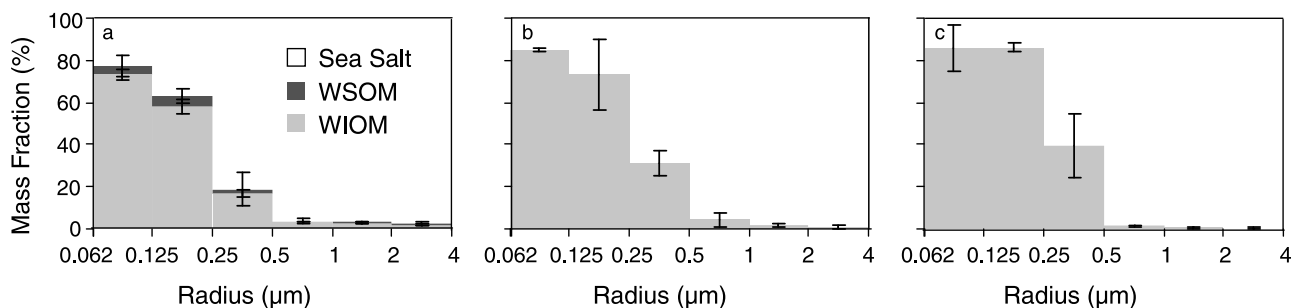
Figure 6. Mass fraction of sea salt, WSOM, and WIOM as a function of particle radius sampled at approximately 70% RH (a) for seawater bubble-bursting chamber experiments with fresh seawater, conducted in a shipboard laboratory in a plankton bloom over the northeast Atlantic (May–June 2006); (b) for clean marine air at Mace Head, Ireland, May–June 2006; and (c) for clean marine air 200–300 km offshore west-northwest of Mace Head in a plankton bloom coincident in time with aforementioned samples. Adapted from *Facchini et al.* [2008].

a function of SSA particle size as evaluated with a thermodynamic model [*Oppo et al.*, 1999]. Despite the small mass fraction of organic matter in larger particles (radius of 2–4 μm at 50–70% RH), the total mass of organic matter in these particles was approximately half the total organic mass in aerosol particles with radius (at these RH values) less than 4 μm. Facchini et al. also reported that the mass ratio of WIOM to sea salt was similar to that observed in aerosol samples at Mace Head.

4.1.4. Surf Zone Measurements

[90] The production of SSA in a surf zone was determined by *Clarke et al.* [2006] from measurements on a 20 m tower, 20–30 m from the water's edge on a beach in Hawaii, during onshore winds (typical wind speed of 7 m s^{-1}). Aerosol properties were characterized using a differential mobility analyzer (DMA), an OPC, and an aerodynamic particle sizer (APS), which together covered the size range 0.01 μm < r_{80} < 8 μm. The DMA and OPC included options for sampling aerosol at ambient temperature or at 300–360°C to permit determination of size distributions of volatile and residual refractory aerosol (the latter being typically sea salt, nonvolatile organics, dust, or soot). These instruments were complemented with two condensation particle counters (CPCs), one operated at ambient temperature and the other at 360°C; a tandem DMA (TDMA) and a humidified TDMA (HTDMA) to examine the thermal and humidification response of selected sizes; and a three-wavelength nephelometer to determine particle light scattering. Inlets for all these instruments were placed at heights of 5, 10, and 20 m and sampling was cycled at regular intervals.

[91] Comparison of measurements at these three heights showed that the highest level was not influenced by surf production and could thus be used for determining the upwind background concentration. SSA production in the surf zone was evaluated from the SSA concentrations measured at 5 m after correction for background concentrations using the 20 m data. The production flux per white area was determined as described in section 3.5 using a mean whitecap fraction in the surf zone of 40%, based on visual examinations of images. Substantial production of particles with dry radius less than 0.05 μm was found.

[92] Heated and ambient sample volumes were used by *Clarke et al.* [2006] to discriminate between refractory aerosol particles, assumed to be mainly sea salt, and other components. To further ascertain whether the detected particles were sea salt, the investigators made several tests. First, they noted the strong correlation between the concentrations of the refractory particles, most of which had dry radii less than 0.05 μm, and light scattering, which would be dominated by particles with dry radius greater than 0.25 μm. Chemical analysis using a flame photometric aerosol sodium detector confirmed that particles with r_{80} > 0.09 μm were composed mainly of sea salt. SSA particles with r_{80} of 0.05 μm (previously heated to 300°C) exhibited a humidity growth factor near 1.8 from low RH to RH of 76%, as expected for sea salt particles, from which Clarke et al. concluded that these particles were composed mainly or entirely (80% up to possibly 100%) of sea salt. They further concluded that most of the particles with $r_{80} \gtrsim 0.03$ μm produced from breaking waves were primarily sea salt. Based on their measurements, Clarke et al. presented an SSSF that extended to r_{80} as small as 0.01 μm. This formulation, presented in Appendix A and discussed in section 5.1, is shown in Figure 4 as a normalized size distribution.

4.1.5. Summary

[93] The whitecap method requires the ability to measure or model the whitecap fraction, W, under a given set of conditions to known accuracy and demonstration that the whitecap fraction so determined yields, within a given uncertainty, the same size-distributed flux per white area as obtained in laboratory experiments or field studies. So far, these goals have not been achieved. Demonstrating that field measurements of W are reproducible and transferable would seem, at minimum, to require simultaneous measurements by multiple groups using different platforms (e.g., shipborne, aircraft, satellite, and fixed offshore platforms) and techniques at a variety of locations differing in controlling properties such as fetch and surfactant content. Simultaneous field measurements of production flux per white area would then allow comparison with flux per white area determined in laboratory experiments. Finally, algorithms for calculating W would have to be compared to measurements under a wide

variety of conditions and locations by different investigators using different techniques. Only when all these requirements are fulfilled would it seem that the SSSF and the associated uncertainty can be considered accurately parameterized and confidently represented in models. However, the laboratory experiments have demonstrated that the size-dependent flux per white area depends on the means by which the white area was created, raising intrinsic questions concerning the applicability and accuracy of the whitecap method, especially with regard to the assumption of a universal production flux per white area.

4.2. Micrometeorological Methods

4.2.1. Eddy Correlation Measurements

[94] Eddy correlation measurements were made by *Geever et al.* [2005] at a 22 m tower at Mace Head, Ireland, over a 4 week period in June and July 1992 during which U_{22} was between 7 and 18 m s^{-1}. Data were restricted to periods when the winds were from the ocean to the land and during high tide, when the distance from the base of the tower to the water was approximately 80 m. Total concentrations of particles with ambient radii from 0.005 to 0.5 μm (RH not reported) were measured by a CPC, and total concentrations of particles with dry radii from 0.05 to 0.5 μm were measured by an OPC; these measurements together with 3-D wind speed measurements were used to determine particle fluxes (Appendix A). The wind speed dependences of the fluxes in the two size ranges were essentially the same. A potential concern with these measurements is coastal influence and effects of surf-produced aerosol on particle fluxes. Footprint analysis by O'Dowd, de Leeuw, and colleagues [*Geever et al.*, 2005] showed that the region contributing to the measured fluxes was almost entirely over water both at high and low tide, at which the distance from the base of the tower to the water was 180 m. However, at low tide at wind speeds less than 10 m s^{-1} measured fluxes showed little correlation with wind speed and were greater than at high tide, indicating influence of the exposed intertidal zone and thereby raising concern over the applicability of such measurements even at high tide to determining SSA production fluxes representative of the open ocean. Drag coefficients measured during high tide conditions yielded a slightly stronger dependence on wind speed than mid North Atlantic values but were comparable to values from the North Sea when water depth was greater than 30 m, from which Geever et al. concluded that fluxes measured during high tide conditions were characteristic of open ocean values.

[95] Fast sizing and counting of aerosol particles, required for the application of the eddy correlation technique to determine the size-dependent production flux, has become feasible with the development of the Compact Light Aerosol Spectrometer Probe (CLASP) [*Hill et al.*, 2008], which measures the size distribution of particles with radii of 0.1–7 μm at a frequency of 10 Hz. CLASP is a compact and lightweight OPC which can be mounted close to the wind sensor with minimal flow distortion and a short inlet tube. The combination of high sample rate, high flow rate (50 cm^3 s^{-1}),

and compact design makes CLASP highly suitable for determining aerosol production flux. The accuracy of the size determination, which is by means of light scattering, depends on particle shape and index of refraction.

[96] Eddy correlation measurements using a CLASP and a traditional OPC (Passive Cavity Aerosol Spectrometer Probe (PCASP)) to determine SSA fluxes were conducted at the 560 m pier at the Field Research Facility (FRF) in Duck (North Carolina, USA) in autumn 2004 and 2005 [*de Leeuw et al.*, 2007; *Norris et al.*, 2008]. The sonic anemometer and the aerosol inlets were mounted at the seaward end of the pier at a height of 16 m above mean sea level. *De Leeuw et al.* [2007] reported measurements of fluxes in three partly overlapping ranges of r_{80} as inferred from the reported dry radii measured with the PCASP equipped with an inlet heated at 300°C: 0.11–0.15, 0.15–0.19, and 0.11–0.375 μm and as an integrated flux over the r_{80} range from 0.11–9.0 μm, when the wind was from the ocean at U_{10} between 3 and 16 m s^{-1}; flux results for wind speeds lower than 7 m s^{-1} were considered unreliable. Based on the analysis of a small subset of the data, the gross particle number fluxes increased with increasing wind speed. These fluxes were fitted to a power law U^b, with values of b between 2.9 and 3.4, although the integrated flux could be better fitted (in terms of minimizing the variance) by a linear function of U_{10} than by a cubic one. *Norris et al.* [2008] measured SSA particle fluxes in six size ranges of ambient radius from 0.145 to 1.6 μm during twenty 20 min periods in October 2005, during which the wind was from the ocean with U_{10} from 4 to 12 m s^{-1}. Fluxes were converted to r_{80} values for U_{10} of 5, 10, and 12 m s^{-1} and were fitted as linear functions of wind speed for each of the six size ranges; these fluxes are discussed in section 5 and, normalized to the maximum value at each wind speed, presented in Figure 4, from which they can be seen to exhibit different size dependences from the majority of the production fluxes from the laboratory experiments. Reported fluxes were not corrected for dry deposition (cf. equation (6)); this correction was estimated as 2–30%, depending on the dry deposition formulation employed, well less than the estimated overall uncertainty, suggesting that these measurements may yield an accurate determination of the production flux. Although whitecap fraction was not reported in this study, simultaneous measurement of this quantity in conjunction with such eddy correlation measurements would permit another means of determining the flux per white area, an essential element of the whitecap method. CLASP has also been used to determine SSA production flux on a cruise in the North Atlantic in the spring of 2007 [*Brooks et al.*, 2009].

4.2.2. Gradient Method

[97] The gradient method (section 3.4.2) was applied by *Petelski and Piskozub* [2006] to determine the SSA production flux from 61 measurements of vertical profiles of the aerosol concentration obtained during four cruises in Arctic seas (Norwegian Sea, Greenland Sea, and Barents Sea) in 2000–2003 [*Petelski*, 2003; *Petelski and Piskozub*, 2006]. The wind speed range was 5 m s^{-1} < U_{10} < 12 m s^{-1} and

stability conditions were close to neutral. Concentrations of particles with ambient radii from 0.25 to 15 μm, at RH varying between 65 and 95%, were measured with an OPC [*Petelski*, 2005]; a single instrument was used for consecutive measurements at five levels between 5 and 20 m above sea level, with at least four 2 min measurements at each level.

[98] There are several concerns with this work. For many of the size ranges, the concentrations showed no obvious decrease with height [*Petelski and Piskozub*, 2006, Figures 3 and 4], with scatter around the logarithmic profile fit much larger than the stated relative uncertainties in the concentrations of 1% for particles with radius 1 μm to 20% for radius 10 μm. *Petelski and Piskozub* [2006] considered only those size bins for which the concentrations could be fitted to logarithmic profiles in height with a given accuracy, although only 60% of all measured profiles matched this criterion; such a procedure might be expected to bias the results. A wind speed dependence of U_{10}^3 was drawn on a graph of the calculated flux of surface area, although this dependence does not seem to be supported by statistical analysis (a linear least squares fit of the logarithm of the flux versus the logarithm of the wind speed results in an exponent of 1.75 ± 0.45 if all the data are included or 1.07 ± 0.71 if two data for $U_{10} < 3$ m s^{-1} are excluded).

4.3. Chemical Composition of Sea Spray Aerosol

[99] The size-dependent chemical composition of SSA, especially the distribution of organic material, is important in determining the RH-dependent growth of SSA particles and their ability to serve as CCN. Although prior work going back to the 1940s has shown the presence of organic material in SSA particles (section 1), only recently have studies attempted to quantify the organic mass fraction as a function of particle size and elucidate the production mechanisms. Here recent field measurements that complement studies that have shown substantial organic fraction of laboratory-generated SSA are examined.

[100] In a series of field measurements at Mace Head, Ireland, conducted in clean marine air with minimal anthropogenic or terrestrial influences (wind from ocean to land; number concentration of particles with radii at 40–70% RH greater than 0.007 μm less than 700 cm^{-3} and black carbon mass concentration less than 50 ng m^{-3}), O'Dowd and colleagues [*O'Dowd et al.*, 2004; *Cavalli et al.*, 2004; *Yoon et al.*, 2007] found substantially greater concentrations of organic matter in SSA during periods of high biological activity than during periods of low biological activity, which occurred during winter and during which the composition was predominantly sea salt. The enrichment of organic matter was much greater for SSA particles with ambient radius (at approximately 70% RH) in the range 0.03–0.5 μm than in the range 1–4 μm (Figure 7). During periods of low biological activity, particles with ambient radii greater than 0.25 μm were composed almost entirely of sea salt, with only 2–3% of the mass consisting of organic material and a substantial fraction of that was WSOM. For smaller particles (ambient radius 0.06–0.25 μm), sea salt accounted for about 70% of the mass, with the principal

remaining components being nss sulfate and organic carbon, each contributing about 15%. Of the organic aerosol mass, roughly 60% was WIOM. Also during high biological activity periods, larger particles (ambient radius 0.5–4 μm) were composed almost entirely of sea salt, although the organic mass fraction increased marginally to about 5%. However, in contrast to the low biological activity periods, organic material contributed 60% to the mass of particles with ambient radius in the range 0.125–0.25 μm, with the organic fraction increasing to 85% for particles with ambient radius 0.03–0.06 μm. Also striking was that the WIOM constituted approximately two-thirds of the total organic aerosol mass. Approximately half of the total WIOM mass resided in particles with ambient radius less than 0.5 μm.

[101] The hypothesis that WIOM was primary in origin was examined by O'Dowd and colleagues [*Ceburnis et al.*, 2008] by means of the vertical gradients of concentrations of aerosol constituents. Measurements were made of chemically speciated mass concentration for particles with ambient radii less than 0.5 μm at heights of 3, 10, and 30 m above the shore at Mace Head. Footprint analysis determined that the peak contribution to the flux was approximately 1.5–3 km offshore and that the vast majority of the contribution was from less than 10 km. These measurements showed that concentrations of sea salt and WIOM decreased with increasing height between 3 and 10 m (Figure 8), indicative of a surface source, whereas concentrations of WSOM and nss sulfate increased with increasing height over the same range, indicative of an atmospheric source. A concern with this study is that at times the measurements at the lower two heights were influenced by surface properties differently from the measurements at the highest level as discussed in section 4.2.1; it is thus likely that in such situations the flow at these heights was perturbed by the land and hence that observed gradients were not representative of mixing processes in the unperturbed atmosphere and cannot be used to derive quantitative flux information on transport and removal processes. Nevertheless, the gradients suggest important qualitative information on production processes, namely a surface, or primary, source for WIOM but a surface sink for WSOM, pointing to secondary aerosol formation processes. A further caveat to quantitative interpretation is that an undetermined fraction of WSOM may have originally been produced as primary WIOM and through chemical aging may have become more oxidized and hence water soluble. The similarity of mass ratio of WIOM to sea salt in ambient aerosols measured simultaneously over productive waters in the northeast Atlantic and at Mace Head by *Facchini et al.* [2008], noted above, provides additional evidence for a primary source of the WIOM in marine aerosol.

[102] A series of field studies by Bigg, Leck, and colleagues suggests that aerosol particles with dry radius smaller than 0.1 μm produced by bubble bursting over the ocean consist almost entirely of organic matter [*Bigg and Leck*, 2008]. In these studies, the particles were sampled by an impactor operating at vacuum, and their chemical properties were examined with transmission electron microscopy [*Bigg*
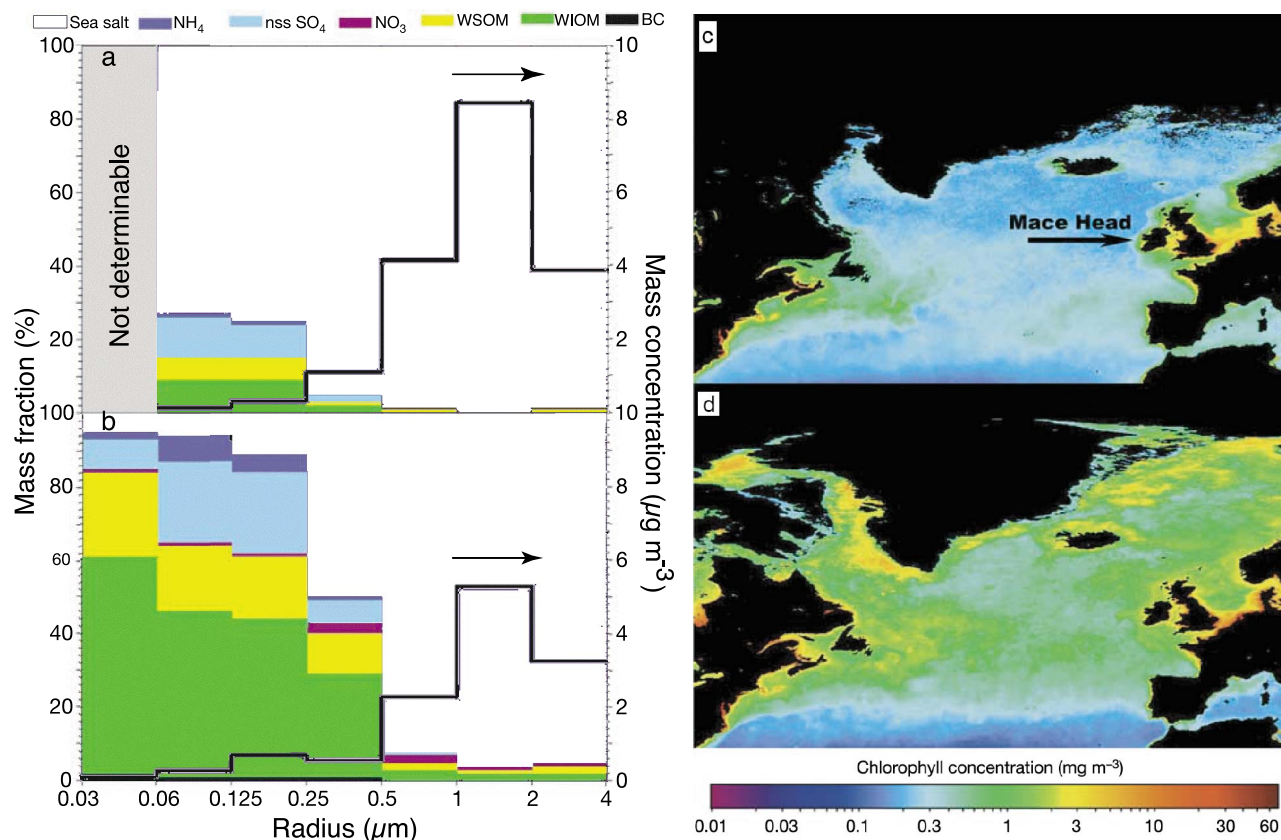
Figure 7. Average mass concentration of total particulate matter (black line, right axis) and mass fraction (colors, left axis) of sea salt, NH_4, nss SO_4, NO_3, WSOM, WIOM, and black carbon (BC) in several size ranges for North Atlantic marine aerosol sampled at Mace Head, Ireland, in clean marine air during periods of (a) low biological activity, November (2002), January (2003), and February (2003) and (b) high biological activity, March-October (2002). Radius corresponds to relative humidity approximately 70%. For low biological activity mass concentrations of aerosol constituents other than sea salt were below detection limits for the size range 0.03–0.06 μm. Oceanic chlorophyll-a concentrations over the North Atlantic for periods of (c) low and (d) high biological activity are 5 year averages (1998–2002) over the same months as for the composition measurements, based on satellite measurements of ocean color (courtesy of Sea-viewing Wide Field-of-view Sensor (SeaWiFS) Project, NASA Goddard Space Flight Center, and Orbital Imaging Corporation (ORBIMAGE)). Adapted from *O'Dowd et al.* [2004].

and Leck, 2001]. Initially, *Leck and Bigg* [1999] and *Bigg and Leck* [2001] reported occurrences of a relatively large concentration (up to 300 cm^{-3}) of solid, water-insoluble aerosol particles with dry radii less than about 0.025 μm in the Arctic marine boundary layer. These particles were accompanied by larger particles ($r_{dry} > 0.05$ μm), obviously of marine origin such as bacteria and fragments of diatoms that showed very similar characteristics to colloidal particles present in bulk seawater.

[103] Strong temperature inversions during the measurements of *Leck and Bigg* [1999] excluded the possibility of a tropospheric source, and the presence of these particles in stable air masses over the ice that had not been in contact with open water for at least 4 days suggested a surface source for the observed particles. To identify such a source, *Bigg et al.* [2004] sampled the microlayer of open water between ice floes in the Arctic and reported the presence of

suspended particulate organic matter with dry radii of 0.005–0.025 μm. Comparing the properties of the particles from the Bigg et al. microlayer samples to those of aerosol particles previously observed in the overlaying atmosphere in the Arctic Ocean, *Leck and Bigg* [2005a, 2005b] concluded that the particles originated from the ocean surface microlayer and were ejected into the atmosphere via bubble bursting.

[104] Subsequent studies in tropical regions have shown the presence of particles with r_{80} of a few hundredths of micrometers having chemical composition similar to that observed in particles in the Arctic, including exopolymer gels, marine microorganisms, fragments of marine biota, and bacteria; sea salt was markedly absent from such particles [*Leck and Bigg*, 2005b, 2008]. This, according to these investigators, suggests a common pattern over the ocean. The implications of these findings and the discrepancy
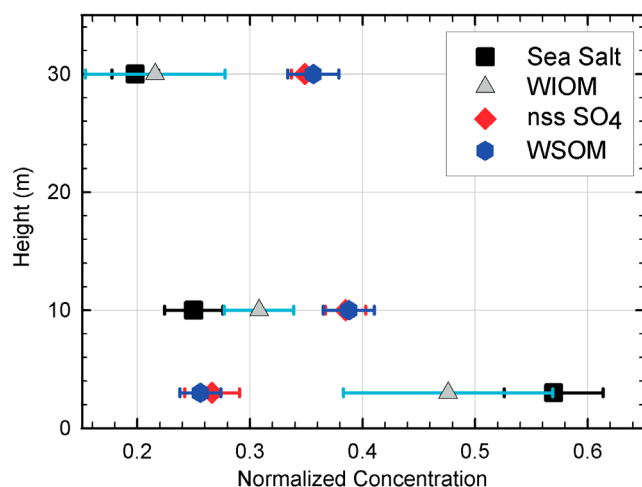
Figure 8. Vertical profiles of mass concentration of sea salt, WIOM, non-sea salt sulfate, and WSOM at Mace Head, Ireland, normalized to the sum of the concentrations of the species at the three heights, for particle radius (at ambient relative humidity) less than 0.5 μm sampled in clean marine air. All values are averages of nine individual 7 day samples analyzed from April–October 2005 except WIOM, which is shown for an average of three samples where a positive WIOM flux was observed and which represented periods when the organic-enriched waters were within the flux footprint as discussed in the text. Uncertainty bars represent the standard deviation from the normalized concentration average. Adapted from *Ceburnis et al.* [2008].

[*Leck and Bigg*, 2008] between these results and those of others are discussed in section 6.2.

5. PARAMETERIZATIONS OF THE SEA SPRAY PRODUCTION FLUX

[105] In view of the importance of the SSA as background, nonanthropogenic, aerosol over much of the planet, much effort has been directed to representing this aerosol in chemical transport models and climate models to examine its effects and those of anthropogenic aerosols on clouds, atmospheric radiation, atmospheric chemistry, and air quality. Such models generally simulate the life cycle of aerosols and therefore represent emissions, new particle formation, chemical and physical transformations, interactions with clouds, and removal by wet and dry deposition. An essential component of such life cycle models is representation of the size- and composition-dependent emission of aerosol particles as a function of time and location, specifically including primary production of SSA particles as a function of meteorological and other controlling variables. Since the publication of LS04, several new estimates of such fluxes have been presented or may be calculated from reported laboratory studies discussed in section 4.1.3. These newer formulations are discussed below and presented in Figure 9 for r_{80} (or r_{amb} or d_p) between 0.005 and 25 μm. To provide context, several previous flux estimates are also included in Figure 9. Both the recent and older formulations discussed

in this section are listed in Appendix A together with the applicable size and wind speed ranges.

[106] Nearly all formulations of the SSA production flux presented before 2004 were discussed, evaluated, and compared by LS04. Based on their analysis of these formulations and numerous other data sets these investigators presented the parameterization for the production flux of sea salt aerosol particles for 0.1 μm < r_{80} < 25 μm, which is presented in Figure 9 for $U_{10} = 8$ m s^{-1} together with its associated uncertainty to allow comparison of formulations based on newly available measurements. Several other parameterizations of the SSA production flux discussed in section 3.1 are also presented in Figure 9 at $U_{10} = 8$ m s^{-1}: those of *Smith et al.* [1993] and LS04 (together with associated uncertainty) based on the steady state dry deposition method; that of LS04 (together with associated uncertainty) based on the statistical wet deposition method; that of *Nilsson et al.* [2001] based on eddy correlation; and that of *Monahan et al.* [1986], extrapolation of this formulation by *Gong* [2003], and formulations of *Mårtensson et al.* [2003] and *de Leeuw et al.* [2000], all based on the whitecap method. The parameterizations of Mårtensson et al. and of de Leeuw et al. used the MO'M80 formulation for W as a function of U_{10} (equation (9)). The flux reported by *Nilsson et al.* [2001], a particle number production flux without size resolution, is plotted as if the flux is independent of d_p (approximately equal to r_{80}) over the indicated size range, such that the measured number flux is obtained as an integral over this range.

5.1. Whitecap Method

[107] Laboratory experiments and field measurements that have been or might be used to infer the SSA production flux per white area and its dependence on water temperature, salinity, and surfactant concentration were described in section 4.1.3. The investigations by *Tyree et al.* [2007] and *Keene et al.* [2007] provided sufficient information to permit determination of the production flux per white area. As noted in section 4.1.3, the magnitudes of these production fluxes also differed greatly depending on experimental conditions such as the bubble volume flux, resulting in large differences even among SSA production flux estimates from a given study. These estimates, used together with the dependence of W on wind speed according to MO'M80, yield size-dependent SSA production fluxes.

[108] The size dependence of the production flux per white area in the representation $dF_{wc}/d\log r_{80}$ was approximated by *Tyree et al.* [2007] as a single lognormal, with the geometric mean r_{80} between approximately 0.085 and 0.115 μm and the geometric standard deviation between approximately 1.6 and 1.8 depending on conditions, specifically bubble volume flux and pore size of the diffuser used to produce the bubbles (their Table 1). The magnitude of the concentration of the particles thus produced increased linearly with bubble volume flux (their Figure 5), implying that the production flux per white area (taken as the surface area of water in the apparatus) increased nearly quadratically with bubble volume flux according to equation (10) (Figure 5),
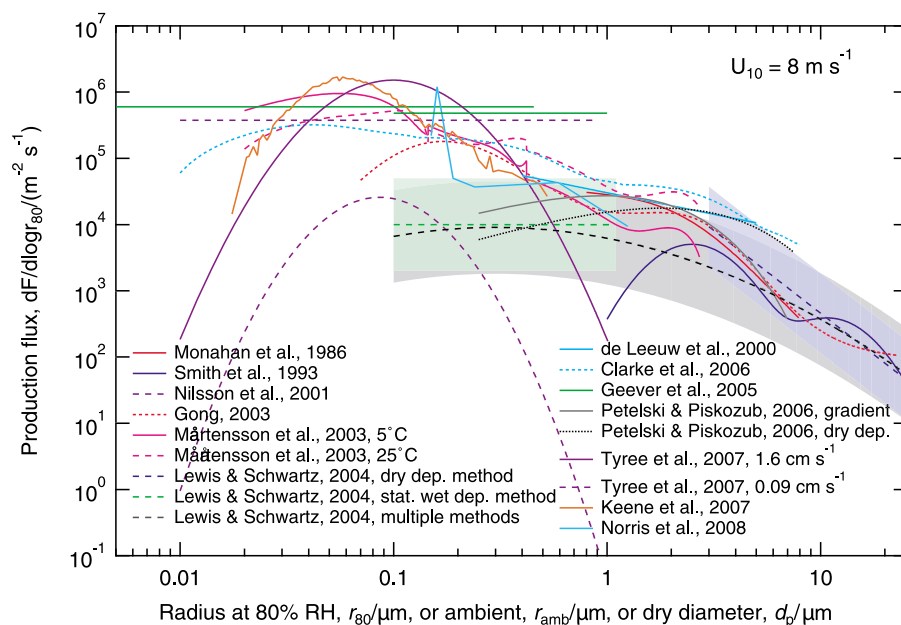
Figure 9. Parameterizations of size-dependent SSA production flux discussed in text and presented in the Appendix A, evaluated for wind speed $U_{10} = 8$ m s^{-1} (or $U_{22} = 8$ m s^{-1} for *Geever et al.* [2005]). Also shown are central values (curves) and associated uncertainty ranges (bands) from review of *Lewis and Schwartz* [2004], which denote subjective estimates by those investigators based on the statistical wet deposition method (green), the steady state deposition method (blue), and taking into account all available methods (gray); no estimate was provided for $r_{80} < 0.1$ μm. Lower axis denotes radius at 80% relative humidity, r_{80}, except for formulations of *Nilsson et al.* [2001], *Mårtensson et al.* [2003], and *Clarke et al.* [2006] which are in terms of dry particle diameter, d_p, approximately equal to r_{80} and those of *Geever et al.* [2005], *Petelski and Piskozub* [2006] (dry deposition method), and *Norris et al.* [2008] which are in terms of ambient radius, r_{amb}. Formulation of *Petelski and Piskozub* [2006] by the dry deposition method is based on expression in Appendix A. Formulations of *Tyree et al.* [2007] are for artificial seawater of salinity 33 at the two specified bubble volume fluxes. Formulations of *Nilsson et al.* [2001] and *Geever et al.* [2005] of particle number production flux without size resolution are plotted arbitrarily as if the flux is independent of r_{amb} over the size ranges indicated to yield the measured number flux as an integral over that range.

varying by nearly a factor of 60 for the different bubble volume fluxes for salinity 33. Examples of size-dependent production fluxes for artificial seawater of salinity 33 at two different bubble volume fluxes are shown in Figure 9 for $U_{10} = 8$ m s^{-1}, based on the MO'M80 parameterization for W.

[109] The SSA production flux per white area determined from the laboratory studies of *Keene et al.* [2007] exhibits a nearly linear dependence on bubble volume flux (their Figures 3 and 4), in contrast to the quadratic dependence found by *Tyree et al.* [2007] (Figure 5). An estimate of the SSA production flux at $U_{10} = 8$ m s^{-1} based on the production flux per white area for a single bubble volume flux from Keene et al. together with the MO'M80 formulation for W is shown in Figure 9.

[110] Measurements of SSA production resulting from a surf zone were used by *Clarke et al.* [2006] (section 4.1.4) to derive a new formulation for the size-dependent SSA production flux per white area for dry particle diameter (approximately equal to r_{80}) range 0.01–8 μm. This formulation together with the MO'M80 formulation for W provides a formulation for the SSA production flux; this is shown in Figure 9 for $U_{10} = 8$ m s^{-1}. According to this formulation, the daily rate of increase of the number concentration of

aerosol particles (assumed to be uniformly distributed over a marine boundary layer height of 0.5 km) for $U_{10} = 10$ m s^{-1} would be nearly 150 cm^{-3}. As discussed in section 4, Clarke et al. concluded that the majority of particles were sea salt particles.

[111] With respect to application of the whitecap method, in addition to uncertainty arising from the SSA production flux per white area, any uncertainty in whitecap fraction W also transfers directly to production flux. From examination of Figure 2, this uncertainty at $U_{10} = 8$ m s^{-1} appears to be roughly a factor of $\overset{\times}{\div}5$. Also if the lower values of W shown in Figure 2 relative to previous measurements are sustained by further observations, a high bias in W from values calculated by the MO'M80 parameterization by roughly a factor of 3 at this wind speed, previous estimates of production fluxes using that expression for W would appear to likewise be biased high by such a factor.

5.2. Eddy Correlation

[112] Eddy correlation measurements by *Geever et al.* [2005] at Mace Head (section 4.2.1) in each of two size ranges, $r_{amb} = 0.005$–0.5 μm and $d_p = 0.1$–1 μm, corrected for dry deposition to yield production fluxes, were expressed

as exponential functions of wind speed at 22 m above the sea surface, U_{22}. The resulting fluxes are plotted in Figure 9 for $U_{22} = 8$ m s^{-1}, as if the fluxes in the representation $dF/d\log r_{amb}$ (or $dF/d\log d_p$) are independent of r_{amb} (or d_p) over the respective size ranges, such that the measured number fluxes are equal to the integrals over these size ranges. According to these expressions, the daily increases in the number concentration of aerosol particles (assumed uniformly distributed over a marine boundary layer height of 0.5 km) for $U_{10} = 10$ m s^{-1} would be 320 and 135 cm^{-3} for the two size ranges.

[113] Noting that an exponential wind speed dependence can introduce an artificial bias in sea spray production at low wind speeds, *O'Dowd et al.* [2008] refitted the data in the larger size range as a power law for their regional climate model (section 5.6). This fit agreed with that presented by *Geever et al.* [2005] to within ~20% for U_{22} greater than 6 m s^{-1}, below which there were only two measurements; in view of the limited range of the measurements, it would seem that either functional form (or perhaps others) would yield equally good fits to the observations and thus it is not possible to identify a preferred wind speed dependence.

[114] Eddy correlation measurements of *Norris et al.* [2008] at Duck, North Carolina, were parameterized in terms of an exponential dependence on either U_{10} or u_* in six ranges of ambient radius. There was no clear reduction in the scatter of the flux estimates based on u_* compared to that based on U_{10}. As these measurements were not corrected for dry deposition, they yield net fluxes rather than production fluxes, although as noted in section 4.2.1, the corrections are likely small. The fluxes according to this formulation are shown in Figure 9 for $U_{10} = 8$ m s^{-1}. According to this formulation, the daily rate of increase of the number concentration of aerosol particles (assumed to be uniformly distributed over a marine boundary layer height of 0.5 km) for $U_{10} = 10$ m s^{-1} would be near 50 cm^{-3}.

5.3. Gradient Method

[115] The size-dependent production flux formulation presented by *Petelski and Piskozub* [2006], based on the gradient method using measurements of the vertical distribution of aerosol concentration, was modified by *Andreas* [2007; see also *Petelski and Piskozub*, 2007] to include a factor of κ, the von Karman constant. According to this formulation, the size dependence of the production flux depends on wind speed. This production flux, including the factor of κ, is presented in Figure 9 for $U_{10} = 8$ m s^{-1}. As noted in section 4.2.2, there are serious concerns with these measurements that limit the confidence that can be placed in this parameterization.

5.4. Steady State Dry Deposition Method

[116] The steady state dry deposition method was applied by *Petelski and Piskozub* [2006] to determine SSA production fluxes for ambient radii 0.25–7.5 μm based on concentrations of aerosol particles measured during cruises to the Arctic [*Petelski*, 2005]. The dry deposition velocity required to obtain the production flux from measured concentrations

was parameterized using a formulation of *Carruthers and Choularton* [1986], which includes only gravitational settling and turbulent diffusion (and not impaction, molecular diffusion, or growth of particles due to increased RH near the sea surface); this formulation yields dry deposition velocities that are considerably greater than those from most other formulations for r_{80} less than several micrometers. Measured concentrations were converted by *Petelski* [2005] to r_{80} values and fitted to the product of an exponential function of wind speed (despite a poor correlation) and a factor that gives the dependence on r_{80}, with a multiplicative uncertainty given as a factor of 7. Concentrations were plotted by *Petelski* [2005] for radii up to 7.5 μm, although the resulting production fluxes were plotted for radii up to only 5 μm by *Petelski and Piskozub* [2006]; as noted in section 3.2, the dry deposition method can be accurately applied only for r_{80} greater than approximately 3 μm. Additionally, as the concentrations measured by *Petelski* [2005] were not specific as to composition and included all marine aerosol particles, it was implicitly assumed that all particles counted were sea salt particles, with resultant overestimation of the production flux by the proportion of particles that were not SSA particles. The SSA production flux according to the formulation of *Petelski and Piskozub* [2006] is presented in Figure 9 (without the multiplicative uncertainty) for $U_{10} = 8$ m s^{-1}, evaluated according to the expression in Appendix A, which employs values of the drag coefficient and gravitational settling velocity not specified by these investigators.

5.5. Other Formulations

[117] Several investigators have used combinations of different SSSF formulations in models. This is evident in the models listed in Table 1. One such recent approach is that of *Caffrey et al.* [2006], which was based on the *Monahan et al.* [1986] formulation for r_{80} from 0.3 to 5 μm (although the Monahan et al. expression had been given by the original investigators for $r_{80} = 0.8$–8 μm) together with that of *Smith et al.* [1993] for r_{80} from 5 to 30 μm, as corrected by *Hoppel et al.* [2002], to account for what those investigators had considered spume drops (although it has not been established that those particles in this range were spume drops). Caffrey et al. accounted for the findings of *Mårtensson et al.* [2003] and *Clarke et al.* [2006] of a large production flux of particles with 0.02 μm < r_{80} < 0.2 μm by multiplying the *Monahan et al.* [1986] production flux (extended to $r_{80} = 0.02$ μm) by a factor (their equation (2))

$$C(r_{80}) = 0.794^{\left(r_{80}^{-0.855}\right)} \left(1 + \frac{0.4}{r_{80}}\right), \qquad (11)$$

where r_{80} is in μm (here the expression is given in terms of r_{80} rather than r_{dry} as given by Caffrey et al., with r_{80} taken as $2r_{dry}$). Production, transport, wet and dry deposition, and clear-air and in-cloud reactions of sea salt aerosol were represented in a 33 bin (0.02 μm < r_{80} < 50 μm) sectional model. For the conditions examined, SSA contributed 20–30% of the CCN concentration for the activation threshold taken as $r_{80} = 0.066$ μm.

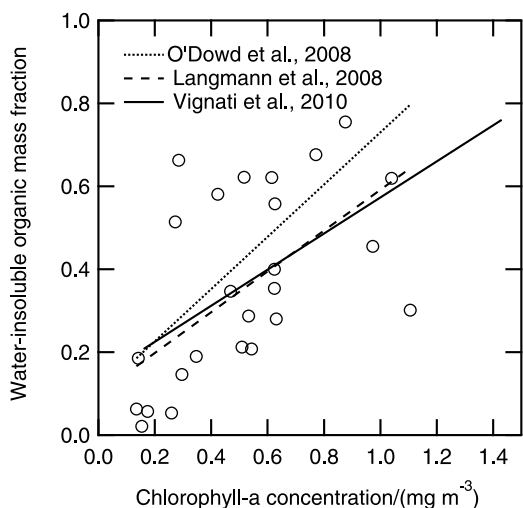**Figure 10.** Mass fraction of water-insoluble organic matter in sea spray aerosol with $0.1 \, \mu m \leq r_{amb} \leq 0.5 \, \mu m$ measured at Mace Head, Ireland, under clean marine conditions as a function of spatial average oceanic surface water chlorophyll-a concentration over an upwind grid of 1000 km × 1000 km as determined from MODIS satellite measurements of ocean color, revised from *O'Dowd et al.* [2008] and provided by C. O'Dowd (2010). Original fit presented by *O'Dowd et al.* [2008] and fits to revised data presented by *Langmann et al.* [2008b] (corrected by *Vignati et al.* [2010]) and *Vignati et al.* [2010] are also shown.

[118] Yet another production flux formulation based on that of *Monahan et al.* [1986] was presented by *Zakey et al.* [2008], who extended the Monahan et al. production flux (which had been given only for $r_{80} \geq 0.8 \, \mu m$) to $r_{80} = 0.015 \, \mu m$, multiplied by a factor to better reproduce high concentrations of SSA particles reported by *O'Dowd et al.* [1997]. Specifically, for $0.015 \, \mu m < r_{80} < 0.2 \, \mu m$ this factor is given by

$$C(r_{80}) = \exp\left\{ -6.43 \left[\log\left(\frac{r_{80}}{0.2 \, \mu m} \right) \right]^2 \right\} \qquad (12)$$

(as above, this expression is presented here in terms of r_{80} rather than r_{dry}, with r_{80} taken as $2r_{dry}$). This production flux formulation was employed in a regional climate model to determine the climate influences of sea salt aerosol. As the model represented SSA by only two size bins and as the r_{80} range of the lower size bin was $0.1–2 \, \mu m$, it would seem that the consequences of the modification to the production flux would be minimal, especially so as the reported emissions and concentrations were presented on a mass basis.

[119] Although formulations such as those of *Caffrey et al.* [2006] and *Zakey et al.* [2008] permit calculation of SSA production fluxes to r_{80} as low as $0.02 \, \mu m$ or below in large-scale models, it would seem that little confidence can be placed in such formulations or in the resultant calculations, especially in the extended size ranges owing to the large extrapolations and the paucity of data upon which they were based. As seen in Figure 9 there remains substantial

uncertainty in SSA production flux estimates in this size range.

5.6. Organic Production Formulation

[120] A key finding of recent work is the identification of a large contribution of biogenic WIOM to SSA (section 4.3). O'Dowd and colleagues have presented several formulations of the production flux of this substance and its representation in global models [*O'Dowd et al.*, 2008; *Langmann et al.*, 2008a, 2008b; *Vignati et al.*, 2010] based on the concentration of chlorophyll-a in the ocean surface layer as determined by satellite observations as a proxy for the mass fraction of WIOM in sea spray, Φ_{om}. These observations together with seasonal variation of Φ_{om} determined from measurements of aerosol chemical composition have been combined with an SSA production flux formulation to yield the oceanic production flux of WIOM associated with sea spray production and to examine WIOM emissions in several model studies.

[121] The relation between Φ_{om} and chlorophyll-a concentrations was investigated by *O'Dowd et al.* [2008] using aerosol composition measurements from the 3 year data set of *Yoon et al.* [2007] from Mace Head, Ireland, in which only clean marine air masses were sampled. It was assumed, based on experimental work discussed in section 4.3, that the aerosol mass for r_{80} less than approximately 1 μm was composed mainly of sea salt and WIOM, with a minor contribution from WSOM, arbitrarily taken as 5% of the WIOM mass concentration. Chlorophyll-a concentration, *Chl*, was taken as the spatial average over a grid of 1000 km × 1000 km upwind of Mace Head. A linear fit of Φ_{om} to *Chl* for 37 data points was presented by *O'Dowd et al.* [2008] and a revised fit, taking into account small corrections to the chemical analysis, was presented by *Langmann et al.* [2008b] (as corrected by *Vignati et al.* [2010]). More recently a fit to a subset (24) of these data was presented by *Vignati et al.* [2010] as

$$\Phi_{om} = 0.435 \left(\frac{Chl}{mg \, m^{-3}} \right) + 0.14, \ Chl < 1.43 \, mg \, m^{-3} \qquad (13)$$

(the range of validity was incorrectly stated as $Chl < 1.43 \, \mu g \, m^{-3}$ in their equation (3)). The different fits are shown in Figure 10. Only about 30% of the variance of Φ_{om} is accounted for by any of the fits.

[122] To obtain a formulation for the size-dependent production flux of WIOM in SSA, *O'Dowd et al.* [2008] assumed that the size dependence of the SSA production flux was given by a lognormal distribution with the geometric mean value of r_{80} given as a function of time of year, so as to capture changes in Φ_{om} (although a more physically based quantity such as water temperature or chlorophyll-a concentration would be more appropriate). The magnitude of the SSA production flux was given by the formulation of *Geever et al.* [2005] for particles with dry diameter $d_p = 0.1–1 \, \mu m$, which was refitted to a power law as $F \ (m^{-2} \ s^{-1}) = 1.854 \times 10^3 \ U_{22}^{2.706}$. The WIOM mass fraction Φ_{om} was constrained to a maximum value of 0.9.
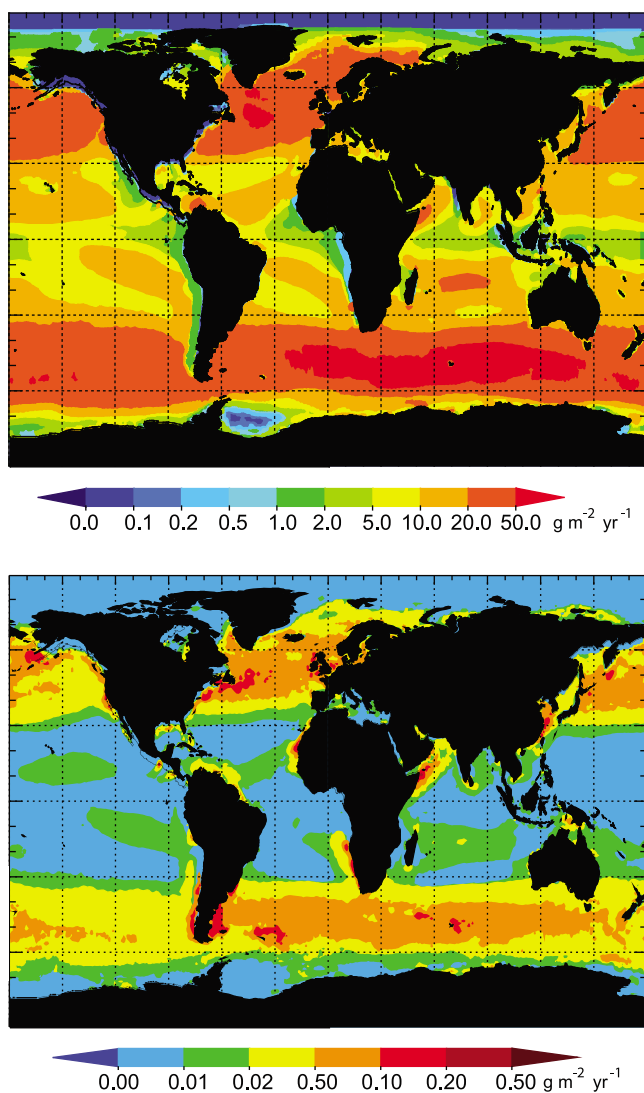
Figure 11. Global distribution of mass flux of (top) sea salt and (bottom) water-insoluble organic matter in sea spray with $0.1 \ \mu m < r_{80} < 1 \ \mu m$ averaged over a 1 year period in 2002–2003 using the TM5 chemical transport model [*Vignati et al.*, 2010; E. Vignati, private communication, 2010].

This procedure yielded a parameterization of the production flux of SSA number and chemical composition for particles with an approximate r_{80} range $0.1–1 \ \mu m$ and was combined with monthly average wind speed fields (from SeaWinds on the QuickScat satellite) and chlorophyll-a concentrations (from Moderate Resolution Imaging Spectroradiometer (MODIS) Aqua and Terra satellites) to produce estimates of the global annual production of WIOM as 2.3 Tg C yr^{-1} for 2003 and 2.8 Tg C yr^{-1} for 2006 [*Langmann et al.*, 2008b].

[123] A similar approach was used by *Vignati et al.* [2010] to determine the production flux of WIOM associated with sea spray in the accumulation mode (approximate r_{80} range $0.1–1 \ \mu m$), for which the size dependence of the production flux was assumed to be a lognormal with geometric mean radius at 80% RH equal to $0.09 \ \mu m$ and the magnitude of the production flux was that of *Gong et al.* [2003]. The maxi-

mum value of Φ_{om} was constrained to 0.76. This formulation was used in a global chemical transport model to determine the production of WIOM and sea salt in this mode for a 1 year period in 2002–2003 (Figure 11). Global annual emissions of WIOM and sea salt in this mode were 8.2 and 24 Tg, respectively. It should be noted that there is likely a significant but to date unquantified flux of WIOM in particles with $r_{80} > 1 \ \mu m$ [*Facchini et al.*, 2008]. The production rate for WIOM estimated by *Vignati et al.* [2010] was nearly 3 times that reported by *Langmann et al.* [2008b]; no reasons for the difference were presented. A possible explanation is that the model of Langmann et al., in contrast to that of Vignati et al., used a single fixed particle size ($r_{80} = 0.09 \ \mu m$) and did not account for possible variation of particle size with *Chl*.

[124] Although a calculation such as this can hardly be taken as a definitive estimate in view of the uncertainties associated with the production flux formulation, the estimate of the organic fraction of the primary SSA emission flux, and the poor correlation between satellite determinations of chlorophyll-a concentrations and organic mass fraction, this methodology suggests an approach for modeling these emissions on a global scale as input to chemical transport models and climate models.

6. DISCUSSION

[125] As discussed in section 1, there is continuing and indeed heightened interest in characterization of the number concentration, composition, and other properties of SSA and in the processes that govern its production. Unfortunately, the present state of understanding of production, concentrations, and removal rates of SSA particles is so low that it is not possible to constrain the mass emission flux even to an order of magnitude, as reflected in the differing emission rates shown in Figure 1, and the situation for particle number production is even more uncertain.

[126] This review has examined recent findings regarding the size-dependent production of SSA and parameterizations of this production flux since the critical review of *Lewis and Schwartz* [2004]. New work has added a substantial body of findings to those which were presented in that review. An important new finding is the recognition that sea spray contains other substances in addition to sea salt and that the major and in some instances dominant contribution to SSA in some size ranges is from organics, especially at smaller sizes. Along with this finding comes the recognition that SSA production extends to much lower sizes than were previously recognized, with both laboratory experiments and field measurements showing substantial production of SSA at values of r_{80} below $0.1 \ \mu m$ and down to as low as $0.01 \ \mu m$, as many of these smaller particles are composed primarily of organic substances. However, despite the new work, there seems to be little convergence on understanding important elements of the SSA production process, as characterized by quantities needed to determine SSA production fluxes such as the flux per white area and the whitecap fraction. This discussion examines the several approaches taken in recent

work to measure the quantities pertinent to the determination of SSA production flux, its dependence on controlling variables, and the numerical representation of this production flux.

6.1. Laboratory Investigations of SSA Production

[127] Key among the findings of recent work is the demonstration in laboratory experiments that the SSA production flux per white area can depend strongly, by up to 2 orders of magnitude, on the volume flux of air in bubbles passing through the white area (Figure 5). However, experiments to date have explored only a very limited subset of the physical and chemical variables controlling SSA production flux per white area. With respect to physical conditions, the studies of *Tyree et al.* [2007] and *Keene et al.* [2007] relied on artificial constraints on the size of the bubble swarm reaching the surface, specifically confinement of the resulting white area by the walls of the vessel in which these bubbles were produced. Whether such a constraint is a good mimic of the barrier to lateral diffusion of bubbles in an unconfined situation such as the open ocean following entrainment of air during wave breaking is not known. One fruitful line of future investigation would be systematic examination of the SSA production flux as the flow rate of air is varied through an array of multiple diffusers (frits) in a vessel sufficiently large that the spread of the bubble swarm would not be limited by the vessel walls. Likewise it would seem essential to examine other possible reasons for differences between the production flux per white area in the studies of *Mårtensson et al.* [2003], *Tyree et al.* [2007], *Keene et al.* [2007], and *Fuentes et al.* [2010] such as dependence of production flux per white area on the depth of the diffuser producing the bubbles, which differed in these experiments by more than an order of magnitude, from a few centimeters to more than a meter. Another fruitful line of investigation might be the systematic examination of the effects of temperature on bubble formation, bubble dynamics, and bubble bursting as components of the SSA production process. Experiments such as these would permit measurement of the bubble spectrum and volume flux that might be compared to such fluxes following wave breaking in the open ocean.

[128] Oceanic bubble spectra obtained to date are averages over long periods and thus include breaking waves and background spectra which do not contain the large bubbles generated just after wave breaking, which are responsible for the generation of film drops. These very large bubbles are probably not generated in any of the laboratory experiments discussed above. Considerations such as these also invite determination of the bubble spectrum and volume flux resulting from wave breaking as a function of location and time relative to wave breaking in laboratory studies and in the open ocean and relating bubble volume flux and SSA production in such studies to "whiteness" determined by optical measurements. Also, a systematic examination of the dependence of SSA production flux on bubble volume flux (and perhaps other variables) beyond the measurements reported to date would be useful, especially given the substantial differences reported by different investigations shown in Figure 5. Such studies would be valuably informed by laboratory investigations examining the dependence of SSA production on means of bubble production such as that of *Fuentes et al.* [2010]. It might be noted that for none of these methods is it established that the bubble spectrum and resultant SSA production are representative of open ocean conditions. In this regard the conclusion reached by some of the investigators that a weir is more appropriate than bubbles produced by diffusers for generating SSA has little justification.

[129] A further open question amenable to laboratory investigation is the mechanism responsible for the temperature dependence of SSA production that has been observed in laboratory experiments [*Mårtensson et al.*, 2003; *Sellegri et al.*, 2006], as temperature might affect bubble generation at the frit employed to generate the bubbles and the dynamics of bubble rise in addition to the production of particles associated with bubble bursting through the temperature dependence of viscosity, surface tension, or other controlling properties. Systematic examination of these dependences might lead to improved understanding and parameterization of the overall dependence of SSA production on temperature.

6.2. Composition of SSA

[130] A very important line of investigation in recent studies has been the dependence of SSA composition as a function of particle size in laboratory experiments and field measurements and the role of seawater composition on particle composition. These studies have shown, especially for particles with $r_{80} < 0.25$ μm, that organic material can comprise a substantial fraction of SSA particles that approaches unity, especially under conditions of high biological activity [*O'Dowd et al.*, 2004; *Facchini et al.*, 2008]. It seems increasingly likely that production of particles highly enriched in organic material derives from fragmentation of the film cap from which much of the seawater has drained prior to bursting, leaving behind a film that is highly enriched in surfactant material. Laboratory studies with flowing seawater (on ships or at coastal laboratories) would be well suited to systematic examination of such influences, especially as studies with organic compounds introduced into laboratory-prepared artificial seawater as proxies for actual oceanic organic material have not proved very successful in reproducing the effects observed in actual seawater. These studies also raise questions regarding the attribution of high-production fluxes of SSA particles to inorganic sea salt in instances where the composition has not been determined by chemically specific methods. It appears [e.g., *Bigg and Leck*, 2008] that the water-insoluble organic matter associated with very small particles may be persistent at temperatures as high as 300°C, which have been used in many studies to distinguish what has been taken as refractory material such as inorganic sea salt from substances such as sulfates and secondary organic matter which are volatilized at such temperatures. Thus, the use of volatility alone is not sufficient to determine the composition of particles that originate from the

ocean surface and suggest the need for specific chemical determination in future such studies.

[131] A major development in the past several years has been sustained measurements of the size-distributed composition of marine aerosol at a coastal site downwind of open ocean. By restricting the measurements to the oceanic sector it has been possible to obtain a much larger data set than would be available from cruises of limited duration. Although there is much precedent for such measurements at island and coastal sites [*Prospero*, 2002] that has established the role of long-range transport of mineral dust and continental anthropogenic aerosols to the marine environment, the new measurements show the value of much better size resolution in the range $r_{80} < 1$ μm together with determination of the size-dependent organic component of the aerosol. Importantly, these measurements have shown that the organic material is present predominantly in particles of $r_{80} \lesssim 0.5$ μm. Examination of vertical profiles of composition (Figure 8) provides convincing evidence that the organic material, specifically WIOM, has an origin at the sea surface, i.e., is a component of SSA.

[132] Extended measurements of size-distributed composition of marine aerosols over several years [*O'Dowd et al.*, 2004; *Facchini et al.*, 2008] have permitted examination of the hypothesis that WIOM is of biological origin, specifically from surfactant materials in the surface layer that arise from biological activity, perhaps exudates or chemical decomposition products of organisms. The data from these measurements have been employed in a first systematic attempt to relate organic material in marine aerosol to biological activity in seawater by examination of correlation with *Chl* obtained from satellite measurements of ocean color [*O'Reilly et al.*, 1998]. Although aerosol organic fraction exhibited some correlation with *Chl* ($r^2 = 0.3$), there is much variation in this fraction that is not accounted for in the oceanic chlorophyll data product (Figure 10). As this variation is much greater than the scatter between in situ measurements of *Chl* and the satellite data product [*O'Reilly et al.*, 1998], it would seem that *Chl* is not wholly adequate as a proxy for the biological activity responsible for the organic material comprising the aerosol. Nonetheless, the relationship between aerosol organic matter and satellite-determined oceanic chlorophyll concentration provides convincing evidence of the role of biological activity in producing this organic matter.

[133] The correlation of organic matter in SSA with satellite-derived *Chl* found by O'Dowd and colleagues [*Vignati et al.*, 2010] has been incorporated into a parameterization of the organic component of a SSA production flux to calculate the global distribution of WIOM production. However, this correlation is based only on measurements at a single nonrepresentative site being a region of high biological productivity; this situation suggests the need for additional similar studies at other locations. For these reasons, at the present stage of understanding calculations such as those of Vignati et al. should perhaps be viewed more as proof of concept than as definitive estimates of the globally distributed production of primary marine organic aerosol. Certainly, the insights gained thus far by the extended measurement campaigns by O'Dowd and colleagues at the Mace Head, Ireland, site suggest the utility of conducting such measurements at other sites characterized by different temperature, different biological productivity, and the like to build a more comprehensive global picture of the composition of marine aerosols generally and of the concentration and properties of sea spray aerosol.

[134] Although the identification and quantification of organic material in very small SSA particles represents a substantial advance, an important piece of the picture that is still missing is the mixing state (internal versus external) of sea salt and organic matter in particles in the r_{80} range from approximately 0.05 to 0.2 μm. This mixing state would be expected to influence the ability of these particles to serve as CCN and consequently their turnover times against removal through wet deposition. The suggestion of recent research that many, perhaps most, of the SSA particles with $r_{80} \lesssim 0.1$ μm consist of WIOM thus has important implications for the budget of these primary aerosol particles. The need for information on particle mixing state suggests the utility of alternative means of characterizing the composition and properties of SSA particles. Aerosol mass spectrometry and single-particle aerosol mass spectrometry provide real-time information on aerosol composition that has greatly informed understanding of aerosol properties and processes in terrestrial environments but that has thus far seen limited application in the marine environment and specifically for characterization of SSA particles. It seems likely as well that much important information on the properties of SSA particles would be gained from developing and applying techniques that can determine the composition of particles with $r_{80} < 0.1$ μm, which are difficult to study by mass spectrometry such as transmission electron microscopy, which can examine the composition and structure of individual particles, or more exotic techniques such as X-ray absorption fine structure, which can determine composition and oxidation state of material present in ensembles of particles.

[135] The variability in the amount and nature of organic material and the resulting surfactants in seawater would appear to be major sources of variability in the SSA production flux. Based on a combination of laboratory experiments with observations on the open ocean and at the coastal site at Mace Head, *Facchini et al.* [2008] showed that the composition of particles generated in laboratory experiments with bursting bubbles was similar to that observed in aerosols in the open ocean. Furthermore, the seasonality of sea spray emissions and chemical composition follows the chlorophyll cycle obtained using satellite measurements [*Sellegri et al.*, 2006]. When biological activity is low in the ocean with resultant low concentrations of organic matter in the ocean surface layer, sea spray is comprised predominantly of inorganic sea salt. In contrast, when biological activity is high and organic matter is present at the ocean surface, this organic matter is enriched in sea spray particles with $r_{80} < 0.25$ μm. These considerations suggest that improving knowledge in this area will require combinations

of laboratory and field experiments and that this effort will require multidisciplinary cooperation among oceanographers, marine biologists, meteorologists, physicists, and chemists to understand the effects of biological species such as phytoplankton and algae on the formation, physical properties, and composition of SSA.

[136] Although O'Dowd and colleagues [*O'Dowd et al.*, 2004; *Cavalli et al.*, 2004; *Yoon et al.*, 2007; *Facchini et al.*, 2008] report the fraction of the mass of SSA particles that is composed of organics varying, depending on the season and the size of the particles, from 2–3% to 60–80% (section 4.3), *Bigg and Leck* [2008] argue that bubble-mediated particles with $r_{80} < 0.1$ µm are purely organic (section 4.3). In contrast, the experiments by *Clarke et al.* [2006] argued that particles with $r_{80} > 0.03$ µm produced from breaking waves in the surf zone were composed almost entirely of sea salt. The contrasting findings raise the question of whether *O'Dowd et al.* [2004] and *Leck and Bigg* [2008] observed the same type of particles. For example, the size distributions of concentration reported by *Bigg et al.* [2004] appeared as two separate modes, whereas *O'Dowd et al.* [2004] observed a continuous size distribution of organic aerosols.

6.3. Whitecap Fraction

[137] A further important line of recent investigation is the examination of the dependence of the whitecap fraction on controlling factors. Recent studies using digital photographic techniques have indicated systematically lower whitecap fraction at a given wind speed (by as much as a factor of 4 or so) than has characterized the bulk of previous determinations of this quantity as summarized by LS04. The reasons for this difference are not known, although one possibility is differences in technique, for example, differences in the dynamic range of digital photography versus that of film; a similar situation resulted in the whitecap fraction as determined by analog video being an order of magnitude lower than that determined by film photography. It is clear that the reasons for these differences need to be better understood than they are at present.

[138] Studies examined in section 4.1.1 reported advances in image processing, specifically in defining thresholds that distinguish white area from nonwhite area. However, although such approaches to defining thresholds remove the subjectivity from determining white area in individual images, this subjectivity is transferred to the choice of the threshold for the batch processing. More intrinsically, it is not established which if any threshold yields a white area that corresponds to that for which the flux per white area has been determined in laboratory studies. It seems likely that there may be variation in the "whiteness" that characterizes the bubble swarm that follows a breaking wave as the bubble volume flux diminishes with time following a wave breaking event; a whitecap property such as this would be much more useful than an arbitrary threshold of "white" in relating SSA production flux to white area and ultimately in developing more accurate parameterizations for SSA production flux.

[139] A major strength of the digital photography technique is the ability to quantitatively examine the temporal variation of white area both by following the course of white area and whiteness subsequent to the breaking of individual waves and by statistical techniques such as examination of the temporal autocorrelation of whiteness, which may yield information on the statistical independence of successive photographs and on the duration of white area following wave breaking as a function of wind speed thus leading to improved estimates of whitecap behavior and of SSA production flux.

[140] Another recent advance is the availability of satellite determination of whitecap fraction through microwave radiometry. Initial developments show that this approach offers the potential for further understanding and parameterizing this quantity and for determining W globally on spatial scales of 50 km with daily or better temporal resolution, which could in turn diminish the uncertainty of SSA production as obtained with the whitecap method. However, at present there are discrepancies of an order of magnitude or more between whitecap fraction determined by satellite-borne microwave radiometers and those determined by photographic measurements at visible wavelengths, especially the high values of W found at low wind speed by the microwave measurements (Figure 3); possible reasons for these discrepancies are examined in section 4.1.2. Based on these comparisons satellite measurements are not sufficiently accurate at present to provide reliable estimates of whitecap fraction. It would seem essential to use airborne radiometers in conjunction with simultaneous airborne photographic measurements to facilitate further developments of this approach.

6.4. SSA Production Flux Parameterization

[141] Many parameterizations of the SSA source function continue to be based on the whitecap method, according to which the SSA production flux is evaluated as the product of the production flux per white area, assumed to be a constant in both the magnitude of the flux and the size dependence, independent of the nature or properties of the white area, and the whitecap fraction, a function of meteorological and ocean conditions but in practice parameterized mainly in terms of wind speed (equation (9)). It should be stressed that the separability of the production flux into the product of two such independent quantities remains an unproved assumption. Indeed this separability is subject to increasing question, especially on the basis of recent laboratory studies and field measurements summarized in Figure 4, which show strong differences in the size dependence of the SSA production flux under different conditions. These differences, if not measurement artifacts, are orders of magnitude in some size ranges. Likewise the measurements of the production flux per white area of *Tyree et al.* [2007] and *Fuentes et al.* [2010] indicate that the magnitude of this quantity can depend strongly on the nature of the white area. Finally, the composition, especially of particles with $r_{80} < 0.25$ µm, depends strongly on the organic composition of the seawater as determined by in situ measurement or as

inferred from proxy measurements. In sum, these measurements raise important questions over the accuracy of the whitecap method in its current formulation (equations (3), (8), and (9)), especially as this method has provided parameterizations for the SSA production flux which are widely used by the aerosol modeling community. It would thus seem essential to reexamine the premises of the whitecap method in laboratory experiments and field measurements to determine how this method can be reformulated.

[142] Alternatively, the SSA production flux determined by field measurements for particular meteorological conditions and ocean state can be compared to that evaluated by the whitecap method for the wind speed of the measurement and/or to that evaluated for whitecap fraction. In this respect, the measurements of *Clarke et al.* [2006] of SSA production in the surf zone and of *de Leeuw et al.* [2007] and *Norris et al.* [2008] of SSA production at a coastal site during onshore winds provide determinations of SSA production under specific meteorological and oceanic conditions. Such measurements, in principle, could be extended to a variety of conditions. It would also be important to increase the size resolution of such measurements in view of the large variation in particle properties such as CCN activity within the range of size bins of existing instrumentation. The surf zone method would seem limited in its application to rather specific situations and might suffer from site-specific conditions that make the results not representative of the open ocean (e.g., the influence of bottom drag on the wave breaking process). Eddy correlation with fast, size-resolved measurements of the net particle flux, which may be employed on long piers, offshore platforms, or ships in the deep ocean, might provide a repertoire of measurements that would permit evaluation of the whitecap method and/or become the basis for a more differentiated picture of the SSA production flux and its dependence on controlling variables.

[143] Recent estimates of the SSA production flux (Figure 9) appear to be greater than previous estimates, especially toward smaller particle sizes. Although these new estimates coincide with that of LS04 for the largest particles ($r_{80} \gtrsim 3$ μm), toward smaller sizes they are increasingly higher, by up to 1–2 orders of magnitude at $r_{80} = 0.1$ μm, near which size these fluxes, in the representation $dF/d\log r_{80}$, exhibit their maximum values. Possible reasons for and consequences of this behavior are discussed in section 6.5.

6.5. Consistency Between SSA Production and Observed Particle Concentrations

[144] As the number concentration of aerosol particles in clean marine air, often as low as 200 cm^{-3} (section 3), is controlled by transport, production, and removal, consideration of rates of removal processes together with reported number concentrations leads to a check on the consistency of estimates of SSA production flux by various formulations.

[145] Removal processes are wet deposition, dry deposition, and coagulation onto larger particles and cloud drops, of which wet deposition is dominant in most circumstances. Coagulation in the marine atmosphere is almost certainly

not important for two reasons: first, the low concentration of aerosol particles that could scavenge such smaller particles and second, the low diffusion coefficients of these small particles, with that for particles with $r_{80} > 0.01$ μm being too low for this to be an important process. Coagulation on cloud drops is slow for similar reasons and is diminished further by the time that particles spend in clouds at the top of the marine boundary layer. For particles of the sizes under consideration, dry deposition, through gravitational sedimentation, impaction on and diffusion to the sea surface, although highly uncertain, is expected to be so slow that characteristic removal times would be at least several days to a week. Removal through activation during nonprecipitating periods might still occur, but cloud drop concentrations are too low for this to be a major removal mechanism, and additionally, a large fraction of the marine aerosol particles of the size range under consideration are too small to activate in the low-updraft conditions of the marine environment. The major removal mechanism is thus almost certainly wet deposition, through both activation to form cloud drops that precipitate and scavenging by falling hydrometeors, which typically occurs on a time scale of several days. Thus, unless other currently unknown or unappreciated loss processes are found, it must be concluded that characteristic turnover times of SSA particles with $r_{80} < 0.1$ μm are several days.

[146] A turnover time of 3 days [LS04, p. 72], together with the assumption of a typical marine boundary layer height of 0.5 km and the observation that the marine boundary layer is largely decoupled from the free troposphere (implying little transport out of the marine boundary layer), allows estimation of the number concentration of SSA particles that would be expected to be present in the marine boundary layer for a given SSA production flux. For this flux taken as 1×10^6 m^{-2} s^{-1} as is indicated by several of the production flux formulations shown in Figure 9, the rate of increase in concentration would be nearly 200 cm^{-3} d^{-1}, resulting in a steady state number concentration of sea spray particles alone of about 500 cm^{-3}. Such a concentration would be comparable to or exceed typical measured number concentrations of all marine aerosol particles in clean conditions, several hundred per cubic centimeter (section 3.1), raising concerns over formulations yielding such large production fluxes. This concern is heightened by the fact that aerosol particles in the clean marine boundary layer may derive from sources other than production at the sea surface and the resultant possibility that SSA particles often constitute only a fraction, perhaps only a small fraction, of measured total particle number concentrations. Apportionment of the particles that derive from primary production at the sea surface is difficult and this difficulty hinders extension of the statistical wet deposition method beyond sea salt aerosol (as by LS04) to sea spray aerosol.

7. CONCLUSIONS

[147] A major finding of recent work is the recognition of the large contribution of organic substances to SSA particles, especially in locations of high biological activity,

which becomes increasingly important with decreasing particle size and may be dominant for $r_{80} < 0.25$ μm, leading to the distinction noted in section 1 between *sea salt* particles (the focus of the review by LS04) and *sea spray* particles. Possible consequences of this difference in composition are differences in properties such as cloud-drop activation and resultant error in models that do not account for these differences.

[148] Determinations of the SSA production flux have been made at sizes smaller than those previously examined, with some formulations extending to particle size as low as $r_{80} = 0.01$ μm; no estimate for the production flux of sea salt aerosol particles with $r_{80} < 0.1$ μm was presented by LS04. However, as noted above, uncertainties remain in the composition of such particles and in what is responsible for the variable amount of organic material in these particles. Additionally, the magnitude and the size distribution of the production flux of particles with $r_{80} < 0.3$ μm are both highly variable (Figures 4 and 9), and laboratory experiments have demonstrated that the means by which the white area is produced results in large differences in both of these quantities that cannot be accounted for by factors such as temperature. Consequently, it must be concluded that the assumption, central to applications of the whitecap method, that the SSA production flux per white area is independent of the means by which that white area is produced is not valid, and thus determinations of the SSA production flux based on the whitecap method are potentially subject to large error. A possible fruitful direction for research would be to investigate the dependence of the SSA production flux on the means of production of white area, as discussed in section 6.1.

[149] The best estimate for the production flux of SSA particles with $r_{80} > 1$ μm remains that given by LS04 based on multiple methods, with uncertainty a multiplicative factor of $\overset{\times}{\div} 4$–5 (Figure 9; dashed black line and gray shaded region). For decreasing r_{80} from 1 to ~0.3 μm, recent flux determinations are increasingly greater than the best estimate of LS04, and for smaller sizes, they are greater still. However, a concern with such large SSA production flux formulations is that they imply number concentrations for SSA particles in the marine boundary layer that are unrealistically high as discussed in section 6.5. The realization that some or much of the aerosol may consist of organic matter rather than sea salt may resolve some of but by no means all this discrepancy.

[150] Recent advances in determination of the whitecap fraction W, also central to evaluation of the SSA production flux by the whitecap method, by both photographic methods and satellite retrievals may eliminate some of the subjectivity in measurement of this quantity, but direct relation to SSA production is lacking. Recent determinations of W by digital photographic measurements are systematically lower, by up to a factor of 4, than those previously determined by film photography for reasons that are not yet understood. Satellite retrieval of W by brightness temperature at microwave frequencies is a promising possibility, but this approach is currently unable to capture the dependence of

this quantity on wind speed that is exhibited in photographic measurements at visible wavelengths.

[151] Based on long-term measurement of aerosol chemical composition and its relation to biological activity at a coastal site (Mace Head, Ireland), it is clear that similar data sets from other sites could permit assessment of the generality of conclusions drawn from those measurements and more broadly on the factors that control the properties of marine aerosols. Additionally, measurements of composition and structure of individual marine aerosol particles with $r_{80} < 0.1$ μm at multiple sites and over multiple seasons would provide a wealth of data that could help elucidate sources and production mechanisms. Laboratory experiments of SSA production under varying conditions and determination of the composition of these laboratory-generated particles may provide some insight into controlling mechanisms, but it would seem that direct measurement of SSA fluxes, e.g., by eddy correlation measurements, would yield a quicker route to determination of the SSA production flux and in any event would be essential to evaluate models of the production flux.

[152] Despite the many gains in understanding in recent years, the uncertainty in the SSA production flux remains sufficiently great that present knowledge of this quantity cannot strongly constrain the representation of emissions of SSA in chemical transport models or climate models that include aerosols. As a consequence, it is not yet possible to improve the modeling of these emissions much beyond the state of affairs represented in Figure 1, which shows a nearly 2 orders of magnitude spread in current estimates of global annual SSA emissions. It is also clear that this situation cannot be resolved by demonstration of the ability to generate reasonable concentration fields with one or another source function, given the demonstrated ability of such greatly varying emissions to yield concentration fields that compare reasonably with observations [*Textor et al.*, 2006]. Rather it would seem essential that the SSA production flux be constrained directly by field observations or preferably be overconstrained by consistency of determinations by multiple approaches.

[153] In addition to representing mass concentrations of SSA in chemical transport models and climate models, it is essential that such models also include some representation of SSA number concentration, both magnitude and size distribution, given the importance of these aerosol properties: magnitude affects cloud properties and both magnitude and size distribution affect the optical depth (commonly used as a measure of skill of such models) and atmospheric radiation transfer. Finally, as it is becoming clear that the organic fraction of SSA depends on particle size and likely on the composition of seawater as influenced by biological activity, it would seem important that this component of SSA be represented in models, especially as composition may exert a strong influence on the cloud nucleating properties of these aerosols, affecting the microphysical properties of marine clouds and the sensitivity of cloud properties to perturbation by anthropogenic aerosols.

TABLE A1. Coefficients for the Expression for the SSA Production Flux of *Mårtensson et al.* [2003] for Salinity 33 in Each of Three Size Ranges[a]

	d_p Range (μm)		
	0.02–0.145	0.145–0.419	0.419–2.8
a_0	$-(1.00013 + 0.11063T) \times 10^2$	$(1.6786 - 0.02589T) \times 10^3$	$(6.0442 + 0.8375T) \times 10^1$
a_1	$(3.8735 - 0.011532T) \times 10^4$	$-(2.1336 - 0.045437T) \times 10^4$	$-(1.2545 + 0.15994T) \times 10^2$
a_2	$-(3.9944 + 0.11009T) \times 10^5$	$(1.1611 - 0.03129T) \times 10^5$	$(9.9094 + 1.2027T) \times 10^1$
a_3	$(1.6611 + 2.2779T) \times 10^5$	$-(2.8549 - 0.092314T) \times 10^5$	$-(3.3435 + 0.37789T) \times 10^1$
a_4	$(5.8236 - 0.98918T) \times 10^6$	$(2.5742 - 0.09416T) \times 10^5$	$(4.0196 + 0.41664T)$

[a]Temperature T is in °C. The expression does not yield values that match at the junctions of the intervals. The coefficients listed here yield values that are within 0.25% of those of *Mårtensson et al.* [2003]; rounding the coefficients may yield results that differ by a greater amount.

APPENDIX A: SSA PRODUCTION FLUX FORMULATIONS

[154] This appendix presents expressions for the SSA production flux based on previously published formulations. The units of total and size-dependent fluxes (F_{eff}, $dF_{eff}/d\log r_{80}$, $dF_{int}/d\log r_{80}$, $dF_{int}/d\log d_p$, $dF_{eff}/d\log r_{amb}$, and $dF_{net}/d\log r_{amb}$) are m^{-2} s^{-1}; U_{10} and U_{22} are m s^{-1}; and d_p (dry mobility diameter; $d_p \approx r_{80}$ for most sizes), r_{amb} (ambient radius), and r_{80} are μm.

A1. Steady State Dry Deposition Method

[155] Expressions based on prior formulations are as follows:
[156] 1. From *Smith et al.* [1993],

$$\frac{dF_{eff}}{d\log r_{80}} = 1400 \times \exp(0.16\, U_{10}) \exp\left\{-3.1\left[\ln\left(\frac{r_{80}}{r_1}\right)\right]^2\right\}$$
$$+ 0.76 \times \exp\left(2.2\, U_{10}^{1/2}\right) \exp\left\{-3.3\left[\ln\left(\frac{r_{80}}{r_2}\right)\right]^2\right\},$$

where $r_1 = 2.5$ μm and $r_2 = 11$ μm, for $r_{80} = 1$–25 μm (as noted above, this formulation cannot be accurately applied to particles with $r_{80} \lesssim 3$ μm) and for $U_{10} < 34$ m s^{-1}.

[157] 2. Following *Lewis and Schwartz* [2004],

$$\frac{dF_{eff}}{d\log r_{80}} = \left(800\, \frac{U_{10}^{2.5}}{r_{80}^{2.5}}\right) \overset{\times}{\div} 4,$$

for $r_{80} = 3$–25 μm and $U_{10} = 5$–20 m s^{-1}.
[158] 3. From *Petelski and Piskozub* [2006],

$$\frac{dF_{eff}}{d\log r_{80}} = \frac{70 \exp(0.21\, U_{10})\, r_{80}^3 \exp(-0.58\, r_{80})}{1 - \exp\left(\frac{-0.11\, r_{80}^2}{U_{10}}\right)} \overset{\times}{\div} 7,$$

for $r_{80} = 0.25$–7.5 μm (as noted above, this formulation cannot be accurately applied to particles with $r_{80} \lesssim 3$ μm) and for $U_{10} < 17$ m s^{-1}; this expression was obtained from that presented by the original investigators with drag coefficient taken as 0.0013 and gravitational terminal velocity (Stokes' law) as given by equation (2.6–8) of LS04.

A2. Statistical Wet Deposition Method

[159] *Lewis and Schwartz* [2004], presented the formulation

$$\frac{dF_{eff}}{d\log r_{80}} = 10^4 \overset{\times}{\div} 5,$$

for $r_{80} = 0.1$–1 μm and $U_{10} = 5$–20 m s^{-1}.

A3. Whitecap Method

[160] Previously published formulations for $dF_{wc}/d\log r_{80}$ have been converted to $dF_{int}/d\log r_{80}$ using $W(U_{10})$ from *Monahan and Ó Muircheartaigh* [1980], as follows:
[161] 1. From *Monahan et al.* [1986], based on laboratory experiments

$$\frac{dF_{int}}{d\log r_{80}} = 3.2\, U_{10}^{3.41} r_{80}^{-2}\left(1 + 0.057\, r_{80}^{1.05}\right)$$
$$\times \exp\left\{2.74 \times \exp\left[-2.4(0.38 - \log r_{80})^2\right]\right\},$$

for $r_{80} = 0.8$–8 μm.
[162] 2. From *Gong* [2003], modified from *Monahan et al.* [1986]

$$\frac{dF_{int}}{d\log r_{80}} = 3.2 U_{10}^{3.41} r_{80} \times \left(1 + 0.057\, r_{80}^{3.45}\right)$$
$$\times \exp\left\{ \begin{array}{l} 3.68 \times \exp\left[-5.33(0.433 - \log r_{80})^2\right] \\ -4.7 \ln r_{80}[1 + \Theta r_{80}]^{-0.017 r_{80}^{-1.44}} \end{array} \right\},$$

with $\Theta = 30$, for $r_{80} = 0.07$–20 μm.
[163] 3. Following *Mårtensson et al.* [2003], based on laboratory experiments

$$\frac{dF_{int}}{d\log d_p} = U_{10}^{3.41}\left(a_4 d_p^4 + a_3 d_p^3 + a_2 d_p^2 + a_1 d_p + a_0\right),$$

for $d_p = 0.02$–2.8 μm; the coefficients for salinity 33, which are linear functions of temperature and take different values in each of three size ranges, are presented in Table A1.

TABLE A2. Coefficients for the Expression for the SSA Production Flux of *Clarke et al.* [2006] in Each of Three Size Ranges[a]

	d_p Range (μm)		
	0.01–0.132	0.132–1.2	1.2–8
a_0	-1.920×10^2	1.480×10^2	1.727×10^1
a_1	3.103×10^4	4.485×10^2	3.222×10^1
a_2	-7.603×10^5	-2.524×10^3	-2.071×10^1
a_3	8.402×10^6	3.852×10^3	4.677
a_4	-4.393×10^7	-2.4603×10^3	-4.658×10^{-1}
a_5	8.794×10^7	5.733×10^2	1.733×10^{-2}

[a]The coefficients listed here yield values that are within 1% of those of *Clarke et al.* [2006]; rounding the coefficients may yield results that differ by a greater amount.

TABLE A3. Coefficients for the Expression for the Net SSA Production Flux of *Norris et al.* [2008] in Each of Six Size Ranges

	r_{amb} Range (μm)					
	0.145−0.155	0.155−0.165	0.165−0.21	0.21−0.27	0.27−0.9	0.9−1.6
a_0	2.7×10^3	9.3×10^2	1.7×10^2	2.2×10^2	4.3×10^2	7.2×10^2
a_1	0.55	0.90	0.71	0.64	0.46	0.32

[164] 4. From *de Leeuw et al.* [2000], based on surf zone measurements

$$\frac{dF_{int}}{d \log r_{80}} = 4.0 \times \exp(0.23\,U_{10}) \times U_{10}^{3.41} \times r_{80}^{-0.65},$$

for $r_{80} = 0.4$–5 μm and $U_{10} = 0$–9 m s^{-1}.

[165] 5. Following *Clarke et al.* [2006], based on surf zone measurements

$$\frac{dF_{int}}{d \log d_p} = U_{10}^{3.41} \left(a_5 d_p^5 + a_4 d_p^4 + a_3 d_p^3 + a_2 d_p^2 + a_1 d_p + a_0 \right),$$

for $d_p = 0.01$–8 μm; the coefficients, which take on different values in each of three different size ranges, are presented in Table A2.

A4. Micrometeorological Methods

[166] Expressions based on prior formulations are as follows:

[167] 1. From *Nilsson and Rannik* [2001] and *Nilsson et al.* [2001], based on eddy correlation

$$F_{eff} = 1.9 \times 10^4 \exp(0.46\,U_{10}),$$

for $d_p > 0.01$ μm and $U_{10} = 4$–13 m s^{-1}.

[168] 2. From *Geever et al.* [2005], based on eddy correlation measurements

$$F_{eff} = 1.9 \times 10^5 \exp(0.23\,U_{22}),$$

for $r_{amb} = 0.005$–0.5 μm and $U_{22} = 7$–18 m s^{-1}, and

$$F_{eff} = 6.5 \times 10^4 \exp(0.25\,U_{22}),$$

for $d_p = 0.1$–1 μm and $U_{22} = 4$–17 m s^{-1}.

[169] 3. Following *Petelski and Piskozub* [2006], modified by *Andreas* [2007], based on the gradient method

$$\frac{dF_{eff}}{d \log r_{amb}} = 1.2 \times 10^3 \exp[0.52\,U_{10} - (0.05\,U_{10} + 0.64)r_{amb}]$$
$$\times r_{amb},$$

for $r_{amb} = 0.25$–7 μm and $U_{10} = 5$–12 m s^{-1}.

[170] 4. From *Norris et al.* [2008] for the net flux (i.e., not corrected for dry deposition), based on eddy correlation

$$\frac{dF_{net}}{d \log r_{amb}} = a_0 \exp(a_1\,U_{10}),$$

for $U_{10} = 4$–12 m s^{-1}, where the coefficients a_i, which take on different values in each of six size ranges, are presented in Table A3.

A5. Multiple Methods

[171] *Lewis and Schwartz* [2004] presented the formulation

$$\frac{dF_{eff}}{d \log r_{80}} = 50\,U_{10}^{2.5} \exp\left\{ -\left(\frac{1}{2}\right) \left[\frac{\ln\left(\frac{r_{80}}{r_1}\right)}{\ln(4)} \right]^2 \right\} \overset{\times}{\div} 5,$$

for $r_{80} = 0.1$–25 μm and $U_{10} = 5$–20 m s^{-1}, where $r_1 = 0.3$ μm.

REFERENCES

Andreae, M. O., and D. Rosenfeld (2008), Aerosol-cloud-precipitation interactions. Part 1. The nature and sources of cloud-active aerosols, *Earth Sci. Rev.*, *89*, 13–41, doi:10.1016/j.earscirev.2008.03.001.

Andreas, E. L (1992), Sea spray and the turbulent air-sea heat fluxes, *J. Geophys. Res.*, *97*, 11,429–11,441, doi:10.1029/92JC00876.

Andreas, E. L (2007), Comments on "Vertical coarse aerosol fluxes in the atmospheric surface layer over the North Polar Waters of the Atlantic" by Tomasz Petelski and Jacek Piskozub, *J. Geophys. Res.*, *112*, C11010, doi:10.1029/2007JC004184.

Anguelova, M. D. (2008), Complex dielectric constant of sea foam at microwave frequencies, *J. Geophys. Res.*, *113*, C08001, doi:10.1029/2007JC004212.

Anguelova, M. D., and F. Webster (2006), Whitecap coverage from satellite measurements: A first step toward modeling the variability of oceanic whitecaps, *J. Geophys. Res.*, *111*, C03017, doi:10.1029/2005JC003158.

Aziz, M. A., S. C. Reising, W. E. Asher, L. A. Rose, P. W. Gaiser, and K. A. Horgan (2005), Effects of air-sea interaction parameters on ocean surface microwave emission at 10 and 37 GHz, *IEEE Trans. Geosci. Remote Sens.*, *43*, 1763–1774, doi:10.1109/TGRS.2005.848413.

Bettenhausen, M. H., C. K. Smith, R. M. Bevilacqua, N.-Y. Wang, P. W. Gaiser, and S. Cox (2006), A nonlinear optimization

algorithm for WindSat wind vector retrievals, *IEEE Trans. Geosci. Remote Sens.*, *44*, 597–610, doi:10.1109/TGRS.2005. 862504.

Bigg, E. K., and C. Leck (2001), Properties of the aerosol over the central Arctic Ocean, *J. Geophys. Res.*, *106*, 32,101–32,109, doi:10.1029/1999JD901136.

Bigg, E. K., and C. Leck (2008), The composition of fragments of bubbles bursting at the ocean surface, *J. Geophys. Res.*, *113*, D11209, doi:10.1029/2007JD009078.

Bigg, E. K., C. Leck, and L. Tranvik (2004), Particulates of the surface microlayer of open water in the central Arctic Ocean in summer, *Mar. Chem.*, *91*, 131–141, doi:10.1016/j.marchem. 2004.06.005.

Blanchard, D. C. (1963), The electrification of the atmosphere by particles from bubbles in the sea, *Prog. Oceanogr.*, *1*, 73–112, doi:10.1016/0079-6611(63)90004-1.

Blanchard, D. C. (1964), Sea to air transport of surface active material, *Science*, *146*, 396–397, doi:10.1126/science.146. 3642.396.

Blanchard, D. C. (1983), The production, distribution, and bacterial enrichment of the sea-salt aerosol, in *Air-Sea Exchange of Gases and Particles*, edited by P. S. Liss and W. G. N. Slinn, pp. 407–454, D. Reidel, Dordrecht, Netherlands.

Blanchard, D. C., and L. D. Syzdek (1970), Mechanism for the water-to-air transfer and concentration of bacteria, *Science*, *170*, 626–628, doi:10.1126/science.170.3958.626.

Blanchard, D. C., and L. D. Syzdek (1972), Concentration of bacteria in jet drops from bursting bubbles, *J. Geophys. Res.*, *77*, 5087–5099, doi:10.1029/JC077i027p05087.

Blanchard, D. C., and L. D. Syzdek (1975), Electrostatic collection of jet and film drops, *Limnol. Oceanogr.*, *20*, 762–774, doi:10.4319/lo.1975.20.5.0762.

Blanchard, D. C., L. D. Syzdek, and M. E. Weber (1981), Bubble scavenging of bacteria in freshwater quickly produces bacterial enrichment in airborne jet drops, *Limnol. Oceanogr.*, *26*, 961–964, doi:10.4319/lo.1981.26.5.0961.

Bower, K., T. Choularton, J. Latham, J. Sahraei, and S. Salter (2006), Computational assessment of a proposed technique for global warming mitigation via albedo-enhancement of marine stratocumulus clouds, *Atmos. Res.*, *82*, 328–336, doi:10.1016/j. atmosres.2005.11.013.

Brady, M., and G. E. Legge (2009), Camera calibration for natural image studies and vision research, *J. Opt. Soc. Am. A Opt. Image Sci. Vis.*, *26*, 30–42, doi:10.1364/JOSAA.26.000030.

Brooks, I. M., et al. (2009), Physical exchanges at the air-sea interface: UK-SOLAS field measurements, *Bull. Am. Meteorol. Soc.*, *90*, 629–644, doi:10.1175/2008BAMS2578.1.

Businger, J. A. (1986), Evaluation of the accuracy with which dry deposition can be measured with current micrometeorological techniques, *J. Clim. Appl. Meteorol.*, *25*, 1100–1124, doi:10.1175/1520-0450(1986)025<1100:EOTAWW>2.0.CO;2.

Caffrey, P. F., W. A. Hoppel, and J. J. Shi (2006), A one-dimensional sectional aerosol model integrated with mesoscale meteorological data to study marine boundary layer aerosol dynamics, *J. Geophys. Res.*, *111*, D24201, doi:10.1029/2006JD007237.

Callaghan, A. H., and M. White (2009), Automated processing of sea surface images for the determination of whitecap coverage, *J. Atmos. Oceanic Technol.*, *26*, 383–394, doi:10.1175/ 2008JTECHO634.1.

Callaghan, A. H., G. B. Deane, and M. D. Stokes (2008a), Observed physical and environmental causes of scatter in whitecap coverage values in a fetch-limited coastal zone, *J. Geophys. Res.*, *113*, C05022, doi:10.1029/2007JC004453.

Callaghan, A. H., G. de Leeuw, L. Cohen, and C. D. O'Dowd (2008b), Relationship of oceanic whitecap coverage to wind speed and wind history, *Geophys. Res. Lett.*, *35*, L23609, doi:10.1029/2008GL036165.

Carruthers, D. J., and T. W. Choularton (1986), The microstructure of hill cap clouds, *Q. J. R. Meteorol. Soc.*, *112*, 113–129, doi:10.1002/qj.49711247107.

Cavalli, F., et al. (2004), Advances in characterization of size-resolved organic matter in marine aerosol over the North Atlantic, *J. Geophys. Res.*, *109*, D24215, doi:10.1029/2004JD005137.

Ceburnis, D., C. D. O'Dowd, S. G. Jennings, M. C. Facchini, L. Emblico, S. Decesari, S. Fuzzi, and J. Sakalys (2008), Marine aerosol chemistry gradients: Elucidating primary and secondary processes and fluxes, *Geophys. Res. Lett.*, *35*, L07804, doi:10.1029/2008GL033462.

Charlson, R. J., S. E. Schwartz, J. M. Hales, R. D. Cess, J. A. Coakley Jr., J. E. Hansen, and D. J. Hoffman (1992), Climate forcing by anthropogenic aerosols, *Science*, *255*, 423–430, doi:10.1126/science.255.5043.423.

Chin, M., P. Ginoux, S. Kinne, O. Torres, B. N. Holben, B. N. Duncan, R. V. Martin, J. A. Logan, A. Higurashi, and T. Nakajima (2002), Tropospheric aerosol optical thickness from the GOCART model and comparisons with satellite and Sun photometer measurements, *J. Atmos. Sci.*, *59*, 461–483, doi:10.1175/1520-0469 (2002)059<0461:TAOTFT>2.0.CO;2.

Cipriano, R. J., and D. C. Blanchard (1981), Bubble and aerosol spectra produced by a laboratory "breaking wave," *J. Geophys. Res.*, *86*, 8085–8092, doi:10.1029/JC086iC09p08085.

Cipriano, R. J., D. C. Blanchard, A. W. Hogan, and G. G. Lala (1983), On the production of Aitken nuclei from breaking waves and their role in the atmosphere, *J. Atmos. Sci.*, *40*, 469–479, doi:10.1175/1520-0469(1983)040<0469:OTPOAN>2.0.CO;2.

Cipriano, R. J., E. C. Monahan, P. J. Bowyer, and D. K. Woolf (1987), Marine condensation nucleus generation inferred from whitecap simulation tank results, *J. Geophys. Res.*, *92*, 6569–6576, doi:10.1029/JC092iC06p06569.

Clarke, A. D., S. R. Owens, and J. Zhou (2006), An ultrafine sea-salt flux from breaking waves: Implications for cloud condensation nuclei in the remote marine atmosphere, *J. Geophys. Res.*, *111*, D06202, doi:10.1029/2005JD006565.

Day, J. A. (1964), Production of droplets and salt nuclei by the bursting of air-bubble films, *Q. J. R. Meteorol. Soc.*, *90*, 72–78, doi:10.1002/qj.49709038307.

de Leeuw, G., F. P. Neele, M. Hill, M. H. Smith, and E. Vignati (2000), Sea spray aerosol production by waves breaking in the surf zone, *J. Geophys. Res.*, *105*, 29,397–29,409, doi:10.1029/ 2000JD900549.

de Leeuw, G., M. M. Moerman, C. J. Zappa, W. R. McGillis, S. J. Norris, and M. H. Smith (2007), Eddy correlation measurements of sea spray aerosol fluxes, in *Transport at the Air-Sea Interface*, edited by C. S. Garbe, R. A. Handler, and B. Jähne, pp. 297–311, doi:10.1007/978-3-540-36906-6_21, Springer, Heidelberg, Germany.

Dentener, F., et al. (2006), Emissions of primary aerosol and precursor gases for the years 2000 and 1750 prescribed data-sets for AeroCom, *Atmos. Chem. Phys.*, *6*, 4321–4344, doi:10.5194/ acp-6-4321-2006.

Detwiler, A., and D. C. Blanchard (1978), Aging and bursting bubbles in trace-contaminated water, *Chem. Eng. Sci.*, *33*, 9–13, doi:10.1016/0009-2509(78)85061-1.

Drennan, W. M., P. K. Taylor, and M. J. Yelland (2005), Parameterizing the sea surface roughness, *J. Phys. Oceanogr.*, *35*, 835–848, doi:10.1175/JPO2704.1.

Easter, R. C., S. J. Ghan, Y. Zhang, R. D. Saylor, E. G. Chapman, N. S. Laulainen, H. Abdul-Razzak, L. R. Leung, X. Bian, and R. A. Zaveri (2004), MIRAGE: Model description and evaluation of aerosols and trace gases, *J. Geophys. Res.*, *109*, D20210, doi:10.1029/2004JD004571.

Erickson, D. J., J. T. Merrill, and R. A. Duce (1986), Seasonal estimates of global atmospheric sea-salt distributions, *J. Geophys. Res.*, *91*, 1067–1072, doi:10.1029/JD091iD01p01067.

Facchini, M. C., et al. (2008), Primary submicron marine aerosol dominated by insoluble organic colloids and aggregates, *Geophys. Res. Lett.*, *35*, L17814, doi:10.1029/2008GL034210.

Freilich, M. H., and B. A. Vanhoff (2006), The accuracy of preliminary WindSat vector wind measurements: Comparisons with NDBC buoys and QuikSCAT, *IEEE Trans. Geosci. Remote Sens.*, *44*, 622–637, doi:10.1109/TGRS.2006.869928.

Frouin, R., M. Schwindling, and P.-Y. Deschamps (1996), Spectral reflectance of sea foam in the visible and near-infrared: In situ measurements and remote sensing implications, *J. Geophys. Res.*, *101*, 14,361–14,371, doi:10.1029/96JC00629.

Fuentes, E., H. Coe, D. Green, G. de Leeuw, and G. McFiggans (2010), Laboratory-generated primary marine aerosol via bubble-bursting and atomization, *Atmos. Meas. Tech.*, *3*, 141–162, doi:10.5194/amt-3-141-2010.

Gaiser, P. W., et al. (2004), The WindSat spaceborne polarimetric microwave radiometer: Sensor description and early orbit performance, *IEEE Trans. Geosci. Remote Sens.*, *42*, 2347–2361, doi:10.1109/TGRS.2004.836867.

Geever, M., C. D. O'Dowd, S. van Ekeren, R. Flanagan, E. D. Nilsson, G. de Leeuw, and Ü. Rannik (2005), Submicron sea spray fluxes, *Geophys. Res. Lett.*, *32*, L15810, doi:10.1029/2005GL023081.

Gong, S. L. (2003), A parameterization of sea-salt aerosol source function for sub- and super-micron particles, *Global Biogeochem. Cycles*, *17*(4), 1097, doi:10.1029/2003GB002079.

Gong, S. L., L. A. Barrie, and J.-P. Blanchet (1997), Modeling sea-salt aerosols in the atmosphere: 1. Model development, *J. Geophys. Res.*, *102*, 3805–3818, doi:10.1029/96JD02953.

Gong, S. L., L. A. Barrie, and M. Lazare (2002), Canadian Aerosol Module (CAM): A size-segregated simulation of atmospheric aerosol processes for climate and air quality models—2. Global sea-salt aerosol and its budgets, *J. Geophys. Res.*, *107*(D24), 4779, doi:10.1029/2001JD002004.

Gong, S. L., et al. (2003), Canadian Aerosol Module: A size-segregated simulation of atmospheric aerosol processes for climate and air quality models—1. Module development, *J. Geophys. Res.*, *108*(D1), 4007, doi:10.1029/2001JD002002.

Grini, A., G. Myhre, J. K. Sundet, and I. S. A. Isaksen (2002), Modeling the annual cycle of sea salt in the global 3D model Oslo CTM2: Concentrations, fluxes, and radiative impact, *J. Clim.*, *15*, 1717–1730, doi:10.1175/1520-0442(2002)015<1717:MTACOS>2.0.CO;2.

Guan, C., W. Hu, J. Sun, and R. Li (2007), The whitecap coverage model from breaking dissipation parametrizations of wind waves, *J. Geophys. Res.*, *112*, C05031, doi:10.1029/2006JC003714.

Hill, M. K., B. J. Brooks, S. J. Norris, M. H. Smith, I. M. Brooks, G. de Leeuw, and J. J. N. Lingard (2008), A Compact Lightweight Aerosol Spectrometer Probe (CLASP), *J. Atmos. Oceanic Technol.*, *25*, 1996–2006, doi:10.1175/2008JTECHA1051.1.

Hoffman, E. J., and R. A. Duce (1976), Factors influencing the organic carbon content of marine aerosols: A laboratory study, *J. Geophys. Res.*, *81*, 3667–3670, doi:10.1029/JC081i021p03667.

Hoppel, W. A., G. M. Frick, and J. W. Fitzgerald (2002), Surface source function for sea-salt aerosol and aerosol dry deposition to the ocean surface, *J. Geophys. Res.*, *107*(D19), 4382, doi:10.1029/2001JD002014.

Intergovernmental Panel on Climate Change (2007), *Climate Change 2007: The Physical Science Basis: Working Group I Contribution to the Fourth Assessment Report of the Intergovernmental Panel on Climate Change*, edited by S. Solomon et al., Cambridge Univ. Press, New York.

Jessup, A. T., C. J. Zappa, M. R. Loewen, and V. Hesany (1997), Infrared remote sensing of breaking waves, *Nature*, *385*, 52–55, doi:10.1038/385052a0.

Kaimal, J. C., and J. J. Finnigan (1994), *Atmospheric Boundary Layer Flows: Their Structure and Measurement*, 289 pp., Oxford Univ. Press, New York.

Keene, W. C., et al. (2007), Chemical and physical characteristics of nascent aerosols produced by bursting bubbles at a model air-sea interface, *J. Geophys. Res.*, *112*, D21202, doi:10.1029/2007JD008464.

Koch, D., G. A. Schmidt, and C. V. Field (2006), Sulfur, sea salt and radionuclide aerosols in GISS ModelE, *J. Geophys. Res.*, *111*, D06206, doi:10.1029/2004JD005550.

Koepke, P. (1986), Remote sensing signature of whitecaps, in *Oceanic Whitecaps and Their Role in Air-Sea Exchange Processes*, edited by E. C. Monahan and G. M. Niocaill, pp. 251–260, D. Reidel, Dordrecht, Netherlands.

Kokhanovsky, A. A. (2004), Spectral reflectance of whitecaps, *J. Geophys. Res.*, *109*, C05021, doi:10.1029/2003JC002177.

Kroeker, K. L. (2009), Photography's bright future, *Commun. ACM*, 52, 11–13, doi:10.1145/1461928.1461933.

Lafon, C., J. Piazzola, P. Forget, O. le Calve, and S. Despiau (2004), Analysis of the variations of the whitecap fraction as measured in a coastal zone, *Boundary Layer Meteorol.*, *111*, 339–360, doi:10.1023/B:BOUN.0000016490.83880.63.

Lafon, C., J. Piazzola, P. Forget, and S. Despiau (2007), Whitecap coverage in coastal environment for steady and unsteady wave field conditions, *J. Mar. Syst.*, *66*, 38–46, doi:10.1016/j.jmarsys.2006.02.013.

Langmann, B., S. Varghese, E. Marmer, E. Vignati, J. Wilson, P. Stier, and C. O'Dowd (2008a), Aerosol distribution over Europe: A model evaluation study with detailed aerosol microphysics, *Atmos. Chem. Phys.*, *8*, 1591–1607, doi:10.5194/acp-8-1591-2008.

Langmann, B., C. Scannell, and C. D. O'Dowd (2008b), New directions: Organic matter contribution to marine aerosols and cloud condensation nuclei, *Atmos. Environ.*, *42*, 7821–7822, doi:10.1016/j.atmosenv.2008.09.002.

Latham, J. (1990), Control of global warming?, *Nature*, *347*, 339–340, doi:10.1038/347339b0.

Leck, C., and E. K. Bigg (1999), Aerosol production over remote marine areas—A new route, *Geophys. Res. Lett.*, *26*, 3577–3581, doi:10.1029/1999GL010807.

Leck, C., and E. K. Bigg (2005a), Biogenic particles in the surface microlayer and overlaying atmosphere in the central Arctic Ocean during summer, *Tellus Ser. B*, *57*, 305–316, doi:10.1111/j.1600-0889.2005.00148.x.

Leck, C., and E. K. Bigg (2005b), Source and evolution of the marine aerosol: A new perspective, *Geophys. Res. Lett.*, *32*, L19803, doi:10.1029/2005GL023651.

Leck, C., and E. K. Bigg (2008), Comparison of sources and nature of the tropical aerosol with the summer high Arctic aerosol, *Tellus Ser. B*, *60*, 118–126, doi:10.1111/j.1600-0889.2007.00315.x.

Lewis, E. R. (2008), An examination of Köhler theory resulting in an accurate expression for the equilibrium radius ratio of a hygroscopic aerosol particle valid up to and including relative humidity 100%, *J. Geophys. Res.*, *113*, D03205, doi:10.1029/2007JD008590.

Lewis, E. R., and S. E. Schwartz (2004), *Sea Salt Aerosol Production: Mechanisms, Methods, Measurements and Models—A Critical Review*, Geophys. Monogr. Ser., vol. 152, 413 pp., AGU, Washington, D. C.

Liu, X., and J. E. Penner (2002), Effect of Mt. Pinatubo H_2SO_4/H_2O aerosol on ice nucleation in the upper troposphere using a global chemistry and transport model (IMPACT), *J. Geophys. Res.*, *107*(D12), 4141, doi:10.1029/2001JD000455.

Marmorino, G. O., and G. B. Smith (2005), Bright and dark ocean whitecaps observed in the infrared, *Geophys. Res. Lett.*, *32*, L11604, doi:10.1029/2005GL023176.

Mårtensson, E. M., E. D. Nilsson, G. de Leeuw, L. H. Cohen, and H. C. Hansson (2003), Laboratory simulations of the primary marine aerosol production, *J. Geophys. Res.*, *108*(D9), 4297, doi:10.1029/2002JD002263.

Massel, S. R. (2007), *Ocean Waves Breaking and Marine Aerosol Fluxes*, 323 pp., Springer, New York.

Middlebrook, A. M., D. M. Murphy, and D. S. Thomson (1998), Observation of organic material in individual particles at Cape Grim during the First Aerosol Characterization Experiment (ACE 1), *J. Geophys. Res.*, *103*, 16,475–16,483, doi:10.1029/97JD03719.

Monahan, E. C., and I. G. Ó Muircheartaigh (1980), Optimal power-law description of oceanic whitecap coverage dependence on wind speed, *J. Phys. Oceanogr.*, *10*, 2094–2099, doi:10.1175/1520-0485(1980)010<2094:OPLDOO>2.0.CO;2.

Monahan, E. C., C. W. Fairall, K. L. Davidson, and P. Jones-Boyle (1983), Observed inter-relations between 10 m winds, ocean whitecaps and marine aerosols, *Q. J. R. Meteorol. Soc.*, *109*, 379–392, doi:10.1002/qj.49710946010.

Monahan, E. C., D. E. Spiel, and K. L. Davidson (1986), A model of marine aerosol generation via whitecaps and wave disruption, in *Oceanic Whitecaps and Their Role in Air-Sea Exchange Processes*, edited by E. C. Monahan and G. MacNiocaill, pp. 167–174, D. Reidel, Dordrecht, Netherlands.

Myhre, G., T. K. Berntsen, J. M. Haywood, J. K. Sundet, B. N. Holben, M. Johnsrud, and F. Stordal (2003), Modeling the solar radiative impact of aerosols from biomass burning during the Southern African Regional Science Initiative (SAFARI-2000) experiment, *J. Geophys. Res.*, *108*(D13), 8501, doi:10.1029/2002JD002313.

Nilsson, E. D., and Ü. Rannik (2001), Turbulent aerosol fluxes over the Arctic Ocean: 1. Dry deposition over sea and pack ice, *J. Geophys. Res.*, *106*, 32,125–32,137, doi:10.1029/2000JD900605.

Nilsson, E. D., Ü. Rannik, E. Swietlicki, C. Leck, P. P. Aalto, J. Zhou, and M. Norman (2001), Turbulent aerosol fluxes over the Arctic Ocean: 2. Wind-driven sources from the sea, *J. Geophys. Res.*, *106*, 32,139–32,154, doi:10.1029/2000JD900747.

Nordberg, W., J. Conaway, D. B. Ross, and T. Wilheit (1971), Measurements of microwave emission from a foam-coverd, wind-driven sea, *J. Atmos. Sci.*, *28*, 429–435, doi:10.1175/1520-0469(1971)028<0429:MOMEFA>2.0.CO;2.

Norris, S. J., I. M. Brooks, G. de Leeuw, M. H. Smith, M. M. Moerman, and J. J. N. Lingard (2008), Eddy covariance measurements of sea spray particles over the Atlantic Ocean, *Atmos. Chem. Phys.*, *8*, 555–563, doi:10.5194/acp-8-555-2008.

Novakov, T., C. E. Corrigan, J. E. Penner, C. C. Chuang, O. Rosario, and O. L. Mayol Bracero (1997), Organic aerosols in the Caribbean trade winds: A natural source?, *J. Geophys. Res.*, *102*, 21,307–21,313, doi:10.1029/97JD01487.

O'Dowd, C. D., and G. de Leeuw (2007), Marine aerosol production: A review of the current knowledge, *Philos. Trans. R. Soc. A*, *365*, 1753–1774, doi:10.1098/rsta.2007.2043.

O'Dowd, C. D., M. H. Smith, I. E. Consterdine, and J. A. Lowe (1997), Marine aerosol, sea salt, and the marine sulphur cycle: A short review, *Atmos. Environ.*, *31*, 73–80, doi:10.1016/S1352-2310(96)00106-9.

O'Dowd, C. D., M. C. Facchini, F. Cavalli, D. Ceburnis, M. Mircea, S. Decesari, S. Fuzzi, Y. J. Yoon, and J.-P. Putaud (2004), Biogenically driven organic contribution to marine aerosol, *Nature*, *431*, 676–680, doi:10.1038/nature02959.

O'Dowd, C. D., B. Langmann, S. Varghese, C. Scannell, D. Ceburnis, and M. C. Facchini (2008), A combined organic-inorganic sea-spray source function, *Geophys. Res. Lett.*, *35*, L01801, doi:10.1029/2007GL030331.

Oppo, C., S. Bellandi, N. Degli Innocenti, A. M. Stortini, G. Loglio, E. Schiavuta, and R. Cini (1999), Surfactant components of marine organic matter as agents for biogeochemical fractionation and pollutant transport via marine aerosols, *Mar. Chem.*, *63*, 235–253, doi:10.1016/S0304-4203(98)00065-6.

O'Reilly, J. E., S. Maritorena, B. G. Mitchell, D. A. Siegel, K. L. Carder, S. A. Garver, M. Kahru, and C. McClain (1998), Ocean color chlorophyll algorithms for SeaWiFS, *J. Geophys. Res.*, *103*, 24,937–24,953, doi:10.1029/98JC02160.

Padmanabhan, S., S. C. Reising, W. E. Asher, L. A. Rose, and P. W. Gaiser (2006), Effects of foam on ocean surface microwave emission inferred from radiometric observations of reproducible breaking waves, *IEEE Trans. Geosci. Remote Sens.*, *44*, 569–583, doi:10.1109/TGRS.2006.870234.

Petelski, T. (2003), Marine aerosol fluxes over open sea calculated from vertical concentration gradients, *J. Aerosol Sci.*, *34*, 359–371, doi:10.1016/S0021-8502(02)00189-1.

Petelski, T. (2005), Coarse aerosol concentration over the North Polar Waters of the Atlantic, *Aerosol Sci. Technol.*, *39*, 695–700.

Petelski, T., and J. Piskozub (2006), Vertical coarse aerosol fluxes in the atmospheric surface layer over the North Polar Waters of the Atlantic, *J. Geophys. Res.*, *111*, C06039, doi:10.1029/2005JC003295.

Petelski, T., and J. Piskozub (2007), Reply to comment by Edgar L Andreas on "Vertical coarse aerosol fluxes in the atmospheric surface layer over the North Polar Waters of the Atlantic," *J. Geophys. Res.*, *112*, C11011, doi:10.1029/2007JC004399.

Pitari, G., E. Mancini, V. Rizi, and D. T. Shindell (2002), Impact of future climate and emissions changes on stratospheric aerosols and ozone, *J. Atmos. Sci.*, *59*, 414–440, doi:10.1175/1520-0469(2002)059<0414:IOFCAE>2.0.CO;2.

Prospero, J. M. (2002), The chemical and physical properties of marine aerosols: An introduction, in *Chemistry of Marine Water and Sediments*, edited by A. Gianguzza, E. Pellizzetti, and S. Sammarano, pp. 35–82, Springer, Berlin.

Putaud, J.-P., et al. (2000), Chemical mass closure and assessment of the origin of the submicron aerosol in the marine boundary layer and the free troposphere at Tenerife during ACE-2, *Tellus B*, *52*, 141–168.

Reddy, M. S., and O. Boucher (2004), Global carbonaceous aerosol transport and assessment of radiative effects in the LMDZ GCM, *J. Geophys. Res.*, *109*, D14202, doi:10.1029/2003JD004048.

Reddy, M. S., O. Boucher, Y. Balkanski, and M. Schulz (2005a), Aerosol optical depths and direct radiative perturbations by species and source type, *Geophys. Res. Lett.*, *32*, L12803, doi:10.1029/2004GL021743.

Reddy, M. S., O. Boucher, N. Bellouin, M. Schulz, Y. Balkanski, J.-L. Dufresne, and M. Pham (2005b), Estimates of global multi-component aerosol optical depth and radiative forcing perturbation in the Laboratoire de Meteorologie Dynamique general circulation model, *J. Geophys. Res.*, *110*, D10S16, doi:10.1029/2004JD004757.

Resch, F., and G. Afeti (1992), Submicron film drop production by bubbles in seawater, *J. Geophys. Res.*, *97*, 3679–3683, doi:10.1029/91JC02961.

Reul, N., and B. Chapron (2003), A model of sea-foam thickness distribution for passive microwave remote sensing applications, *J. Geophys. Res.*, *108*(C10), 3321, doi:10.1029/2003JC001887.

Rose, L. A., W. E. Asher, S. C. Reising, P. W. Gaiser, K. M. St. Germain, D. J. Dowgiallo, K. A. Horgan, G. Farquharson, and E. J. Knapp (2002), Radiometric measurements of the microwave emissivity of foam, *IEEE Trans. Geosci. Remote Sens.*, *40*, 2619–2625, doi:10.1109/TGRS.2002.807006.

Satheesh, S. K., and K. K. Moorthy (2005), Radiative effects of natural aerosols: A review, *Atmos. Environ.*, *39*, 2089–2110, doi:10.1016/j.atmosenv.2004.12.029.

Schulz, M., G. de Leeuw, and Y. Balkanski (2004), Sea-salt aerosol source functions and emissions, in *Emission of Atmospheric Trace Compounds*, edited by C. Granier, P. Artaxo, and C. E. Reeves, pp. 333–359, Kluwer, Dordrecht, Netherlands.

Sellegri, K., C. D. O'Dowd, Y. J. Yoon, S. G. Jennings, and G. de Leeuw (2006), Surfactants and submicron sea spray generation, *J. Geophys. Res.*, *111*, D22215, doi:10.1029/2005JD006658.

Slinn, S. A., and W. G. N. Slinn (1980), Predictions for particle deposition on natural waters, *Atmos. Environ.*, *14*, 1013–1016, doi:10.1016/0004-6981(80)90032-3.

Smith, M. H., and N. M. Harrison (1998), The sea spray generation function, *J. Aerosol Sci.*, *29*, suppl. 1, S189–S190, doi:10.1016/S0021-8502(98)00280-8.

Smith, M. H., P. M. Park, and I. E. Consterdine (1993), Marine aerosol concentrations and estimated fluxes over the sea, *Q. J. R. Meteorol. Soc.*, *119*, 809–824, doi:10.1002/qj.49711951211.

Soloviev, A., M. Donelan, H. Graber, B. Haus, and P. Schlussel (2007), An approach to estimation of near-surface turbulence and CO_2 transfer velocity from remote sensing data, *J. Mar. Syst.*, *66*, 182–194, doi:10.1016/j.jmarsys.2006.03.023.

Spiel, D. E. (1995), On the birth of jet drops from bubbles bursting on water surfaces, *J. Geophys. Res.*, *100*, 4995–5006, doi:10.1029/94JC03055.

Stier, P., et al. (2005), The aerosol-climate model ECHAM5-HAM, *Atmos. Chem. Phys.*, *5*, 1125–1156, doi:10.5194/acp-5-1125-2005.

Sugihara, Y., H. Tsumori, T. Ohga, H. Yoshioka, and S. Serizawa (2007), Variation of whitecap coverage with wave-field conditions, *J. Mar. Syst.*, *66*, 47–60, doi:10.1016/j.jmarsys.2006.01.014.

Takemura, T., H. Okamoto, Y. Maruyama, A. Numaguti, A. Higurashi, and T. Nakajima (2000), Global three-dimensional simulation of aerosol optical thickness distribution of various origins, *J. Geophys. Res.*, *105*, 17,853–17,873, doi:10.1029/2000JD900265.

Takemura, T., T. Nakajima, O. Dubovik, B. N. Holben, and S. Kinne (2002), Single-scattering albedo and radiative forcing of various aerosol species with a global three-dimensional model, *J. Clim.*, *15*, 333–352, doi:10.1175/1520-0442(2002)015<0333:SSAARF>2.0.CO;2.

Textor, C., et al. (2006), Analysis and quantification of the diversities of aerosol life cycles within AeroCom, *Atmos. Chem. Phys.*, *6*, 1777–1813, doi:10.5194/acp-6-1777-2006.

Thorpe, S. A. (1992), Bubble clouds and the dynamics of the upper ocean, *Q. J. R. Meteorol. Soc.*, *118*, 1–22, doi:10.1002/qj.49711850302.

Tyree, C. A., V. M. Hellion, O. A. Alexandrova, and J. O. Allen (2007), Foam droplets generated from natural and artificial seawaters, *J. Geophys. Res.*, *112*, D12204, doi:10.1029/2006JD007729.

Vignati, E., M. C. Facchini, M. Rinaldi, C. Scannell, D. Ceburnis, J. Sciare, M. Kanakidou, S. Myriokefalitakis, F. Dentener, and C. D. O'Dowd (2010), Global scale emission and distribution of sea spray aerosol: Sea-salt and organic enrichment, *Atmos. Environ.*, *44*, 670–677, doi:10.1016/j.atmosenv.2009.11.013.

Wang, Q., E. C. Monahan, W. E. Asher, and P. M. Smith (1995), Correlations of whitecap coverage and gas transfer velocity with microwave brightness temperature for plunging and spilling breaking waves, in *Air-Water Gas Transfer*, edited by B. Jähne and E. C. Monahan, pp. 217–225, AEON, Hanau, Germany.

Whitlock, C. H., D. S. Bartlett, and E. A. Gurganus (1982), Sea foam reflectance and influence on optimum wavelength for remote sensing of ocean aerosols, *Geophys. Res. Lett.*, *9*, 719–722, doi:10.1029/GL009i006p00719.

Woodcock, A. H. (1948), Note concerning human respiratory irritation associated with high concentrations of plankton and mass mortality of marine organism, *J. Mar. Res.*, *7*, 56–62.

Woolf, D. K. (2005), Parametrization of gas transfer velocities and sea-state-dependent wave breaking, *Tellus B*, *57*, 87–94.

Yoon, Y. J., et al. (2007), Seasonal characteristics of the physicochemical properties of North Atlantic marine atmospheric aerosols, *J. Geophys. Res.*, *112*, D04206, doi:10.1029/2005JD007044.

Zakey, A. S., F. Giorgi, and X. Bi (2008), Modeling of sea salt in a regional climate model: Fluxes and radiative forcing, *J. Geophys. Res.*, *113*, D14221, doi:10.1029/2007JD009209.

Zhao, D., and Y. Toba (2001), Dependence of whitecap coverage on wind and wind-wave properties, *J. Oceanogr.*, *57*, 603–616, doi:10.1023/A:1021215904955.

E. L Andreas, Seattle Division, NorthWest Research Associates, Inc., 25 Eagle Rdg., Lebanon, NH 03766-1900, USA.

M. D. Anguelova, Naval Research Laboratory, 4555 Overlook Ave., Washington, DC 20375, USA.

G. de Leeuw, Climate Change Unit, Finnish Meteorological Institute, Erik Palmenin Aukio 1, FI-00101 Helsinki, Finland. (gerrit.leeuw@fmi.fi)

C. W. Fairall, NOAA Earth System Research Laboratory, 325 Broadway, Boulder, CO 80305-3328, USA.

E. R. Lewis and S. E. Schwartz, Brookhaven National Laboratory, P.O. Box 5000, Upton, NY 11973-5000, USA.

C. O'Dowd, Centre for Climate and Air Pollution Studies, Environmental Change Institute, National University of Ireland, Galway, University Road, Galway, Ireland.

M. Schulz, Meteorologisk Institutt, Postboks 43 Blindern, N-0313 Oslo, Norway.